CARBOHYDRATE COMPONENTS OF POMACE IN CORN-BASED EXTRUDATES: INTERACTIONS, EXPANSION DYNAMICS, AND STRUCTURE-TEXTURE RELATIONSHIPS

by

ELISA NOEMBERG LAZZARI KARKLE

B.S., Parana Federal University, Brazil, 2004
M.S., Londrina State University, Brazil, 2006

AN ABSTRACT OF A DISSERTATION

submitted in partial fulfillment of the requirements for the degree

DOCTOR OF PHILOSOPHY

Department of Grain Science and Industry
College of Agriculture

KANSAS STATE UNIVERSITY
Manhattan, Kansas

2011

Abstract

Extrusion processing is a technology widely used to make ready-to-eat snack and breakfast cereal products. The raw materials that result in optimal texture and consumer acceptance are mainly those with high levels of starch, which greatly limits the nutritional value of these products. One alternative to enhance the nutritional value is the incorporation of fruits and vegetables. Fruits and vegetables are consistently under-consumed by the American population and incorporation into extruded products may help increase the intake of important nutrients, such as dietary fiber. In the first part of this study a lab-scale twin screw extruder was used for processing directly expanded products based on corn flour and apple pomace (0-28%), resulting in a total dietary fiber content of 1.1-22.5%. Apple pomace increased nucleation and favored axial expansion. The change in cell size and alignment explained the higher mechanical resistance caused by apple pomace. The objective of the second part was to study the effect of preconditioning regimen on the extent of matrix transformation and impact on texture, microstructure and digestibility. The material was processed on a pilot scale extruder. The results showed that increasing the opportunity for hydration increased starch gelatinization at all pomace levels. Apple pomace promoted milder extrusion conditions, resulting in less starch gelatinization and solubilization and reduced starch digestibility. Digestibility was also affected by structure, with a strong correlation between the available starch fraction and cell wall thickness/cell size ratio (r=0.90). The third part of this study was designed to gain a better understanding of the impact of the individual cell wall components (cellulose, lignin, xyloglucan and pectin) on expansion and structure formation. The results suggest that compatibility with starch is critical for good dispersion in the matrix, therefore good expansion and structure forming properties.

CARBOHYDRATE COMPONENTS OF POMACE IN CORN-BASED EXTRUDATES: INTERACTIONS, EXPANSION DYNAMICS, AND STRUCTURE-TEXTURE RELATIONSHIPS

by

ELISA NOEMBERG LAZZARI KARKLE

B.S., Parana Federal University, Brazil, 2004
M.S., Londrina State University, Brazil, 2006

A DISSERTATION

submitted in partial fulfillment of the requirements for the degree

DOCTOR OF PHILOSOPHY

Department of Grain Science and Industry
College of Agriculture

KANSAS STATE UNIVERSITY
Manhattan, Kansas

2011

Approved by:

Major Professor
Sajid Alavi, PhD

Abstract

Extrusion processing is a technology widely used to make ready-to-eat snack and breakfast cereal products. The raw materials that result in optimal texture and consumer acceptance are mainly those with high levels of starch, which greatly limits the nutritional value of these products. One alternative to enhance the nutritional value is the incorporation of fruits and vegetables. Fruits and vegetables are consistently under-consumed by the American population and incorporation into extruded products may help increase the intake of important nutrients, such as dietary fiber. In the first part of this study a lab-scale twin screw extruder was used for processing directly expanded products based on corn flour and apple pomace (0-28%), resulting in a total dietary fiber content of 1.1-22.5%. Apple pomace increased nucleation and favored axial expansion. The change in cell size and alignment explained the higher mechanical resistance caused by apple pomace. The objective of the second part was to study the effect of preconditioning regimen on the extent of matrix transformation and impact on texture, microstructure and digestibility. The material was processed on a pilot scale extruder. The results showed that increasing the opportunity for hydration increased starch gelatinization at all pomace levels. Apple pomace promoted milder extrusion conditions, resulting in less starch gelatinization and solubilization and reduced starch digestibility. Digestibility was also affected by structure, with a strong correlation between the available starch fraction and cell wall thickness/cell size ratio (r=0.90). The third part of this study was designed to gain a better understanding of the impact of the individual cell wall components (cellulose, lignin, xyloglucan and pectin) on expansion and structure formation. The results suggest that compatibility with starch is critical for good dispersion in the matrix, therefore good expansion and structure forming properties.

Table of Contents

List of Figures

List of Tables

Acknowledgements

I would like to acknowledge the contribution of the following people and organizations:

- Dr. Sajid Alavi, for his guidance, involvement and great interest and support towards all aspects of my development as a scientist.
- Drs. Bhadriraju Subramanyam, Mark Haub, Lewis Keller, and Yong-Cheng Shi for their valuable input and involvement since the initial phases of this work.
- Mr. Eric Maichel, Operations Manager of the Extrusion Laboratory, and his student helpers for assistance with extrusion processing and hands-on training.
- Faculty and staff of the Department of Grain Science and Industry, for facilitating the use of various equipments and resources, and overall helpfulness.
- The following companies, for kindly donating materials for the experiments: Tree Top, Didion Milling, Cargill, Tate and Lyle, Meadwestvaco, Bunge, International Fiber Corp., Naturex, and International Flavors and Fragrances.
- The Kansas State University Center for Engagement and Community Development, for funding portions of this work.
- My friends at the Department of Grain Science, specially my labmates Jhoe Stonestreet, Juhyun Yoo, Swathi Kodavali and Dr. XiaoZhi Tang.
- My friends at Grace Baptist Church, for being my family in Manhattan.
- My loving family for their support and encouragement.
- My beloved husband Daniel, for his strength and unconditional love.

CHAPTER 1 - Introduction

1.1 Dietary guidelines and fruit and vegetable consumption

The latest results on childhood obesity from the National Health and Nutrition Examination Survey 2005-2006 showed that 30.1% of children aged 2-19 years were above the 85th percentile of body mass index for age (Ogden et al, 2008). The same survey indicated that the incidence of overweight and obesity in this age group has reached a plateau, with no significant increments from the period 2003-2004. Among adults the prevalence of overweight and obesity is currently 68% (Flegal et al., 2010). There is evidence that the increment for adults has also stabilized, based on rates for the past 10 years. Although these are positive trends, a large segment of the population is at risk for developing adverse health outcomes associated with overweight/obesity.

In addition to the high prevalence of overweight/obesity, several food groups and consequently nutrients are lacking in the American diet. The report issued by the 2010 Dietary Guidelines for Americans Advisory Committee (DGAC, USDA, 2010) identified the intake of dietary fiber, vitamin D, calcium, potassium and unsaturated fatty acids as insufficient. These were termed shortfall nutrients. Fruits and vegetables can be good sources of dietary fiber, calcium and potassium, however intake of this food group has consistently been below the recommended levels. Figure 1-1 illustrates the inadequacy of consumption. Consumption is less than 50% of the recommended intake for fruits and 60% for vegetables.

According to the World Health Organization there is strong evidence that health outcomes such as protection against myocardial infarction, hypertension and certain cancers are obtained with high daily intake of fruits and vegetables (WHO, 2003). High levels of fruit and fiber intake have been associated to lower risk for development of overweight/obesity, which by itself reduces the risk of cardiovascular disease and diabetes, among other metabolic conditions (Zazpe et al, 2011). Low caloric density is the main mechanism by which fruit and vegetables assist in energy balance and weight management (WHO, 2003).

Although the DGAC report calls for minimal processing of fruits and vegetables, it also calls for the engagement of academia and industry in changing the food environment (USDA,

2010). Technological innovations in the use of fruits and vegetables may be a route for increasing consumption. Several organizations have already responded to the call for action by the DGAC. Rowe et al. (2011) present the results of initial dialogues between food scientists and nutritional scientists in addressing the change in food environment. The group identified two key components needed for such change: an offering of balanced food choices aligned with the dietary guidelines, as food scientists in industry and academia reformulate and/or create new products; and nutrition-conscious consumers who adopt new behaviors and demand healthier foods.

1.2 Fruits and vegetables in extruded products

Extrusion processing is a technology widely used to make ready-to-eat snack and breakfast cereal products. In this process, shear, pressure and heat are combined so that the raw materials are mixed, cooked and finally expanded. The resulting products are mainly characterized by an aerated structure, which imparts very unique textural qualities. The raw materials that result in optimal texture and consumer acceptance are mainly those with high levels of starch. This greatly limits the nutritional value of these products. Apart from starch being the base ingredient, these products are commonly coated with oils and/or syrup, adding to the caloric content.

The growing consumer demand for wholesome and healthier foods has impacted the expanded foods segment and it is driving research and industry towards developing novel ready-to-eat expanded products. One option that has been studied for a few decades is the incorporation of fruits and vegetables into expanded products.

The addition of fruits and vegetables to extruded snacks has been studied since the 1980's, with the first published work in 1989, by Maga and Kim. Researchers have since then studied the addition of fruit juice, paste, powders, pomace, peels and seeds into extruded products (Upadhyay et al., 2010; Altan et al., 2008; Yagci and Gogus, 2008; Camire et al, 2007; Maga and Kim, 1989). The use of fruit and vegetable by-products is a growing trend in recent literature. One motivation is the addition of value to food processing residues and reduction of

waste (Yagci and Gogus, 2010). Other drivers are the concentrated nutrient content of the by-products (especially in terms of bioactive compounds) and growing interest in increasing the dietary fiber content of foods (Stojceska et al., 2009; Nawirska and Kwasniewska, 2005; McKee and Latner, 2000).

The typical inclusion levels of fruit and vegetable by-product varies between 2-15%. Upadhyay et al. (2010) applied response surface methodology to optimize the level of carrot pomace in an expanded snack and found 5% to give the best result considering product characteristics and sensory quality. Stojceska et al. (2008) found acceptable sensory scores when incorporating up to 10% cauliflower trimmings into an expanded snack. At 15 and 20% cauliflower inclusion the flavor became unacceptable. The addition of onion powder and potato peels to extrudates has been studied by Camire et al. (2005). At a 2% level, the vegetable material caused no significant effect on expansion, compared to a control of degermed corn meal. The vegetable materials were found to maintain antioxidant activity after extrusion, retarding product oxidation.

The composition of the by-products plays an important role in determining the end quality of the extrudates. Altan et al. (2008) related increase in bulk density to the sugar content of grape pomace. Yanniotis et al. (2007) have demonstrated that different cell wall materials (specifically cellulose and pectin) have very different functionalities upon extrusion. Pectin promoted increase in porosity while cellulose caused a marked decrease. Yagci and Gogus (2008) used this reasoning to explain good expansion of extrudates containing orange peels in a fruit waste mixture.

Despite the information on the effect of fruits and vegetables on quality parameters of extrudates, a thorough analysis of the interaction of the different components is still lacking. For instance, studies have suggested but not proven that the structure of extrudates can be used to control the glycemic index of these products (Donnelly et al., 2008; Chanvrier et al., 2007; Ozer et al, 2006; Slavin et al., 2001). However, the mechanisms of structure formation are still poorly understood for systems with fruit and vegetable materials. Imaging techniques which have been applied for several years for extrudates have only recently been applied to an extrudates containing some form of fiber (Parada et al, 2011).

1.3 Scope of this study

There can be large variations in the composition of fruit and vegetable by-products according to source and previous processing steps (Harris and Smith, 2006). For this work the approach was to choose one highly available fruit by-product to study the effect of addition to extruded snacks. As a second step, fruit and vegetable cell walls were broken down into their four main components and these were studied independently and mixed. Apple pomace was used as the example by-product because of the availability of a consistent supply, and also due to a large body of evidence regarding high fiber and phytonutrient contents. Apple pomace is the material resultant of juice extraction, and consists of peels, seeds, cores and stems. The apple pomace generation in the United States has been estimated to be 27 million kilos (Roberts et al., 2004). The phenolic compounds in this material are responsible for the antioxidant activity (Garcia et al., 2009). In a literature compilation, Bhushan et al. (2008) cite 49 different phenolic compounds that have been reported in apple pomace. The presence of other bioactive components has also been reported, including glutathione, ascorbate and L-cysteine (Lata and Tomala, 2007). Dietary fiber content varies between 51.1-89.8% (36.5-81.6% insoluble and 4.14-14.6% soluble) (Sudha et al., 2007; Figuerola et al., 2005).

The hypotheses upon which this work was based were the following:

1) Matrix components and process dynamics have a significant impact on cellular structure of pomace-added expanded products
2) Mechanical properties are impacted by cellular structure and anisotropy
3) In pomace-added matrices, hydration regimens impact expansion dynamics and mechanical properties
4) Individual cell wall components can be used to understand the impact of pomace addition to directly expanded products

Three experiments were used to test the hypotheses. The objective of the first experiment was to understand the impact of apple pomace on corn-based extrudates, in terms of expansion dynamics and structure formation. Analysis of the internal structure in combination with

composition, and macro-level structural and mechanical properties was used to gain insight into micro-level mechanical properties.

The second experiment was conducted to understand the impact of hydration regimens on the matrix transformation of apple pomace-corn extrudates. It was hypothesized that addition of water in the preconditioner would modify hydration, and the resulting changes in the matrix would impact texture, microstructure and digestibility.

Finally, the third experiment was designed to gain a better understanding of the impact of the individual cell wall components on expansion and structure formation of directly expanded products. The levels of cell wall components used was consistent with their natural occurrence in fruit and vegetable pomaces, as to provide a basis for selecting fruit and vegetable by-products with better functionality.

References

Altan, A., McCarthy, K. L., & Maskan, M. (2008). Twin-screw extrusion of barley-grape pomace blends: Extrudate characteristics and determination of optimum processing conditions. *Journal of Food Engineering, 89*(1), 24-32.

Bhushan, S., Kalia, K., Sharma, M., Singh, B., & Ahuja, P.S. (2008). Processing of apple pomace for bioactive molecules. *Critical Reviews in Biotechnology, 28*, 285-296.

Camire, M.E., Dougherty, M.P. & Briggs, J.L. (2005). Antioxidant-rich food retard lipid oxidation in extruded corn. *Cereal Chemistry, 82*(6), 666-670.

Camire, M. E., Dougherty, M. P., & Briggs, J. L. (2007). Functionality of fruit powders in extruded corn breakfast cereals. *Food Chemistry, 101*(2), 765-770.

Chanvrier, H., Appelqvist, I. A. M., Bird, A. R., Gilbertt, E., Htoon, A., Li, Z., Lillford, P. J., Lopez-Rubio, A., Morell, M. K., & Topping, D. L. (2007). Processing of novel elevated amylose wheats: Functional properties and starch digestibility of extruded products. *Journal of Agricultural and Food Chemistry, 55*(25), 10248-10257.

Donnelly, W. J., Fenelon M. A., Giblin L., & Stanton C. (2008). Obesity. The food research agenda. *International Journal of Dairy Technology*, *61*(1), 11-15.

Figuerola, F., Hurtado, M.L., Estevez, A.M., Asenjo, F. & Chiffelle, I. (2005). Fibre concentrates from apple pomace and citrus peel as potential fibre sources for food enrichment. *Food Chemistry, 91*, 395-401.

Harris, P.J. & Smith, B.G. (2006). Plant cell walls and cell-wall polysaccharides: structures, properties and uses in food products. *International Journal of Food Science and Technology, 41* (S2), 129-143.

Lata, B. & Tomala, K. (2007). Apple peel as a contributor to whole fruit quantity of potentially healthful bioactive compounds. Cultivar and year Implication. *Journal of Agricultural and Food Chemistry, 55*(23), 10795-10802.

Maga, J. A., & Kim, C. H. (1989). Co-Extrusion of rice flour with dried fruits and fruit juice concentrates. *Lebensmittel-Wissenschaft & Technologie, 22*(4), 182-187.

McKee, L.H. & Latner, T.A. (2000). Underutilized sources of dietary fiber: A review. *Plant Foods for Human Nutrition, 55,*285-304.

Nawirska, A. & Kwaśniewska, M. (2005). Dietary fibre fractions from fruit and vegetable processing waste. *Food Chemistry, 91*, 221-225.

Ozer, E. A., Herken E. N., Guzel S., Ainsworth P., & Ibanoglu S. (2006). Effect of extrusion process on the antioxidant activity and total phenolics in a nutritious snack food. *International Journal of Food Science and Technology, 41* (3), 289-93.

Parada, J., Aguilera, J.M. & Brennan, C. (2011). Effect of guar gum content on some physical and nutritional properties of extruded products. *Journal of Food Engineering*, *103*, 324-332.

Roberts, J.S., Gentry, T.S. & Bates, A.W. (2004). Utilization of dried apple pomace as a press aid to improve the quality of strawberry, raspberry and blueberry juices. *Journal of Food Science, 69*(4), 181-190.

Rowe, S., Alexander, N., Almeida, N., Black, R., Burns, R., Bush, L., Crawford, P., Keim, N., Kris-Etherton, P., & Weaver, C. (2011). Food science challenge: Translating the Dietary Guidelines for Americans to bring about real behavior change. *Journal of Food Science, 76*(1), R29-R37.

Slavin, J. L., Jacobs D., & Marquart, L. (2001). Grain processing and nutrition. *Critical Reviews in Biotechnology*, *21*(1), 49-66.

Stojceska, V., Ainsworth, P., Plunkett, A., Ibanoglu, E., & Ibanoglu, S. (2008). Cauliflower by-products as a new source of dietary fibre, antioxidants and proteins in cereal based ready-to-eat expanded. *Journal of Food Engineering, 87*(4), 554-563.

Stojceska, V., Ainsworth, P., Plunkett, A. &Ibanoglu, S. (2009). The effect of extrusion cooking using different water feed rates on the quality of ready-to-eat snacks made from food by-products. *Food Chemistry, 114*, 226-232.

Sudha, M. L., Baskaran, V., & Leelavathi, K. (2007). Apple pomace as a source of dietary fiber and polyphenols and its effect on the rheological characteristics and cake making. *Food Chemistry, 104*(2), 686-692.

Upadhyay, A., Sharma, H.K.& Sarkar, B.C. (2010). Optimization of carrot pomace powder incorporation on extruded product quality by response surface methodology. *Journal of Food Quality*, *33*, 350-369.

USDA, United States Dept. of Agriculture (USDA), Center for Nutrition Policy and Promotion. 2010. *Report of the Dietary Guidelines Advisory Committee on the Dietary Guidelines for Americans, 2010.* Washington, D.C.: USDA. Available from: http://www.cnpp.usda.gov/DGAs2010-DGACReport.htm. Accessed Jan 14, 2011.

WHO, World Health Association. (2003). *Diet, nutrition and the prevention of chronic diseases: report of a joint WHO/FAO expert consultation.* Geneva: WHO.

Yagci, S. & Gogus, F. (2008). Response surface methodology for evaluation of physical and functional properties of extruded snack foods developed from food-by-products. *Journal of Food Engineering, 86*(1), 122-132.

Yagci, S. & Gogus, F. (2010). Effect of incorporation of various food by-products on some nutritional properties of rice-based extruded foods. *Food Science and Technology International*, 15(6), 571-581.

Yanniotis, S., Petraki, A., & Soumpasi, E. (2007). Effect of pectin and wheat fibers on quality attributes of extruded cornstarch. *Journal of Food Engineering, 80*(2), 594-599.

Zarpe, I., Bes-Rastrollo, M., Ruiz-Canela, M., Sanchez-Villegas, A., Serrano-Martinez, M., & Martinez-Gonzalez, M. A. (2011). A brief assessment of eating habits and weight gain in a Mediterranean cohort. *British Journal of Nutrition,* 105, 765-775.

Figure
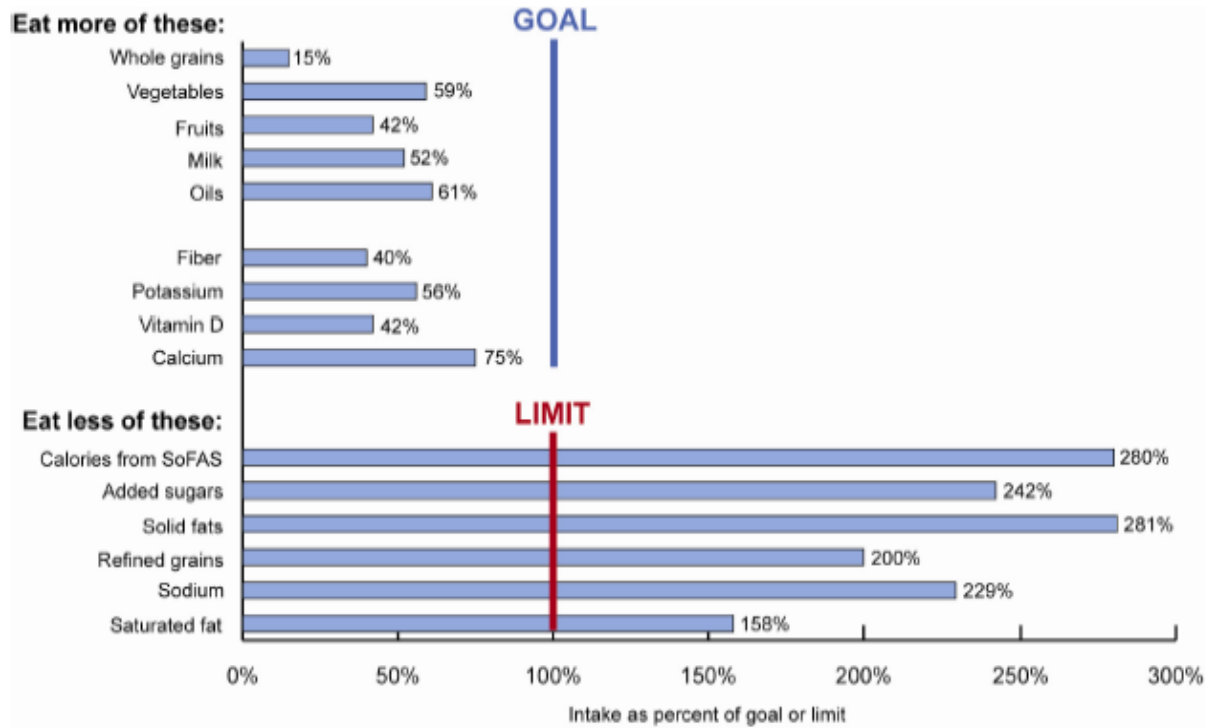
Note: Bars show average intakes for all individuals (ages 1 or 2 years or older) as a percent of the recommended intake level or limit. Recommended intakes for food groups and limits for refined grains, SoFAS, solid fats, and added sugars are based on the USDA 2000-calorie food patterns. Recommended intakes for fiber, potassium, vitamin D, and calcium are based on the highest AI for ages 14 to 70 years. Limits for sodium are based on the AI and for saturated fat on 7 percent of calories.

Data source: What We Eat in America, National Health and Nutrition Examination Survey (WWEIA, NHANES) 2001-2004 or 2005-2006.

Figure 1-1 Inadequacy of current average consumption. Source: USDA, 2010.

CHAPTER 2 - Expansion dynamics, cellular architecture and texture of directly expanded extrudates containing apple pomace

Abstract

Expanded cereal products can deliver significant amounts of fruit and vegetable fibers, however a major hurdle is the accompanying decrease in quality, mainly in terms of texture. Information on the cellular architecture of fiber-added extruded products is scarce. The objective of this work was to understand the relationship between macro and microstructural parameters and texture of high-fiber expanded products. A lab-scale twin screw extruder was used for processing directly expanded products based on corn flour and apple pomace (0-28%), resulting in a total dietary fiber (TDF) content of 1.1-22.5%. Processing moisture content (MC) was 17.5, 20 and 25% for each pomace level. Macro-structural properties (radial expansion, piece density, and specific length) were measured using standard methodology. Micro-structural analysis was conducted using X-ray microtomography to obtain cellular architecture parameters (void fraction, average cell wall thickness –CWT, and average cell size -CS). Average crushing force (F_{cr}), number of spatial ruptures (N_{sr}) and crispness work (W_c) were determined in compression. Addition of pomace decreased radial expansion, but increased specific length, thus piece density of the samples was not affected. CS (0.05-3.43 mm) and CWT (0.12-0.34 mm) were lower for treatments with pomace, while moisture affected only the CWT. CS was significantly correlated to F_{cr} (r=-0.69), W_c (r=-0.69), and N_{sr} (r=0.74), while CWT had no significant correlation with texture parameters. Apple pomace increased nucleation and favored axial expansion. The change in cell size and alignment explains the increased mechanical resistance. It can be inferred from the data that both moisture and apple pomace increase mechanical resistance of the matrix.

2.1. Introduction

The addition of fruits and vegetables to extruded snacks has been studied since the late 1980's. In one of the first published studies (Maga and Kim, 1989) the objective was to introduce flavor inside the extrudates, rather than as a coating. More recently the main motivation has shifted towards increasing the nutritional value of extruded products, as they lack significant amounts of nutrients other than available carbohydrates. Another current driver is the utilization of nutrient rich by-products from the fruit and vegetable processing industry (Stojceska et al., 2008). Researchers have studied the addition of fruit juice, paste, powders, pomace, peels, seeds, and trimmings into extruded products (Stojceska et al, 2010; Altan et al., 2008; Stojceska et al., 2008; Yagci and Gogus, 2008; Camire et al, 2007). While increase in dietary fiber and bioactive components is achieved, the texture of these expanded, foam-like products is adversely impacted (Altan et al., 2008; Yagci and Gogus, 2008). The texture is mainly dependent on the cellular architecture and the mechanical properties of the cell wall material (Agbisit et al, 2007; Babin et al., 2007; Gao and Tan, 1996). While the impact on macrostructure has been widely studied, the mechanism by which fruit and vegetable components (fiber, sugars, acids, etc) affect the microstructure is still poorly understood.

Techniques used to study the microstructure of expanded extrudates include scanning electron microscopy (Warburton et al., 1992), light microscopy (Chanvrier et al., 2007), digital imaging (Stojceska et al., 2008), and more recently X-ray microtomography (XMT). XMT provides a non-invasive means of accessing features such as cell size and cell wall thickness, along with their distributions, which is impossible with 2D imaging (Trater et al., 2005). XMT has been successfully used to analyze the internal structure of extruded samples comprising of starch only (Agbisit et al, 2007; Babin et al. 2007; Cheng et al., 2007), starch with proteins (Cho

and Rizvi, 2009; Cheng et al., 2007; Trater et al., 2005), wheat flour (Robin et al., 2010) and flours with guar gum (Parada et al., 2011). To the best of our knowledge, this technique has not yet been used to study the impact of fruit fibers on the cellular architecture of extrudates.

Apple pomace is a by-product of the apple processing industry and consists of peels and the core, which are dried and ground. The typical composition is 1.2-10.8% moisture, 0.5-1.9% ash, 2.4-7.3% protein, 1.6-4.5% fat, and 51.1-89.8% total dietary fiber (36.5-81.6% insoluble and 4.14-14.6% soluble) (Sudha et al., 2007; Figuerola et al., 2005; Chen et al., 1988). Apple pomace has high total phenolic content and antioxidant activity, which along with the high fiber content, is the main reason it has been extensively studied in the past few years as a potential food ingredient (Suarez et al., 2010; Garcia et al., 2009; Cetkovic et al., 2008; Lata and Tomala, 2007; Sudha et al., 2007).

The objective of this experiment was to understand the impact of apple pomace on the expansion dynamics and cellular architecture of corn-based extrudates. Furthermore, analysis of the microstructure in combination macro-level mechanical properties was used to gain unique insight into micro-level mechanical properties.

2.2. Materials and Methods

2.2.1 Materials and composition

Degermed yellow corn flour (Didion Milling, Cambria, WI) and dried non-sulfured apple pomace (Tree Top Inc., Selah, WA) were the two ingredients used in the study. The proximate

composition of the ingredients was determined using standard methods (AOAC, 2010). This included crude protein (based on nitrogen by combustion method; AOAC 990.03), crude fat (petroleum ether extract method; AOAC 920.39); ash (600°C for 2 h; AOAC 942.05); and starch (glucoamylase method; AOAC 920.40). Particle size of apple pomace was determined by laser diffraction (LS13320 Laser Diffraction PS Analyzer, Beckman Coulter, Brea, CA).

Soluble and insoluble fiber contents of the corn flour and apple pomace were determined using the Megazyme Total Dietary Fiber Assay Procedure (K-TDFR 06/07), which is based on AACC method 32-07 (AACC International, 2009). Briefly, the sample was hydrolyzed with α-amylase, protease and amyloglucosidase. The solution was filtered and the residue collected as the insoluble fiber portion. Soluble fiber in the filtrate was precipitated out with ethanol and collected by filtration. Soluble and insoluble fiber content was corrected for protein and ash in the residues, and the weight of a blank reagent run. Total dietary fiber content was obtained by the sum of the measured soluble and insoluble fractions. Dietary fiber composition was also characterized in terms of cellulose, hemicellulose, lignin and pectin. Cellulose, hemicellulose and lignin were analyzed using an ANKOM Fiber Analyzer (ANKOM Technology, Macedon, NY). An estimate of the pectin content of apple pomace was obtained from literature (11-22%; Gullon et al., 2007; Nawriska and Kwaśniewska, 2005).

Sugar content in apple pomace was determined by high performance liquid chromatography (HPLC; Agilent 1100), using a Phenomenex Rezex ROA organic acid column (130x7.8 mm, 8% H+ ; Phenomenex, CA). Sulfuric acid 0.005N was used as a mobile phase, and the flow rate was 0.6 ml/min at 60°C. Samples were prepared by dispersing one gram pomace in 20mL distilled water at 30°C and stirring with a magnetic stirrer for 15 min. The contents were centrifuged (15 min at 1000xg), and the supernatant diluted and filtered through 0.45 μm.

Results were expressed as combined content of sucrose, glucose and fructose per gram dry matter.

2.2.2 Blend preparation

Corn flour and apple pomace were combined to obtain ratios of 100:0, 83:17, 78:22 and 72:28 (corn flour: apple pomace). These ratios were referred to as 0, 17, 22 and 28% AP, respectively. The apple pomace levels were chosen with the aim to deliver 15, 20 and 25% of the recommended daily value for dietary fiber (25g) in a 30g serving. Each blend was adjusted to moisture levels (MC) of 17.5, 20 and 25% (wet basis or wb), resulting in a 4x3 factorial design with 12 treatments. The required amount of water was added and the material was mixed for 3 minutes on a bench-top mixer (N-50, The Hobart Mfg. Co., Troy, OH). The hydrated blends were placed in sealed plastic bags and allowed to equilibrate overnight under refrigeration. Moisture content of the hydrated blends was verified before extrusion using AOAC standard method 930.15 (2h at 135°C).

2.2.3 Phase transition analysis

The hydrated blends were analyzed on a Phase Transition Analyzer (PTA^{TM}, Wenger Mfg., Sabetha, KS), to determine the softening and flow temperatures (T_s and T_f, respectively). These are analogous to glass transition and melt temperatures, respectively, however unlike the latter they are a measure of deformation and flow behavior of the material under conditions representing extrusion to a certain extent (Liu et al., 2011; Bengoechea et al. 2007). A 2-g

sample was loaded in the chamber with a closed die underneath, and an initial compression of 10 MPa was applied for 15 seconds. The pressure was then fixed at 6MPa and the sample was heated at 10°C/min, with starting temperature of 7°C. T_s was obtained from the mid-point between onset and end of softening (identified by chamber displacement over the threshold of 0.0106 mm/°C). After the softening period the closed die was replaced by a 2 mm capillary die and heating was continued at the same rate and operating pressure. T_f was the temperature at which the material started to flow through the capillary (identified by a steep increase in displacement).

2.2.4 Water interactions

The hydration capacity (C_H) of corn flour and apple pomace was determined using an adaptation of the AACC method 56-20 (AACC International, 2009). The material was weighed (75 mg) into tared 1.5mL centrifuge tubes. Distilled water was added (1.5mL) and the tubes were vortexed to suspend the contents. The material was allowed to hydrate for 10 min, vortexing again after 5 and 10 min. The tubes were then centrifuged at 1,000xg for 15 minutes (Eppendorf centrifuge AG5424, rotor FA-45-24-11, Hamburg, Germany). The supernatant was removed using suction and the precipitate was weighed. C_H was expressed as grams of water absorbed per grams of dry matter. Hydration capacity of extrudates was determined following the same procedure after grinding and sieving to pass 0.42 mm.

Water activity (a_w) of the 12 hydrated blends was determined using a Decagon CX-2 (Pullman, WA) water activity meter. Duplicate measurements were taken for each blends. Water retention (WR_{120}) or the strength of water interactions at high temperatures for each blend was

assessed using the following procedure. A 2 g sample at 17.5% wb moisture content was weighed into a tared aluminum pan. The pans were placed in a convection oven at 120°C and allowed to dehydrate for 5 min. The pans were then weighed and returned to the oven for another 115 min for complete dehydration. The moisture loss at 5 min was calculated as a percentage of initial water in the sample, and then subtracted from 100 to obtain WR_{120}.

2.2.5 Extrusion

The equilibrated blends were extruded using a lab scale twin-screw extruder (Micro-18, American Leistritz Extruder Corp., Somerville, NJ) with a barrel diameter of 18mm and L/D ratio of 29.3. A circular cross-section die with diameter (d_d) of 3.1mm was used. The feed rate was 2.1 ± 0.2 kg/h and the extruder screw speed was set to 350 rpm for all treatments. The screw configuration and temperature profile are shown in Figure 2-1. Extrudates were collected in trays, cut manually and dried in a convection oven at 103°C for 10 minutes. Each blend was prepared and extruded in duplicate.

The specific mechanical energy (SME) for each treatment was calculated using the following relation:

$$SME\ (kJ/kg) = \frac{\frac{\tau - \tau_0}{100} \cdot \frac{N}{N_r} \cdot P_r}{\dot{m}} \tag{1}$$

where τ = % torque, τ_0 = % torque at no-load (17%), N = screw speed (rpm), N_r = rated screw speed (500 rpm), P_r = rated motor power (2.2 kW) and $\dot{m}$ = mass flow rate (kg/s).

2.2.6 Extrudate macrostructure

For each treatment, the length (l_e), diameter (d_e) and mass (m_e) of 20 extrudates were measured and used to obtain the radial expansion ratio (ER), specific length (l_{sp}) and piece density (ρ), as described below.

$$ER = \frac{d_e^{\,2}}{d_d^{\,2}} \tag{2}$$

$$l_{sp}\ (m/kg) = \frac{l_e}{m_e} \tag{3}$$

$$\rho\ (kg/m^3) = \frac{4m_e}{\pi \cdot d_e^2 \cdot l_e} \tag{4}$$

2.2.7 Extrudate microstructure

Microstructural features of the extrudates were analyzed using X-ray microtomography (XMT). One extrudate from each duplicate extrusion run was analyzed. To ensure that the samples were representative, the extrudates were selected based on a diameter matching the average diameter for that treatment. Samples were scanned on an XMT system (Model 1072, Skyscan, Belgium), under the following settings: voltage 40kV, current 248µA, exposure time 1.34 seconds, rotation step 1.35°, sample rotation 180° and magnification 24.6x. Shadow images were reconstructed into a 3D object (software NRecon v. 1.6.1, Skyscan, Belgium), which was virtually sliced into approximately 1,000 cross sections and analyzed (CTAn 1.9.1, Skyscan, Belgium). For analysis, a volume of interest (VOI) was determined by setting a region of interest tightly around the perimeter of each cross section. The VOI dataset was resized by 2 to reduce

the computational burden and reloaded for further processing. The grayscale images were converted into binary images with a threshold of 40 (cell walls converted to white pixels representing the object, and voids converted to black pixels). The despeckling function was applied to the VOI to reduce background noise from the image, and the final processed image was analyzed in 3D. Cell size was obtained from the structure separation function, and cell wall thickness from the structure thickness function. Void fraction was obtained from the ratio of white voxels (cell walls or solid material) to total voxels in the VOI.

2.2.8 Extrudate mechanical properties

Mechanical properties of the extrudates were analyzed using a texture analyzer (TA-XT2) and the Texture Exponent 32 software (both from Stable Micro Systems, Godalming, UK). Twenty extrudates from each treatment were equilibrated to a moisture of 8.0 ±0.5% (wb) using a humidity chamber (30% RH, 94 h). Samples were compressed perpendicular to the direction of extrusion to 80% of their original diameter, using a 38 mm compression plate at a test speed of 2.0 mm/s. The area under the curve (S, mm^2) and the number of peaks (n) greater than 1.5 N were obtained from the force-deformation curves and used to calculate the spatial frequency of ruptures (N_{sr}), average crushing force (F_{cr}) and crispness work (W_c) (Bouvier et al., 1997; Agbisit et al., 2007).

$$N_{sr} \ (mm^{-1}) = \frac{n}{d} \tag{5}$$

$$F_{cr} \ (N) = \frac{S}{d} \tag{6}$$

$$W_c \ (N.mm) = \frac{F_{cr}}{N_{sr}} \qquad\qquad (7)$$

where d = probe travel distance (mm).

2.2.9 Statistical analysis

The experimental design was a 4x3 full factorial with apple pomace (4 levels) and moisture content (3 levels) as the two variables. The mixed procedure (SAS 9.2, SAS Institute Inc., Cary, NC) was used to perform analysis of variance, with the 2 duplicates as random blocks. Differences between treatments were determined using the least square means method (α=0.05). Selected parameters were also analyzed using Pearson's correlation (Excel 2003, Microsoft Corp, Redmond, WA). Significance at 95% confidence was established by $|r| \geq 0.4$ (non-directional, 24 observations) (Lowry, 2010).

2.3. Results and Discussion

2.3.1 Composition of corn flour - apple pomace blends

The proximate composition of apple pomace and corn flour is given in Table 2-1, based on which the calculated composition of their blends is also provided. The composition of apple pomace was within the previously reported range mentioned earlier. The only exception was fat, which was higher (5.4%). It was obvious that the substitution of apple pomace for corn flour would have a large impact on fiber and starch content. The calculated blend compositions predict

30% reduction in starch and almost 9-fold increase in fiber, as pomace level increased from 0 to 28%. The corresponding increase in fat was 2.6 times, although the highest fat content of 2.3% is still not high enough to expect a notable impact on processing or final product characteristics. The fat in apple pomace is mainly contributed by the seeds, which contain 95% triacylglycerols (Nguyen et al., 1984). Although low levels of free fatty acids (less than 1%) have been shown to form inclusion complexes with amylose during extrusion, complexation with triacylglycerols is not as extensive (Desrumaux et al., 1999; Singh et al., 1998; Bhatnagar and Hanna, 1994).

2.3.2 Water interactions

Water activity of hydrated blends (0.779-0.960) was impacted by both moisture content (MC) and apple pomace level (AP), with a significant interaction between the two variables ($p<0.0001$; Table 2-2). As expected a_w increased with MC, however the highest increase was observed in the absence of pomace (0% AP). The trends with respect to AP were also interesting. Under low moisture conditions (MC $\leq$ 20%), a_w generally decreased as AP decreased and the lowest a_w was found at 0% AP. It appears that the starch in corn flour binds water more tightly than apple pomace when moisture is limited ($\leq$ 20% wb), although pomace also has hydrophilic components. The binding of water by starch is mainly at the molecular level via hydrogen bonding. In a compilation of several literature values, Rahman (1995) cited corn flour as having a GAB monolayer value of 0.083 kg water/kg solids. The values for cellulose and pectin, which account for approximately 40% of the dry weight of pomace, are 0.045 and 0.049 kg water/kg solids, respectively. Stronger water binding by starch is also supported by its supramolecular structure. Water is part of the crystalline structure of starch, and the A-type crystals found in corn

starch contain 4 water molecules for every unit cell, which accounts for 7% of the crystal weight (Popov et al., 2009). On the other hand, cellulose crystals do not contain water (Slade and Levine, 1991).

Contrary to the above observations, the highest water activity at 25% MC was found at 0% AP and the addition of apple pomace led to a progressive decrease in a_w. This suggested the predominance of another mechanism for water binding under 'excess' moisture conditions, which involved apple pomace and possibly capillary action. Although these macroscopic scale interactions are weaker than hydrogen bonding, they can bind a much larger amount of moisture to the substrate. This was evident from data for water retention at 120^oC (WR_{120}) and the observations for hydration capacity (C_H) discussed below.

WR_{120} of 17.5% MC blends was lower in the presence of apple pomace and 0% AP had the highest water retention of 20.3% (Table 2-2). This was consistent with a_w data at room temperature, and indicated that even at a temperature close to that encountered during the extrusion process apple pomace was less hydrophilic than corn flour. This observation has implications with regard to extrudate expansion and the role of vapor pressure, which is the primary driving force. It was clear that apple pomace does not hinder expansion by restricting the release of water vapor. This contradicts the hypotheses extended previously for high fiber extrudates, including by our lab group for oat flour – Moringa leaf based expanded extrudates (Liu et al., 2010). Thus water interactions appear to be specific to the fibrous substrate, and a generalization should be avoided.

C_H for corn flour was 1.84 g/g, while that for apple pomace was observed to be 5.51 g/g. This indicated that pomace could absorb almost 3 times more water than corn flour. Based on these data, the calculated C_H for blends ranged from 1.84-2.87 g/g. In comparison C_H of

extrudates ranged from 4.98-6.89 g/g, and was significantly affected by blend moisture but not the level of apple pomace (Figure 2-2). It is apparent that extrusion processing led to a substantial increase in the hydration capacity of both corn flour and apple pomace. C_H of flour increased due to disruption of the compact supramolecular granule structure of starch and gelatinization during extrusion (Yagci and Gogus, 2008; Chang et al., 1998; Artz et al., 1990; Zhu et al., 2010). Differential scanning calorimetry (DSC) results for all treatments indicated complete gelatinization after extrusion (data not shown), although presence of some ungelatinized granules cannot be ruled out if other detection methods such as scanning electron microscopy, polarized light microscopy and X-ray diffraction are employed (Mahasukhonthachat et al., 2010; Altan et al, 2009; Chanvrier et al., 2007). The lignocellulosic structure of apple pomace was also probably disrupted due to thermo-mechanical action (Yoo et al., 2011), leading to greater hydration capacity. At 17.5% and 20% MC apple pomace and corn flour had similar C_H, leading to the lack of a significant effect of apple pomace. At 25% MC, apple pomace structure was not substantially degraded, probably due to milder thermo-mechanical conditions associated with higher in-barrel moisture. Thus hydration capacity at 25% MC was lower, and substitution of starch with pomace led to further reduction in C_H. This effect has also been described by other studies on extrudates with fruit residues (Yagci and Gogus, 2008; Altan et al., 2008).

2.3.3 Phase transition analysis

Phase transition analysis data of corn flour – apple pomace blends are shown in Table 2-3. The softening temperature (T_s) of biopolymers has been shown to be analogous to glass

transition temperature (T_g) obtained using thermal transition data or dynamic rheometry (Bengoechea et al. 2007). At temperatures above T_s the material can be considered to be in the rubbery state and can be compacted under pressure. T_s for blends ranged from 44.4-82.7°C. The lowest values were found at 25%MC and at this moisture level pomace addition had no effect. At low moisture contents (17.5 and 20%MC) addition of apple pomace suppressed the T_s . In corn flour, the amorphous portion of starch is the main fraction that undergoes glass transition, at a T_g of approximately 71.5-91°C in the moisture range of 10 to 55% (Athawale and Lele, 2000; Levine and Slade, 1988).It is likely that compaction was also related to the plasticization of this portion in the corn flour-apple pomace blends, since cell wall materials from fruit and vegetables do not have a detectable T_g in this temperature range (Aguilera et al., 1998). The suppression of the T_s in the presence of pomace can be explained by the reduction in starch content, with higher water availability for the remaining starch. The presence of low molecular weight components such as sugars (2.3% in pomace) may further reduce the T_s. Lower T_s value with increase in moisture is expected due to reduction in the glass transition temperature, and has been reported by other authors (Bengoechea et al. 2007; Liu et al, 2010).

The flow temperature (T_f) represents the temperature at which the blend is plasticized enough that it flows through a capillary. While increase in moisture significantly decreased T_f due to reduction in viscosity, the effect of apple pomace was not significant (p=0.307). The T_f is related to shear viscosity and resistance to flow (Liu et al., 2010). Reduction in starch content with the addition of apple pomace limited viscosity development in the melt. This would reduce the T_f however it was balanced by the presence of cell wall components of apple pomace that do not melt and thus hinder deformation and flow. The net effect was non-significant change in T_f with pomace addition.

2.3.4 Extrusion Processing

Fluctuations in the motor load caused significant variations in the specific mechanical energy or SME (coefficient of variation 19-66%). The average values are shown in Figure 2-3. The flow temperature (T_f) can be a reasonably good predictor for SME, as both are related to viscosity and resistance to flow. Thus higher MC led to a significant decrease in SME, which is similar to the observation for T_f. On the other hand, apple pomace did not have a significant effect on SME (p=0.246), which was also the case for T_f. However, there was a general trend of decrease in SME with pomace level. This was probably due to limitations of feed delivery to the extrusion system, which is based on volumetric control via the feeder screw speed. Higher level of pomace facilitated better flow and higher throughput, thus reducing the SME although not significantly.

2.3.5 Extrudate macrostructure

Variations in apple pomace and moisture content caused a significant impact on the expansion pattern of the extrudates (Figure 2-4). The treatments with no apple pomace had the highest expansion ratio at all moisture contents, and increase in moisture caused significant reduction in radial expansion for all treatments.

Although apple pomace caused radial expansion to decrease by half compared to corn flour alone, at the same time it caused increase in specific length (an indicator of longitudinal expansion). It is interesting to note that piece density was not affected by apple pomace (p=0.086), which implies that the longitudinal expansion compensated for decreased radial

expansion. This is supported by the results for void fraction, which indicate no change in relative volume of the air cells with pomace addition (discussed below). Other authors have also reported that fruit materials rich in pectin and isolated pectin have negatively affected radial expansion but not the density of extrudates (Yagci and Gogus, 2008; Yanniotis et al., 2007). These authors suggest that pectin increases the extensibility of the starch matrix. The pectin content used in these works is within the range of pectin that is present in the corn flour-apple pomace blends (1.9-6.2%, based on reported values of 11 to 22% pectin in apple pomace; Gullon et al., 2007; Nawriska and Kwaśniewska, 2005).

Expanded structures formed by extrusion depend on the balance between vapor pressure inside the bubbles, resistance of the bubble cell walls during vapor flash off and collapse of the structure after expansion. Collapse is mainly caused by low viscosity (which can explain the decreased expansion as moisture content increased), while the extensibility of the matrix can be affected by the fibers in apple pomace. The type of fiber appears to play a role in hindering or enhancing the extensibility of the starch matrix in a particular direction. Cellulose and lignin are mainly insoluble and cellulose has a highly ordered linear structure with crystalline regions. These molecules align in the direction of flow in the extruder, providing resistance to radial expansion and enhancing longitudinal expansion (Moraru and Kokini, 2003). Pectin and hemicellulose are mainly soluble and are branched polymers, thus they are more compatible with the gelatinized starch matrix as compared with cellulose and lignin (Pai et al., 2009). Thus, pectin and hemicelluloses are able to entangle with starch and make part of the expanding matrix. In the apple pomace system both effects are in action, cellulose and lignin promoted resistance to radial expansion, but pectin and hemicellulose imparted extensibility, thus the high longitudinal expansion.

The detrimental effect of fibers in expansion has also been attributed to binding of water, thus reducing the free water available for expansion (Moraru and Kokini, 2003; Jin et al., 1994; Camire and King, 1991). The macrostructure results combined with evidence from the water binding experiments suggest that competition for water is not a relevant mechanism in these systems. The components in corn flour held on to water more aggressively than apple pomace in both the raw and processed blends, and increase in available water did not favor expansion.

Another factor that plays a role in defining the macrostructure is the dilution of starch content in the matrix as the pomace level increases (Altan et al, 2008; Chinnaswamy and Hanna, 1991), reducing the amount of extensible polymers in the bubble cell walls. Dilution of starch explains why better expansion was found with lower levels of pomace (at 17.5% MC). At higher moisture content, not only is there further dilution of starch content by the addition of water, but it also appears that the decrease in viscosity and collapse became more predominant, thus there was no significant difference among fiber levels.

The expansion pattern is consistent with the SME results, as verified by the significant correlations of SME with expansion ratio (r=0.600) and piece density (r=-0.505) (Table 2-4). Increase in moisture content reduces viscosity, lowering the SME. This translates into reduced friction and heat generation, thus lowering both the driving force for expansion and the film forming capacity of the starch matrix. The result in the final product is lower expansion and increased density. Apple pomace also lowered SME, but it is clear that the components (probably pectin) have some degree of film forming capacity, as the density was unchanged upon the addition of pomace.

2.3.6 Extrudate microstructure

A representative XMT image of each treatment in radial and longitudinal sections is given in Figure 2-5. The cell walls are represented in black and the void areas in white, for clarity. Pomace particles are not visible at this scale. The images clearly show that both apple pomace and moisture created great differences in cellular structure. Apple pomace caused the air cells to assume a less radial orientation compared to the treatments with no pomace. This agrees with the argument that fibers might align in the direction of the flow and provide resistance to radial expansion (Moraru and Kokini, 2003). At 0% pomace anisotropic expansion is evident, with a favored radial orientation of the cells. Structural anisotropy has also been reported by Robin et al. (2010) for wheat flour extrudates. Their work was done with no fiber addition and the findings agree with the treatments that were processed without apple pomace.

Despite the lower figures at 28% pomace, the effect of pomace on void fraction (VF) was not significant (Figure 2-6). This agrees with the results of the macrostructure analysis, which indicated no effect of pomace level on piece density. Both VF and piece density are measures of the total volumetric expansion, the former at a microscopic level and the latter at a macroscopic level. The agreement between both measures is therefore expected.

Increase in processing moisture content resulted in more compact structures, with reduced VF. This result is consistent with the macrostructure analysis, which revealed significant effect of moisture in decreasing expansion (radial and longitudinal) and increasing density. The lower T_f at high moisture is an indication of reduced viscosity of these matrices, which were unable to hold the expanded structure and collapsed into compact architectures.

Average cell size (CS) decreased with the addition of apple pomace (Figure 2-6). Despite no statistical difference between 17, 22 and 28% pomace, 28% had the smallest cells. The

volume distribution (exemplified for samples at17.5% moisture - Figure 7) revealed the heterogeneity in CS, which ranged from 0.05 to 3.43 mm. The treatments with apple pomace had a narrower CS distribution, concentrating in the region under 1 mm. The largest cells were found for 0% pomace and measured 3.43 mm. This is almost twice the size of the maximum CS in the treatments with apple pomace (1.87 mm). Apple pomace clearly limited cell growth, probably by interfering with extensibility of the matrix.

Unlike apple pomace, the effect of moisture on CS was not significant. The average values (Figure 2-6) suggest a decrease in CS as moisture increased for 0% pomace, which is also supported by the cumulative distribution curves (Figure 2-8). In fact, at all pomace levels there was a trend towards reduced cell size as moisture content increased.

Although it was not possible to quantify the number of cells, visual examination of the cross sections clearly showed a larger number of smaller cells for the treatments with pomace (Figure 2-5). The visual examination is supported by the cumulative distribution curves of CS (Figure 2-8). For the treatments with pomace, 50% of the cellular volume is comprised of cells between 0.27 and 0.49 mm, while at 0% pomace the 50th percentile falls between 0.71 and 0.94 mm. In starch extrudates entrapped air is considered to be the main nucleation site (Moraru and Kokini, 2003). However, fiber particles are also well recognized nucleation agents (Lue et al., 1991). Using light microscopy, Chanvrier et al. (2007) showed that small cells were located next to bran particles, suggesting this to be a place of weak adhesion within the matrix, thus favoring the formation of nuclei. It is likely that in the treatments with pomace, the fibers played a role in providing discontinuities in the matrix, increasing number of cells. At the same time substitution of pomace for starch creates a less extensible matrix and the nuclei do not expand into large cells. The result is a larger number of small cells.

28

Average cell wall thickness (CWT) was the highest for the treatments with no pomace, ranging from 0.18 to 0.34 mm (Figure 2-6). With the addition of apple pomace the CWT decreased to a range of 0.12 to 0.22 mm, with no difference between 17, 22 or 28% pomace. Given the lack of effect of apple pomace on void fraction, it is logical to expect that a decrease in CS must be accompanied by decrease in CWT, as was the case. Thicker cell walls were found for the treatments processed at 25%MC, compared to 17.5 and 20%MC (Figure 2-6), which is consistent with the increase in density and decrease in void fraction resulting from structure collapse.

There is little quantitative information or discussion on CWT of extrudates with added fruit and vegetable materials. The determination of CWT is difficult using traditional imaging techniques, such as scanning electron microscopy (Trater et al., 2005) Using digital photography and an imaging software, Stojceska et al. (2008) reported CWT values between 0.3 and 0.5 mm for a wheat-based extrudate with up to 33% vegetable powder addition (consisting of cauliflower, onion, tomato and carrot powders). Although the range is higher than in the present study, the authors also found decrease in CWT as the level of vegetable powder increased.

An increase in CWT as CS increases has been reported for starch-based extrudates. Trater et al. (2005) found a positive correlation between these parameters (r=0.56), for corn starch with added whey protein concentrate. The authors discuss that as the cells expand, they coalesce and the walls merge, resulting in fewer cells with thicker walls. Babin et al. (2007) also found a positive correlation between CS and CWT (r=0.82) when analyzing extrudates within the same density range (corn starches with no added ingredients). The authors found that the finest structures (low CS and CWT) were found at high moisture. From the earlier discussion on the effect of fiber on nucleation, it may be that the availability of nucleation sites is one of the

underlying mechanisms of the effect of fiber on decreasing CS and CWT. In the presence of pomace more nucleation sites are available, increasing the number of cells. Reduced matrix extensibility limits cell growth, so cells do not coalesce into larger ones. The resulting structure is formed by a high number of small cells with thin walls. With no pomace addition cells readily expand and merge to form large cells with thick walls. Both final structures had a similar ratio of void volume to total volume, thus same volumetric expansion with strikingly different microstructure.

CWT in combination with particle size can provide some indication on the expansion dynamics. The average particle size of apple pomace was 0.35mm, which is larger than the average CWT (0.12-0.22 mm). Therefore, the particles cannot be contained inside the walls and probably pierced the cells as they expanded (Moraru and Kokini, 2003). The soluble components (pectin and hemicellulose) may leach out of the structure of apple pomace during extrusion, and as mentioned in 3.3.2, these components can entangle with starch and help form the expanding matrix.

2.3.7 Mechanical properties

The average crushing force (F_{cr}) was greatly increased in the presence of apple pomace (Figure 2-9). Such increase can be due to cellular structure, as well as resistance of the solid matrix. Smaller cells and thicker walls are usually the structural cause for increased crushing force, but composition of the matrix can affect the strength of the cell walls at levels that exceed the effect of structure (Barret and Peleg, 1992). The addition of apple pomace had a significant effect on the spatial frequency of ruptures (Nsr), causing a decrease in the number of peaks.

Crispness work (W_c) was increased by the addition of apple pomace, reflecting the increase in energy per crushing peak.

The effect of moisture content was only significant for F_{cr}. Since the samples were equilibrated before mechanical testing, the difference in F_{cr} corresponds to different cell structures created during expansion/collapse, and/or different degrees of transformation of the matrix.

F_{cr} had a high negative correlation with expansion ratio (r=-0.805, Table 2-4). This relationship has been reported for starch extrudates, as larger cells generate a weaker structure (Agbisit et al., 2007; Barret and Peleg, 1992). N_{sr} had a significant negative correlation (r=-0.596) with specific length. This is an indication that the alignment of the air cells with respect to the direction of deformation plays a role in the breaking pattern, as discussed below (3.3.5).

2.3.8 Texture-structure relationships

As mentioned, the direction of expansion, and resulting shape of the air cells, plays an important role in defining texture. The samples with apple pomace showed a more isotropic expansion, with less elongation in the radial direction. Furthermore, CS decreased, thus the length of the walls in the radial direction was decreased compared to 0% pomace (see Figure 2-5). Shorter walls provide resistance (Barret and Peleg, 1992; Trater et al. 2005), thus higher force is required to compress the specimen (schematically shown in Figure 2-10). Conversely, longer walls in the radial direction provide less resistance and the fracture of each one can be recorded under compression, giving more fracture peaks over the same travel distance. This is supported by the significant positive correlation between N_{sr} and expansion ratio (r=0.721). In the structure with short cell walls, each fracture peak would represent the fracture of a group of cells, resulting

31

in lower N_{sr}. This reasoning has been accepted by other authors, including Cho and Rizvi (2009), who support that each peak in the force-distance curve can represent failure of a mass of cells at a time, or breaking of the sample in large pieces. Agbisit et al. (2007) reported reduced N_{sr} for samples with smaller CS and explain that the crushing of several small cells at once is responsible for the increase in magnitude of each crushing peak. This reasoning is also consistent with the higher values of W_c.

Not only is the average CS important in defining mechanical resistance, but also the CS distribution. Babin et al. (2007) have found that greater dispersion in CS caused decrease in mechanical resistance of starch extrudates. The present results also follow this trend, with 0% AP showing lowest F_{cr} and broader CS distribution curves compared to the treatments with pomace.

While increase in F_{cr} is expected with higher CWT, the correlation between these parameters was low and non-significant (r=0.261). Since increase in CWT was accompanied by increase in CS, the latter contributed more in weakening the structure, overcoming any reinforcement caused by thicker walls. The prevalent effect of CS is supported by the significant negative correlation between F_{cr} and CS (r=-0.692).

Plotting F_{cr} as a function of CS some insight can be gained on the mechanical resistance of the matrix itself (Figure 2-11). Within the CS range of 0.3-0.4 mm, the F_{cr} varied as much as 80%. While the level of apple pomace did not follow any consistent trend in this range, the F_{cr} increased along with moisture content. Since CWT did not explain F_{cr}, and F_{cr} can vary within the same CS range, it is clear that higher moisture causes changes that increase the mechanical resistance of the cell walls, independent of cellular architecture. It is likely that increase in moisture promoted greater plasticization (reflected in lower SME and T_f), which reduced the degree of starch depolymerization compared to the lower moisture treatments. Starch

depolymerization is a well known reason for decreased mechanical resistance of extruded products (Robin et al., 2010; Carvalho and Mitchell, 2000; Barret and Peleg, 1992).

The data (Figure 2-11) also supports that apple pomace reinforces the matrix. At 25% MC, each increase in pomace level (0-17-22) caused a 30N increase in F_{cr}, without change in CS. Although the increase in pomace caused lowering of the SME (400.4, 364.5, and 336.3 kJ/kg, respectively), the range is close and the magnitude is not consistent with the increase in F_{cr}. At 20% MC this pattern appears again, with F_{cr} 28>22>17%AP within a CS of 0.37-0.38 mm. The effect of apple pomace on reinforcing the mechanical properties of the matrix might be due to a decrease in starch depolymerization, as discussed above.

2.4. Conclusion

Variations in apple pomace and processing moisture content caused great impact on the texture, macro-, and microstructure of corn-based extrudates. The effect of pomace can be attributed mainly to increased nucleation and shifting the expansion direction to a less radial orientation. While the piece density was not impacted, these effects resulted in smaller, more numerous cells, which were more elongated, thus forming a structure with increased mechanical resistance. It is also suggested that apple pomace reinforces the cell walls independent of cellular architecture. This same effect was found for increase in moisture, possibly by reduction of SME, which limits starch depolymerization. XMT has shown to be a valuable tool in accessing structure/texture relationships in extrudates with apple pomace and its use should be expanded to other fiber-rich extruded products.

References

AACC International. (2009). Approved Methods of Analysis. (11th ed.). St Paul, MN: AACC International Press.

Agbisit, R., Alavi, S., Cheng, E. Z., Herald, T., & Trater, A. (2007). Relationships between microstructure and mechanical properties of cellular cornstarch extrudates. *Journal of Texture Studies, 38*(2), 199-219.

Aguilera, J. M., Cuadros, T. R., & del Valle, J. M. (1998). Differential scanning calorimetry of low-moisture apple products. *Carbohydrate Polymers, 37*(1), 79-86.

Altan, A., McCarthy, K. L., & Maskan, M. (2008). Twin-screw extrusion of barley-grape pomace blends: Extrudate characteristics and determination of optimum processing conditions. *Journal of Food Engineering, 89*(1), 24-32.

Altan, A., McCarthy, K. L., & Maskan, M. (2009). Effect of extrusion cooking of functional properties and in vitro starch digestibility of barley-based extrudates from fruit and vegetable by-products. *Journal of Food Science, 74*(2), E77-E86.

AOAC 2010. *Official Methods of Analysis.* (18th ed., Revision 3). Washington, DC: Association of Official Analytical Chemists.

Artz, W. E., Warren, C., & Villota, R. (1990). Twin-Screw Extrusion Modification of a Corn Fiber and Corn Starch Extruded Blend. *Journal of Food Science, 55*(3), 746-754.

Athawale, V. D., & Lele, V. (2000). Thermal studies on granular maize starch and its graft copolymers with vinyl monomers. *Starch-Starke, 52*(6-7), 205-213.

Babin, P., Della Valle, G., Dendievel, R., Lourdin, D., & Salvo, L. (2007). X-ray tomography study of the cellular structure of extruded starches and its relations with expansion phenomenon and foam mechanical properties. *Carbohydrate Polymers, 68*(2), 329-340.

Badrie, N., & Mellowes, W. A. (1992). Cassava starch or amylose effects on characteristics of cassava (Manihot-esculenta Crantz) extrudate. *Journal of Food Science, 57*(1), 103-107.

Barrett, A. H., & Peleg, M. (1992). Extrudate Cell Structure-Texture Relationships. *Journal of Food Science, 57*(5), 1253-1257.

Bengoechea, C., Arrachid, A., Guerrero, A., Hill, S. E., & Mitchell, J. R. (2007). Relationship between the glass transition temperature and the melt flow behavior for gluten, casein and soya. *Journal of cereal science, 45*(3), 275-284.

Bhatnagar, S. & Hanna, M.A. (1994). Amylose-lipid complex formation during single-screw extrusion of various corn starches. *Cereal Chemistry, 71*(6), 582-587.

Bouvier, J. M., Bonneville, R., & Goullieux, A. (1997). Instrumental methods for the measurement of extrudate crispness. *Agro Food Industry Hi-Tech, 8*(1), 16-19.

Camire, M. E., Dougherty, M. P., & Briggs, J. L. (2007). Functionality of fruit powders in extruded corn breakfast cereals. *Food Chemistry, 101*(2), 765-770.

Camire, M.E. & Clay King, C. (1991). Protein and fiber supplementation effects on extruded cornmeal snack quality. *Journal of Food Science 56*(3), 760-768.

Carvalho, C. W. P., & Mitchell, J. R. (2000). Effect of sugar on the extrusion of maize grits and wheat flour. *International Journal of Food Science and Technology, 35*(6), 569-576.

Cetkovic, G., Canadanovic-Brunet, J., Djilas, S., Savatovic, S., Mandic, A., & Tumbas, V. (2008). Assessment of polyphenolic content and in vitro antiradical characteristics of apple pomace. *Food Chemistry, 109*(2), 340-347.

Chang, Y.K.; Silva, M.R.; Gutoski, L.C.; Sebio, L. & Da Silva, MAAP. (1998) Development of extruded snacks using jatoba (Hymenaea stigonocarpa Mart) flour and cassava starch blends. *Journal of the Science of Food and Agriculture, 78*(1), 59-66.

Chanvrier, H., Appelqvist, I. A. M., Bird, A. R., Gilbertt, E., Htoon, A., Li, Z., Lillford, P. J., Lopez-Rubio, A., Morell, M. K., & Topping, D. L. (2007). Processing of novel elevated amylose wheats: Functional properties and starch digestibility of extruded products. *Journal of Agricultural and Food Chemistry, 55*(25), 10248-10257.

Chen, H., Rubenthaler, G. L., Leung, H. K., & Baranowski, J. D. (1988). Chemical, Physical, and Baking Properties of Apple Fiber Compared with Wheat and Oat Bran. *Cereal Chemistry, 65*(3), 244-247.

Chinnaswamy, R. & Hanna, M.A. (1991). Physicochemical and macromolecular properties of starch-cellulose fiber extrudates. *Food Structure, 10*, 229-239.

Cho, K. Y., & Rizvi, S. S. H. (2009). 3D Microstructure of supercritical fluid extrudates. II: cell anisotropy and the mechanical properties. *Food Research International, 42*(5/6), 603-611.

Desrumaux, A., Bouvier, J. M., & Burri, J. (1999). Effect of free fatty acids addition on corn grits extrusion cooking. *Cereal Chemistry, 76*(5), 699-704.

Figuerola, F., Hurtado, M.L., Estevez, A.M., Asenjo, F. & Chiffelle, I. (2005). Fibre concentrates from apple pomace and citrus peel as potential fibre sources for food enrichment. *Food Chemistry, 91*, 395-401.

Gao, X. & Tan, J. (1996). Analysis of expanded-food texture by image processing. Part II: mechanical properties. *Journal of Food Process Engineering, 19,* 445-456.

Gullón, B., Falaqué, E., Alonso, J.L. & Parajó, J.C. (2007). Evaluation of apple pomace as a raw material for alternative applications in food industries. *Food Technology and Biotechnology, 45*(4), 426-433.

Jin, Z., Hsieh, F. & Huff, H.E. (1994). Extrusion cooking of corn meal with soy fiber, salt and sugar. *Cereal Chemistry, 71*(3), 227-234.

Kim, J. H., Tanhehco, E. J., & Ng, P. K. W. (2006). Effect of extrusion conditions on resistant starch formation from pastry wheat flour. *Food Chemistry, 99*(4), 718-723.

Liu, S., Alavi, S., & Abu-Ghoush, M. (2010). Extruded moringa leaf – oat flour snacks: Physical, nutritional and sensory properties. *International Journal of Food Properties*. doi: 10.1080/10942910903456358.

Lue, S., Hsieh, F., & Huff, H. E. (1991). Extrusion Cooking of Corn Meal and Sugar-Beet Fiber - Effects on Expansion Properties, Starch Gelatinization, and Dietary Fiber Content. *Cereal Chemistry, 68*(3), 227-234.

Maga, J. A., & Kim, C. H. (1989). Co-Extrusion of Rice Flour with Dried Fruits and Fruit Juice Concentrates. *Lebensmittel-Wissenschaft & Technologie, 22*(4), 182-187.

Mahasukhonthachat, K., Sopade, P.A. & Gidley, M.J. (2010). Kinetics of starch digestion and functional properties of twin-screw extruded sorghum. *Journal of Cereal Science, (51),* 392-401.

Moraru CI, & Kokini JL (2003). Nucleation and expansion during extrusion and microwave heating of cereal foods. *Comprehensive Reviews in Food Science and Food Safety, 2*(4), 2 (4) 120-138.

Nawirska, A. & Kwaśniewska, M. (2005). Dietary fibre fractions from fruit and vegetable processing waste. *Food Chemistry, 91*, 221-225.

Nguyen, X.V., Come, D., Lewark, St. & Mazlik, P. (1984). Dormancy breaking and frost-resistance induction in apple embryos as related to changes in reserve and polar lipids. *Physiologia Plantarum, 62*(4), 566-570.

Pai, D.A., Blake, O.A., Hamaker, B.R., Campanella, O.H. (2009). Importance of extensional rheological properties of fiber-enriched corn extrudates. *Journal of Cereal Science*, *50*, 227-234.

Parada, J., Aguilera, J.M., Brennan, C. (2011). Effect of guar gum content on some physical and nutritional properties of extruded products. *Journal of Food Engineering*, *103*, 324-332.

Popov, D., Buléon, A., Burghammer, M., Chanzy, H., Montesant, N., Putaux, J.-L., Potocki-Véronèse, G. & Riekel, C. (2009). Crystal structure of A-amylose : a revisit from synchrontron microdiffraction analysis of single crystals. *Macromoluceluees, 42,* 1167-1174.

Rahman, S. (1995). *Food properties handbook*. Boca Raton: CRC Press, (Chapter 1).

Robin, F., Engmann, J., Pineau, N., Chanvrier, H., Bovet, N., & Della Valle, G. (2010). Extrusion, structure and mechanical properties of complex starchy foams. *Journal of Food Engineering, 98*(1), 19-27.

Slade, L., & Levine, H. (1988). Non-Equilibrium Melting of Native Granular Starch .1. Temperature Location of the Glass-Transition Associated with Gelatinization of A-Type Cereal Starches. *Carbohydrate Polymers, 8*(3), 183-208.

Slade, L & Levine, H. (1991). A food polymer science approach to structure-property relationships in aqueous food systems: non-equilibrium behavior of carbohydrate-water systems. In Levine, H. & Slade, L. (Eds.),*Water relationships in food: advances in the 1980s and trends for the 1990s* (pp.29-101). New York: Plenum Press.

Stojceska, V., Ainsworth, P., Plunkett, A., Ibanoglu, E., & Ibanoglu, S. (2008). Cauliflower by-products as a new source of dietary fibre, antioxidants and proteins in cereal based ready-to-eat expanded. *Journal of Food Engineering, 87*(4), 554-563.

Stojceska, V., Ainsworth, P., Plunkett, A. & Ibanoglu, S. (2009). The effect of extrusion cooking using different water feed rates on the quality of ready-to-eat snacks made from food by-products. *Food Chemistry, 114*, 226-232.

Stojceska, V., Ainsworth, P., Plunkett, A., & Ibanoglu, S. (2010). The advantage of using extrusion processing for increasing dietary fibre level in gluten-free products. *Food Chemistry, 121*(1), 156-164.

Suarez, B., Alvarez, A.L., Garcia, Y.D., del Barrio, G., Lobo, A.P., & Parra, F. (2010). Phenolic profiles, antioxidant activity and in vitro antiviral properties of apple pomace. *Food Chemistry*, *120*, 339-342.

Sudha, M. L., Baskaran, V., & Leelavathi, K. (2007). Apple pomace as a source of dietary fiber and polyphenols and its effect on the rheological characteristics and cake making. *Food Chemistry, 104*(2), 686-692.

Trater, A. M., Alavi, S., & Rizvi, S. S. H. (2005). Use of non-invasive X-ray microtomography for characterizing microstructure of extruded biopolymer foams. *Food Research International, 38*(6), 709-719.

Warburton, S. C., Donald, A. M., & Smith, A. C. (1992). Structure and Mechanical-Properties of Brittle Starch Foams. *Journal of Materials Science, 27*(6), 1469-1474.

Yagci, S., & Gogus, F. (2008). Response surface methodology for evaluation of physical and functional properties of extruded snack foods developed from food-by-products. *Journal of Food Engineering, 86*(1), 122-132.

Yanniotis, S., Petraki, A., & Soumpasi, E. (2007). Effect of pectin and wheat fibers on quality attributes of extruded cornstarch. *Journal of Food Engineering, 80*(2), 594-599.

Yoo, J., Alavi, S., & Vadlani, P. (2011). Thermo-mechanical extrusion pretreatment for conversion of soybean hulls to fermentable sugars. Bioresource Technology. doi: 10.1016/j.biortech.2011.04.092.

Zhu, L.J.; Shukri, R.; de Mesa-Stonestreet, N.J.; Alavi, S.; Dogan, H. & Shi, Y.C. (2010). Mechanical and microstructural properties of soy protein - high amylose corn starch extrudates in relation to physiochemical changes of starch during extrusion. *Journal of Food Engineering, 100*(2), 232-238.

Figures and Tables

Inlet	50°C	65°C	80°C	90°C	110°C	120°C

Spacer (6x5mm)   FSE 30-90   FSE 30-30   FSE 20-60   FSE 15-60   RKB 4-5-20-30°   FSE 15-60   RKB 5-4-20-45°   FSE 15-60   FSE 10-30   FKB 5-4-20-45°   FSE 10-60
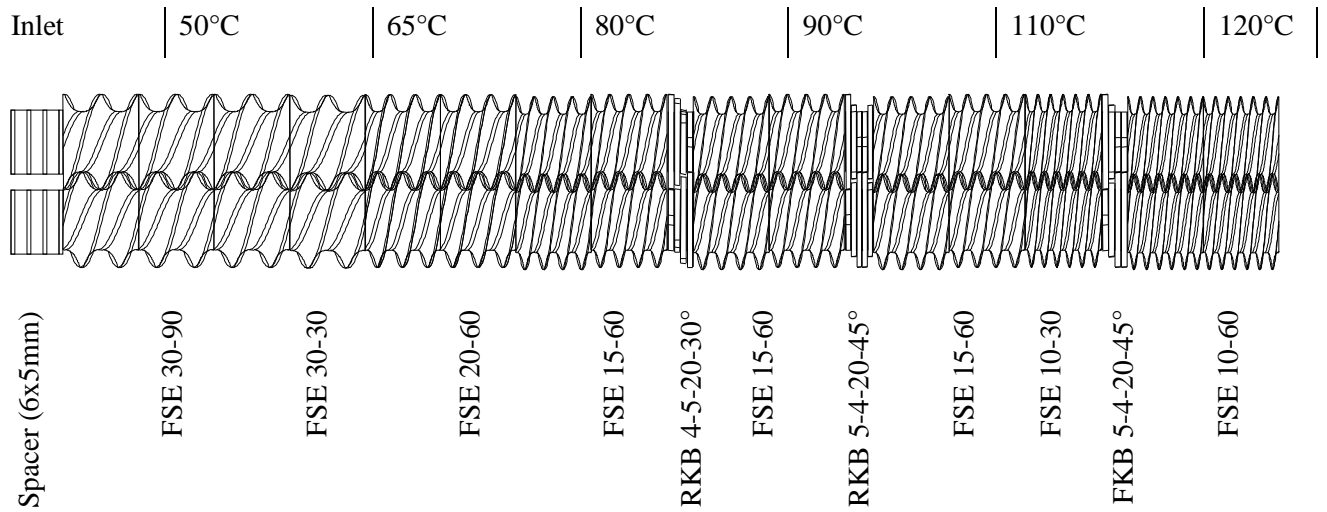
FSE: forward screw element; numbers indicate flight length and total element length, respectively (in mm).
FKB: forward kneading block; numbers indicate number of lobes, lobe length, total length and angle, respectively (length in mm).

Figure 2-1 Screw configuration and temperature profile.

39
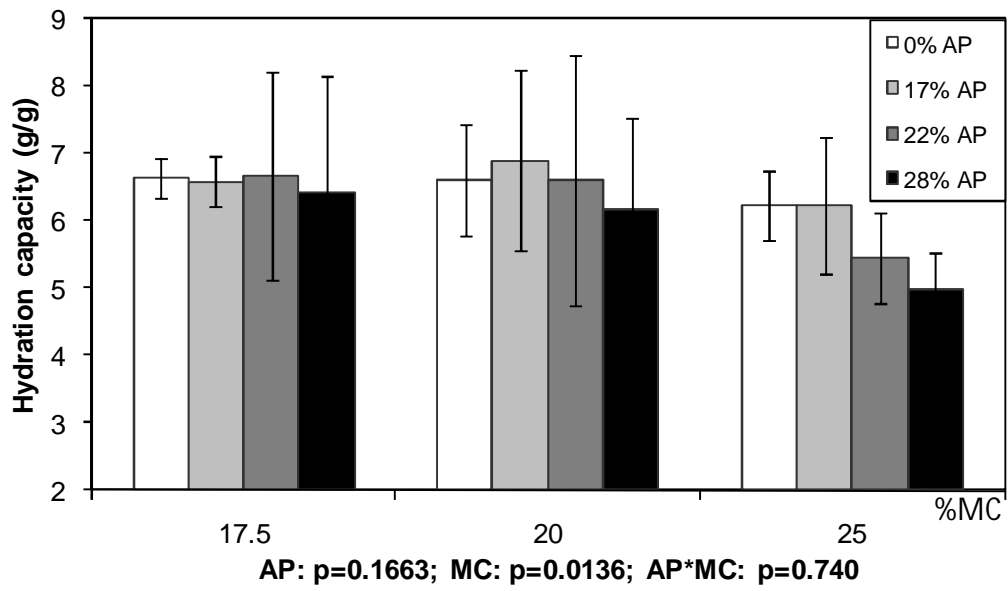
Figure 2-2 Hydration capacity of extrudates (in g/g dry matter). AP: apple pomace content; MC: moisture content.
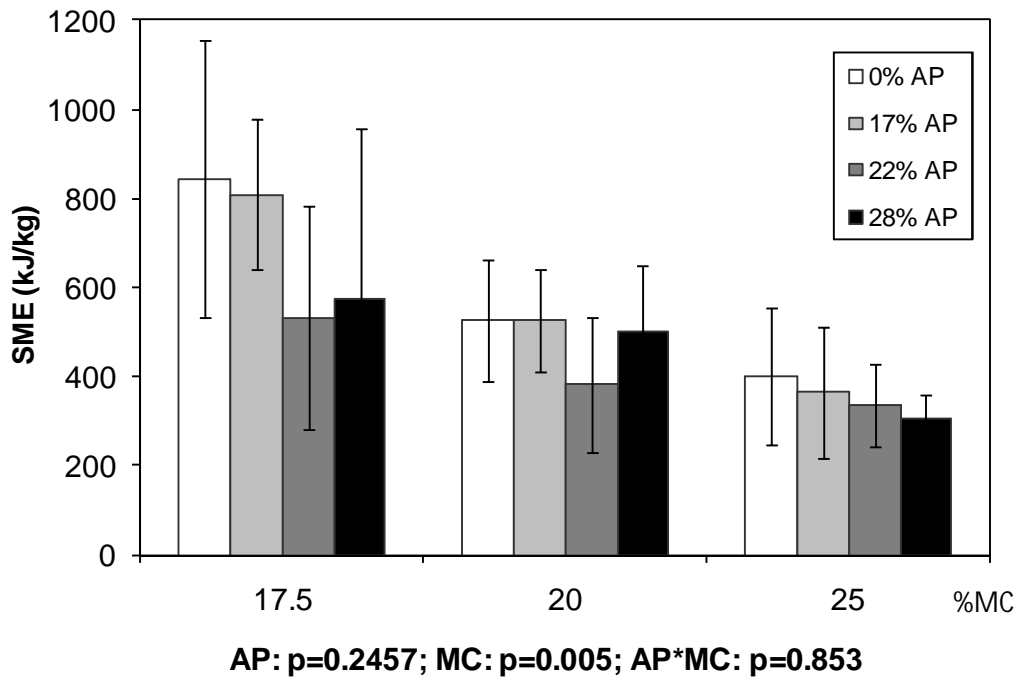
Figure 2-3 Specific mechanical energy (SME) during extrusion processing. AP: apple pomace content; MC: moisture content.
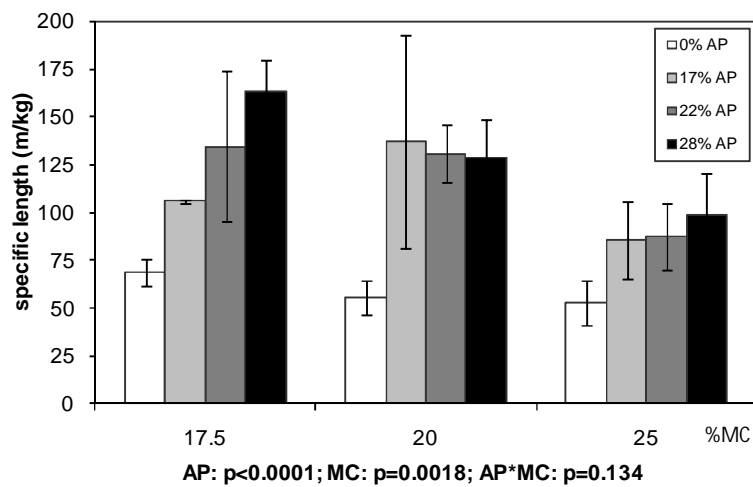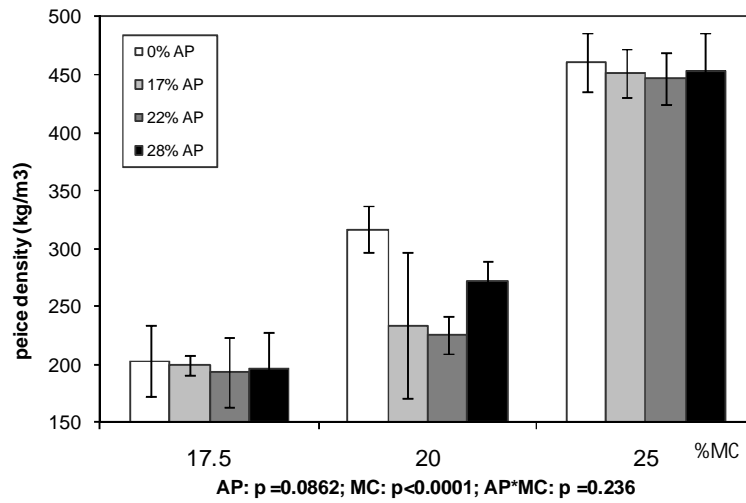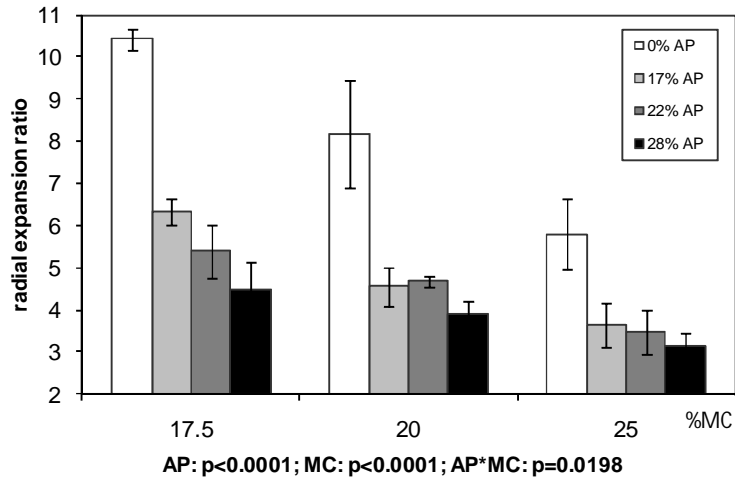
Figure 2-4 Macrostructural parameters of extrudates. AP: apple pomace content; MC: moisture content.
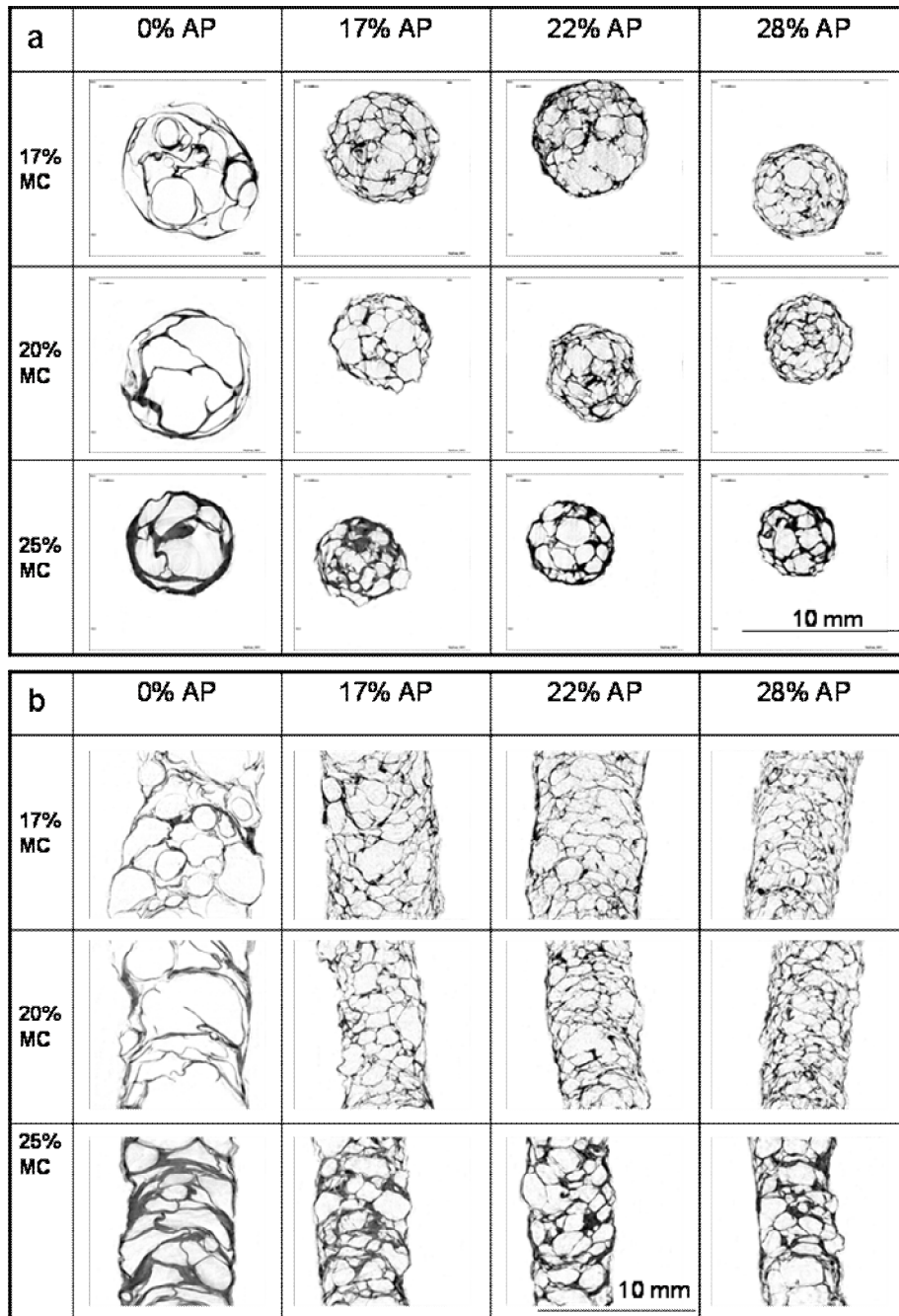
Figure 2-5 XMT images of treatments. Radial (a) and axial (b) views. AP: apple pomace content; MC: moisture content.
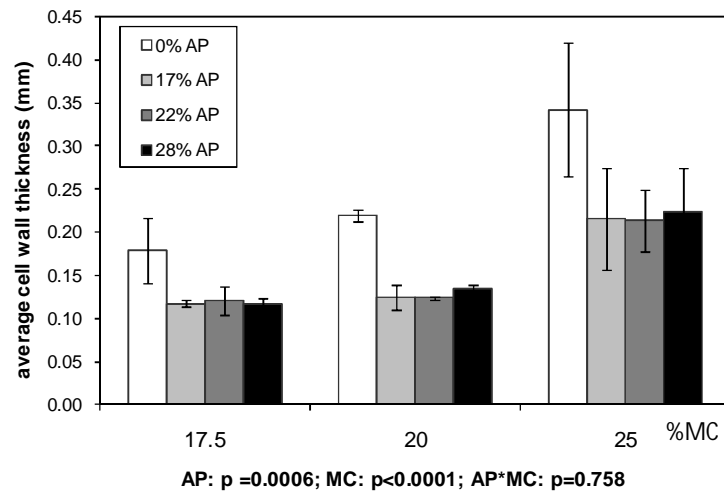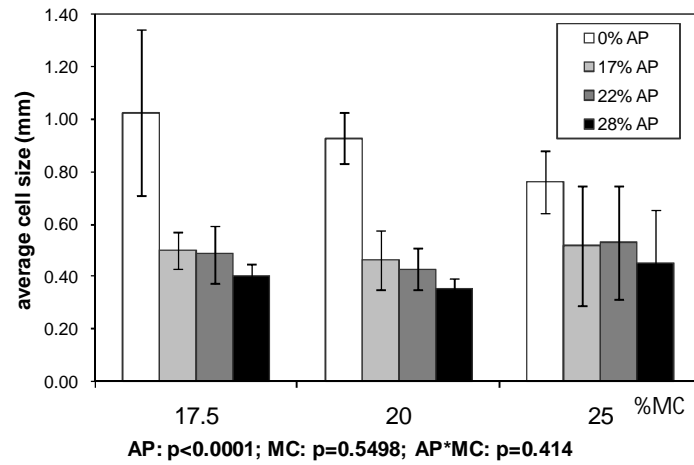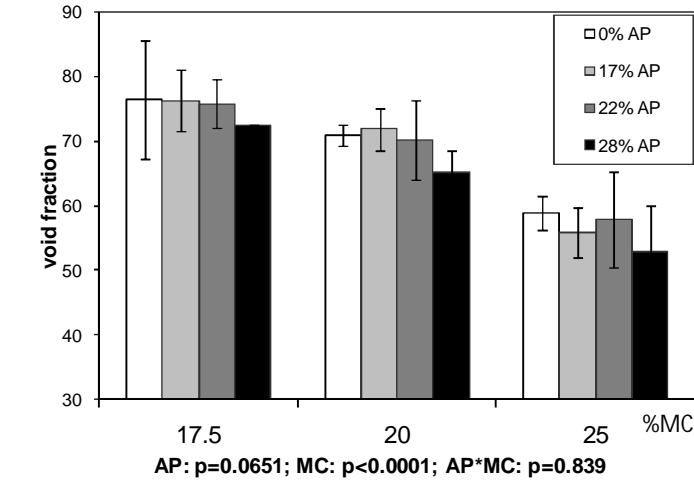
Figure 2-6 Microstructural parameters of extrudates. AP: apple pomace content; MC: moisture content.
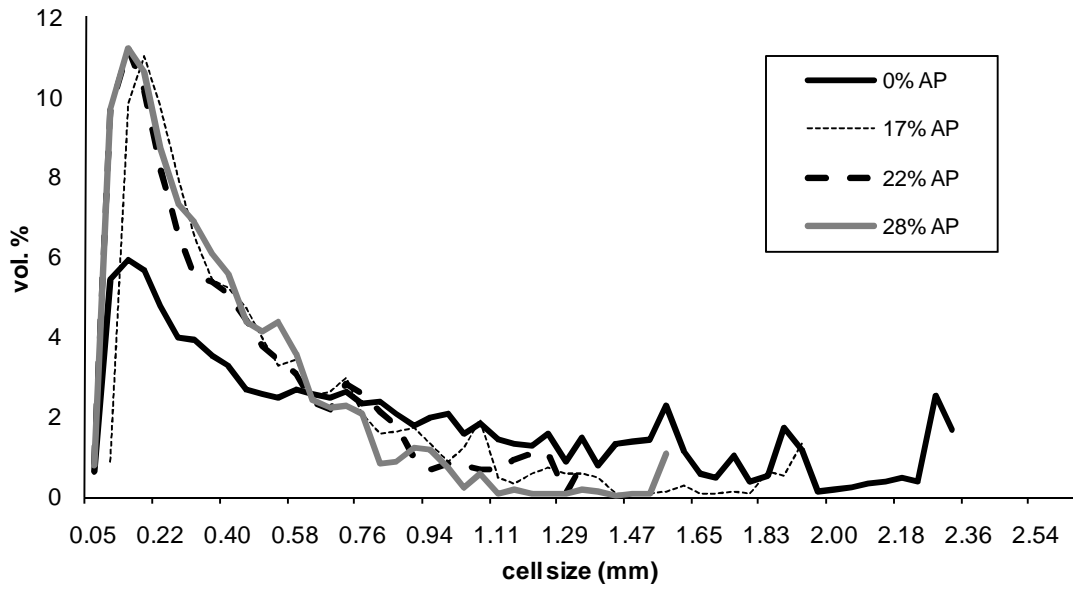
Figure 2-7 Cell size distribution of treatments at 17.5% moisture content. AP: apple pomace level.
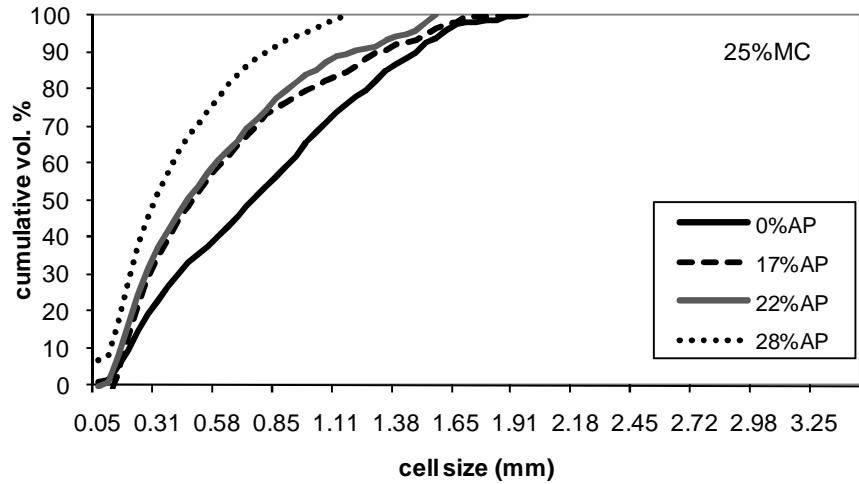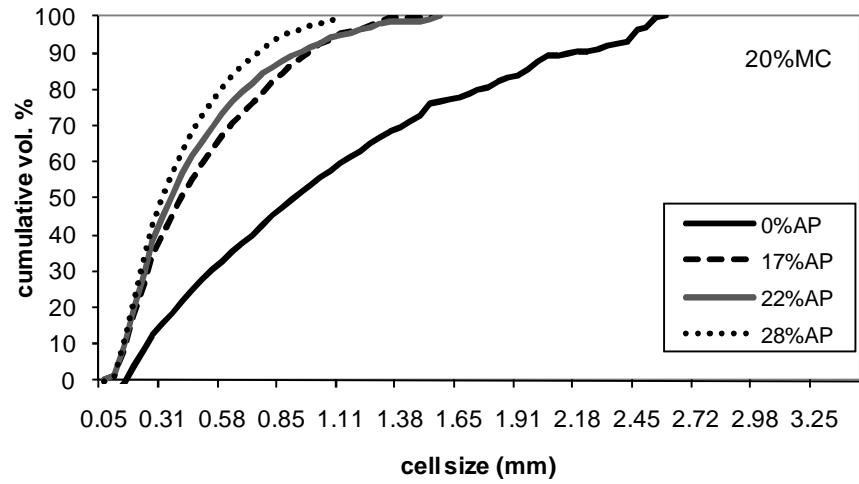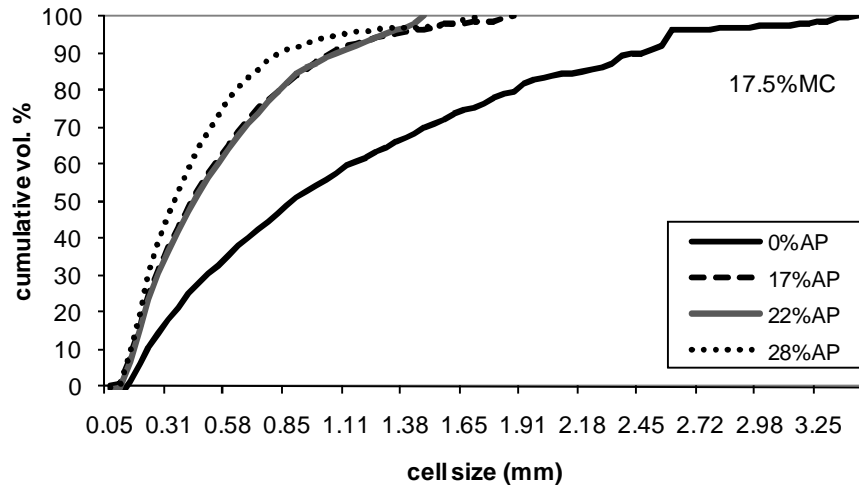
Figure 2-8 Cumulative distribution of cell size. Average values of both duplicates are represented. AP: apple pomace content; MC: moisture content.
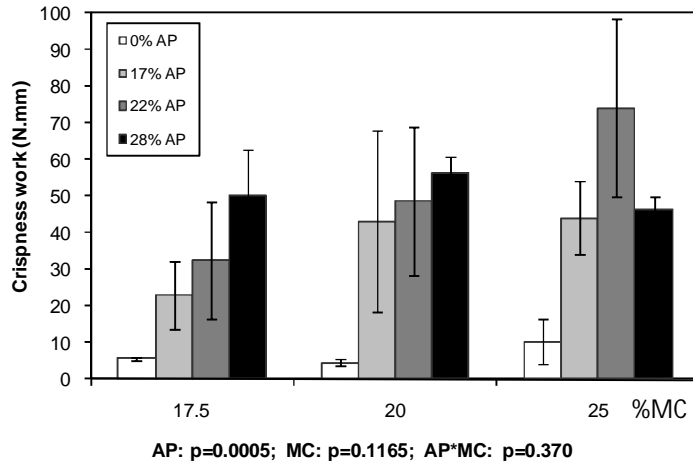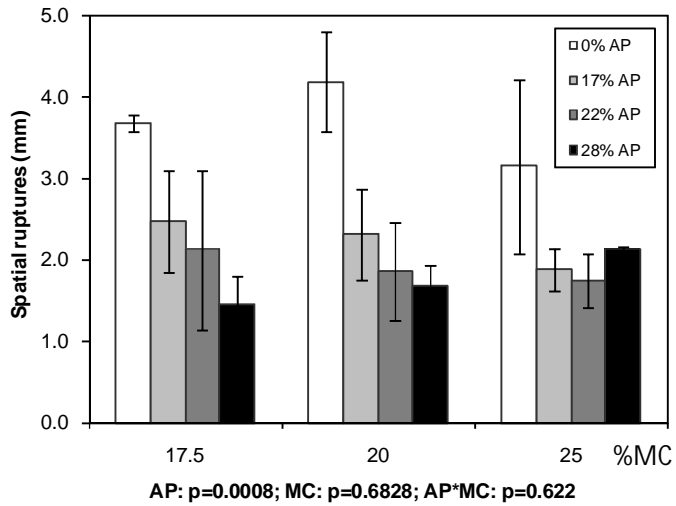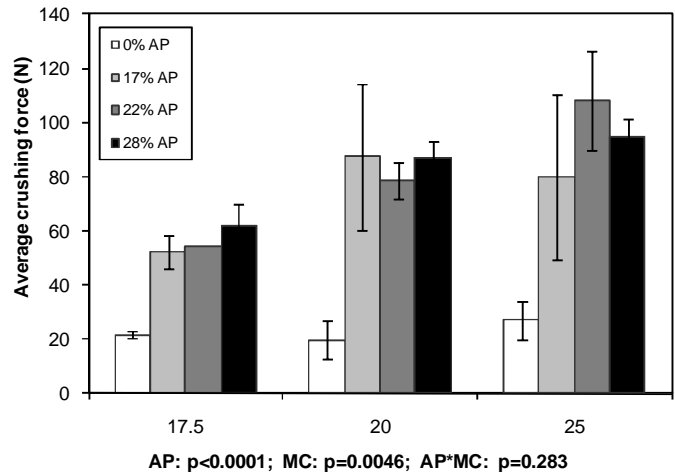
Figure 2-9 Textural parameters of extrudates. AP: apple pomace content; MC: moisture content.
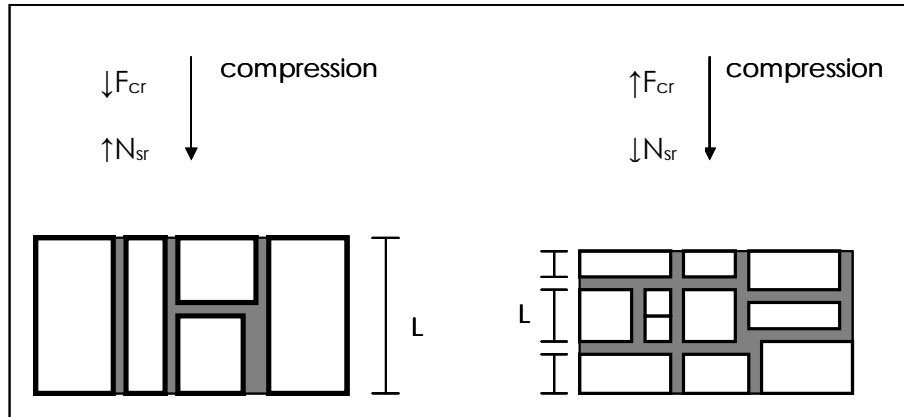
Figure 2-10 Schematic representation of influence of cell size and expansion direction on crushing force.
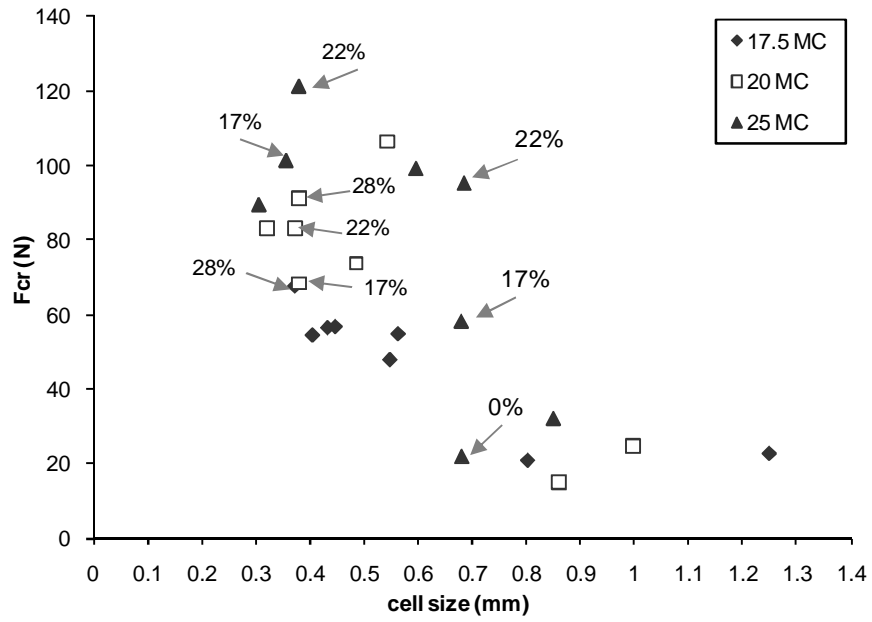
Figure 2-11 Crushing force (F_{cr}) as a function of cell size. Arrows indicate apple pomace levels of selected points. MC: moisture content.

Table 2-1 Proximate composition of apple pomace and corn flour-apple pomace blends (g/100g, d.b.)

	Apple pomace	Corn flour-apple pomace blends			
		0%	17%	22%	28%
Protein	6.4	4.6	4.7	5.0	5.1
Fat	5.4	0.9	1.7	2.0	2.3
Ash	1.4	0.4	0.6	0.6	0.7
Total carbohydrates	86.8	94.1	93.0	92.4	92.0
Starch	0.2	73.3	59.8	56.0	51.3
Total fiber	83.3	3.0	17.0	21.3	26.4
Insoluble	63.3	2.1	13.0	16.3	20.2
Cellulose	22.1				
Lignin	13.7				
Soluble	20.0	0.9	4.0	5.0	6.3
Hemicellulose	10.0				
Sugars	2.3				

Table 2-2 Water activity (a_w) and water retention at 120^oC (WR_{120}) for corn flour - apple pomace blends.

		Apple pomace level			
		0%	17%	22%	28%
a_w	17.5% MC	0.779 [a*]	0.828 [b]	0.812 [c]	0.819 [c]
	20.0% MC	0.803 [d]	0.812 [e]	0.839 [f]	0.872 [g]
	25.0% MC	0.960 [h]	0.947 [i]	0.940 [ij]	0.938 [j]
WR_{120} (%)	17.5% MC	20.34	14.74	14.89	16.34

*Same letters indicate p>0.05.

Table 2-3 Softening and flow temperatures of hydrated raw mixes.

Moisture Content	Softening temperature (°C) Apple pomace level (%)				Flow temperature (°C) Apple pomace level (%)			
	0	17	22	28	0	17	22	28
17.5%	82.7 [a] (2.4)*	78.0 [b] (1.5)	76.8 [b] (0.6)	68.4 [c] (0.2)	164.2 [ab] (0.9)	167.6 [a] (0.6)	164.6 [a] (4.6)	158.7 [b] (0.9)
20%	64.8 [d] (0.3)	64.3 [d] (1.3)	59.4 [e] (0.5)	60.2 [e] (0.2)	149.8 [c] (1.6)	150.6 [c] (4.2)	147.3 [c] (0.7)	146.8 [c] (4.2)
25%	46.4 [f] (1.6)	44.4 [f] (1.5)	46.5 [f] (1.5)	45.7 [f] (2.3)	123.7 [e] (3.7)	125.2 [de] (0.7)	130.1 [d] (2.0)	130.0 [d] (1.9)

*average (SD); same letters within softening/flow temperature indicate p>0.05.

Table 2-4 Pearson's correlation matrix for extrudate parameters and SME

	SME	ER	ρ	l_{sp}	WAI	N_{sr}	F_{cr}	W_c	VF	CWT
ER	0.600*									
ρ	-0.505*	-0.383								
l_{sp}	-0.136	-0.467*	-0.586*							
WAI	-0.065	0.212	-0.508*	0.412*						
N_{sr}	0.190	0.721*	-0.007	-0.596*	0.112					
F_{cr}	-0.430*	-0.805*	0.259	0.389	-0.237	-0.726*				
W_c	-0.335	-0.766*	0.166	0.461*	-0.160	-0.854*	0.902*			
VF	0.666*	0.575*	-0.826*	0.184	0.202	0.272	-0.451*	-0.405*		
CWT	-0.232	0.103	0.805*	-0.772*	-0.350	0.310	-0.261	-0.288	-0.536*	
CS	0.433*	0.775*	0.097	-0.737*	-0.112	0.737*	-0.692*	-0.689*	0.316	0.488*

* indicates $p<0.05$. SME: specific mechanical energy; ER: radial expansion ratio; ρ: piece density; l_{sp}: specific length; WAI: water absorption index; N_{sr}: frequency of spatial ruptures; F_{cr}: crushing force; W_c: crispness work; VF: void fraction; CWT: average cell wall thickness; CS: average cell size

CHAPTER 3 - Extent of matrix transformation in fiber-added extruded products under different hydration regimens and its impact on texture, microstructure and digestibility

Abstract

The objective of this work was to study the effect of three hydration regimens on the extent of matrix transformation, texture, microstructure and digestibility of a corn-based extruded product blended with apple pomace. Blends containing 0, 17, 22 and 28% pomace were hydrated to 17.2% by adding water either into the preconditioner (P), the extruder (E) or dividing half in each (PE). Increasing the opportunity for hydration (P>PE>E) promoted more complete starch gelatinization at all pomace levels. Apple pomace promoted milder extrusion conditions, resulting in less starch gelatinization and solubilization, poor expansion and reduced starch digestibility. Available starch was correlated to cell wall thickness/cell size ratio (r=0.91), which increased with pomace addition. Thus, pomace decreased digestibility by promoting changes in structure and gelatinization. Delayed water addition (E) promoted broader cell size and cell wall thickness distributions, attributed to poor mixing and hydration. Therefore, water incorporation (not just total content) is a key factor in defining extrudate microstructure, texture and digestibility patterns.

3.1 Introduction

In face of the rising prevalence of obesity, there is great interest in developing food products with high nutrient content but reduced energy density. The addition of fiber to commonly consumed products is a way to control caloric density and provide health benefits associated with fiber consumption. The waste stream of fruit and vegetable processing includes materials with high dietary fiber content combined with significant amounts of phytonutrients, thus suitable to address the current need. Extrusion processing has been described as a viable technique for incorporating fruit and vegetable by-products into ready-to-eat products, however there is also need for further research regarding impact on functional and nutritional properties (Karkle et al. 2010; Altan et al. 2009; Altan et al. 2008).

Starch is the main component of directly expanded products. During extrusion, starch undergoes a series of physical and chemical transformations, including water diffusion, granule expansion, gelatinization, depolymerization, decomposition, and complexation (Liu et al., 2009). The extent of starch transformation plays an important role in the functional properties of the final product, and it is dependent on extrusion conditions, characteristics of the starch granule and presence of other components such as protein, fibers and sugars (Chanvrier et al., 2007). It has been shown that molecules that readily hydrate (such as sugars and fibers) may restrict water available to starch and reduce the degree of gelatinization (Tester and Sommerville, 2003). In excess moisture systems it was found that sucrose and glucose reduced gelatinization by binding strongly to water, as well as by penetrating into the granule (Gonera and Cornillon, 2002). The molecules entered the granule, displacing water and reducing plasticization. Polysaccharides

such as fibers are too large to penetrate the granule, and water restriction is mainly due to competition for free water in solution (Tester and Sommerville, 2003).

In extrusion of directly expanded products, moisture content is limited and injection of water directly into the barrel allows for a very short hydration period. Zhang and Hoseney (1998) have found that preconditioning corn grits for 2 min doubled the expansion ratio as compared to water added directly into the extruder. The work was conducted in the context of particle size, but their conclusion that uniform moisture absorption benefits expansion can be applied to systems with water-absorbing components. Mathew et al. (1999) applied this concept for extruded pet food with high protein content and found that injection of water into the preconditioner resulted in better quality parameters. Although the effect of in-barrel moisture has been studied in fruit and vegetable-added systems (Karkle et al., 2010; Yagci and Gogus, 2010; Stojceska et al., 2009), there are no published studies on the effect of different preconditioning regimens. It is hypothesized that addition of water in the preconditioner can increase the chance for components to hydrate. This is an advantage compared to increasing in-barrel moisture in that a better balance can be achieved between hydration and viscosity.

Variation in water addition is known to change the degree of transformation of the matrix, leading to differences in starch digestibility and in microstructure (Karkle et al., 2010; Yagci and Gogus, 2010). Chanvrier et al. (2007) have suggested that extrudate microstructure may be used to control starch susceptibility to enzymatic action, however systematic studies on the relation between these two are lacking. The addition of fruit and vegetable materials to extrudates adds challenges in understanding this relationship due to the complex composition of the cell wall material.

Therefore, the objective of this work was to study the effect of preconditioning regimen on the extent of matrix transformation and its impact on texture, microstructure and digestibility of an extruded snack with added fruit fiber.

3.2 Materials and Methods

3.2.1 Material characterization and blend preparation

The ingredients used were yellow degermed cornmeal (76.8% starch, 99.5% < 420µm, Bunge Milling, St Louis, MO), dried apple pomace (95% < 420µm, Tree Top, Selah, WA), and pregelatinized waxy cornstarch (95% < 450 µm, X-PAN'R, Tate&Lyle, Decatur, IL). The composition of the apple pomace, as provided by the manufacturer, was: 6.3% protein, 4.7% fat, 1.3% ash, 72% total dietary fiber (53.5% insoluble and 18.6% soluble). The composition of cornmeal was 7.5% protein, 0.4% fat, 0.3% ash, 1% insoluble dietary fiber, as provided by the manufacturer.

Moisture content of raw materials was determined by AACC standard method 44-19.01 (oven method at 135˚C; AACC International, 1999). Sugar content in apple pomace was determined by high performance liquid chromatography (HPLC; Agilent 1100), using a Phenomenex Rezex ROA organic acid column (130x7.8 mm, H+ (8%); Phenomenex, CA). 0.005N sulfuric acid was used as a mobile phase, and the flow rate was 0.6 ml/min at 60°C. Samples were prepared by dispersing one gram pomace in 20mL distilled water at 30°C and stirring with a magnetic stirrer for 15 min. The contents were centrifuged (15 min at 1000xg),

and the supernatant diluted and filtered through 0.45 µm. Results were expressed as combined content of sucrose, glucose and fructose per gram dry matter.

Blends were formulated with four cornmeal:apple pomace ratios: 90:0, 73:17, 68:22, and 62:28, with the balance being 10% pregelatinized cornstarch for all blends. Blends are herein referred to by percent apple pomace (AP) added in substitution of cornmeal (0, 17, 22 or 28% AP).

3.2.2 Extrusion processing

Extrusion processing was carried out on a pilot-scale twin-screw extruder (TX-52, Wenger Manufacturing, Sabetha, KS), equipped with a differential diameter cylinder preconditioner with a volumetric capacity of $0.056m^3$ (DDC2, Wenger Manufacturing, Sabetha, KS). The preconditioner paddles were set to forward pitch at the first third of the preconditioner, followed by neutral pitch at the second third, and reverse pitch at the preconditioner outlet. The preconditioner shaft speed was set at 379 rpm, resulting in an average residence time of 2.8 minutes, based on previous experiments. The material was fed into the extruder at 80 kg/h. The extruder set–up consisted of a screw profile typical for directly expanded snacks (Figure 3-1). The screw diameter was 52mm with an L/D ratio of 16. The screw speed was fixed at 300rpm for all treatments. The die head was equipped with a probe to measure the temperature at the center of the product flow. A one-opening circular die of 3.7mm was used. Product was cut at the die exit with three hard knife blades rotating at 530 rpm. The extrudates were dried in a dual pass dryer (4800, Wenger Manufacturing, Sabetha, KS) at 115°C for 18 minutes, with a 7 minute

cooling step. Samples were immediately transferred to thick polyethylene bags and stored at room temperature until analysis.

Each blend was processed under three water addition regimens. First, the water addition was divided equally between the preconditioner and the extruder (coded PE). The next regimen consisted of adding all the water in the extruder (coded E), and lastly the full amount of water was added in the preconditioner (coded P). The target in-barrel moisture content was 17% wet basis, and total water addition was adjusted according to the moisture of each blend (10.1-12.4%). The average in-barrel moisture content achieved was 17.2 ±0.4 for all treatments, calculated based on water injection rates (data acquired every 1.2 seconds) and raw material moisture.

The specific mechanical energy (SME) for each treatment was calculated using

$$SME = \frac{\frac{(T - T_0)}{100} \times \frac{N}{N_r} \times P_r}{\overset{\bullet}{m}} \quad \text{(kJ/kg)} \tag{1}$$

where N = screw speed, N_r = rated screw speed (508rpm), T= percent torque, T_0 = no-load torque (5%), P_r = rated motor power (37.9 kW) and $\overset{\bullet}{m}$ = mass flow rate (kg/s) (Ryu & Ng, 2001). Due to errors in the data acquisition system, it was not possible to collect the torque for the treatments with apple pomace under the PE regimen, thus no SME was computed for the same.

3.2.3 Extent of Gelatinization

Gelatinization was verified by differential scanning calorimetry (DSC) and light microscopy. For the DSC analysis, 12mg of sample was weighed into high volume steel pans. Raw mix was used as is, and extrudates were ground and sieved to <250 µm. Excess water (2x dry weight) was added, the pans were sealed and allowed to hydrate overnight at room temperature. The samples were scanned against an empty pan at a heating rate of 10°C/min, from 10 to150°C (Q100, TA Instruments, New Castle, DE). Endothermic peaks with a signal greater than 0.2mW in the temperature range of 60-90°C were characterized as gelatinization (Chanvrier et al., 2007). All treatments were analyzed in triplicates.

For light microscopy, ground samples were suspended in water (0.1% solids) and mounted onto microscope slides. Samples were viewed under 400 x magnification (Olympus BX51) under polarized light to identify ungelatinized starch granules.

3.2.4 Moisture loss

Moisture loss at the die was computed by subtracting the residual moisture from the in-barrel moisture. Residual moisture is the moisture content of the product at the die exit (before drying). The samples were collected into plastic bags immediately after cutting and moisture was measured according to AACC standard method 44-19.01 (in triplicates).

3.2.5 Water absorption/water solubility

Water absorption index (WAI) and water solubility index (WSI) were measured as described by Anderson et al. (1969). Before analysis the extrudates were ground to pass a 250 µm sieve. Samples were allowed to hydrate in distilled water (1:12) with intermittent mixing, followed by centrifugation. The precipitate was used to compute WAI and the supernatant was dried to obtain the WSI. Results are the average of duplicate measurements and are expressed on dry basis of initial sample. The WSI of the raw materials (cornmeal: 1.86%; apple pomace: 19.68%) was analyzed in the same manner and subtracted from the WSI of the extrudates to identify only solubility promoted by extrusion. The WSI of pregelatinized starch was omitted as the result was 0% solubility due to gelling and complete immobilization of the full amount of water.

3.2.6 In vitro starch digestibility

In vitro starch digestibility was assessed using the Englyst method with a colorimetric end-point, as described by Englyst et al. (1992) and Silvester et al. (1995). Before analysis all samples were ground and sieved to obtain a particle size between 840-1180µm. The particle size was chosen as to retain intact cell wall segments, while being consistent with particle size reduction upon chewing (Jalabert-Malbos et al., 2007). Samples were hydrolyzed with pepsin, then incubated with pancreatin and amyloglucosidase. Samples were collected after 20 and 120 min and measured for glucose content. The remaining hydrolysate was boiled and solubilized with alkali to obtain total starch content of each sample. The following modifications were

applied to the original method: six glass beads of 10mm were used in each tube instead of five 15mm balls; amyloglucosidase from *Rhizopus* was used at an activity of 730U in each hydrolysis tube; invertase was omitted; and stroke length of the water bath was 38 mm and set to 120 strokes/min. Glucose was quantified using a glucose oxidase kit (D-glucose assay procedure, GOPOD format, Megazyme, Ireland). To validate the modifications to the method, wheat flour 70% extraction was run as a reference and compared to the values given by Englyst et al. (1999).

Free glucose in the samples was analyzed using the following procedure: 0.6g of sample was dispersed in 20mL distilled water and placed in a water bath at 100°C for 30 minutes, with gentle shaking. One milliliter of sample was transferred into 2mL 95% ethanol, vortexed and centrifuged at 1,000 x g for 5 minutes. The supernatant was analyzed for glucose using the glucose oxidase assay kit.

Digestibility was expressed in terms of nutritionally relevant starch fractions, as described by Englyst et al. (1992). Rapidly digestible starch (RDS) refers to glucose released after 20 minutes of hydrolysis (corrected for free glucose), and slowly digestible starch (SDS) is glucose released during the remaining 100 minutes of hydrolysis. Resistant starch (RS) is obtained by subtracting the available starch (SDS + RDS) from total starch in the sample. The fractions are expressed as g/100g total starch, not total sample weight, as starch content varies with the different levels of apple pomace addition. The values are the average of at least 3 replicates for the hydrolysis procedure and 2 replicates for free glucose.

3.2.7 Macrostructure

The length (l_e), diameter (D_e) and weight (m_e) were measured for 20 pieces of dried product from each treatment, and used to obtain the radial expansion ratio (ER), specific length (l_{sp}), and piece density (ρ).

$$ER = \frac{D_e{}^2}{D_d{}^2} \tag{2}$$

$$l_{sp} = \frac{l_e}{m_e} \qquad (mm/g) \tag{3}$$

$$\rho = \frac{m_e}{\left[3.14 * \left(\frac{D_e}{2} \right)^2 * l_e \right]} \qquad (kg/m^3) \tag{4}$$

where D_d = die diameter

3.2.8 Microstructure

Microstructural features of the extrudates were analyzed using X-ray microtomography (XMT). One piece of each treatment was scanned. To ensure that the samples were representative, the diameter of the scanned piece matched the average diameter for that treatment. Samples were scanned on an XMT system (Model 1072, Skyscan, Belgium), under the following settings: voltage 40kV, current 244µA, exposure time 1 second, rotation step 0.9°,

sample rotation 180°, magnification 14.48x. Shadow images were reconstructed into a 3D object (software NRecon v. 1.6.1, Skyscan, Belgium), which was virtually sliced into approximately 1,000 cross sections and analyzed (CTAn 1.9.1, Skyscan, Belgium). For analysis, a volume of interest (VOI) was determined by setting a region of interest tightly around the perimeter of each cross section and interpolating for the dataset. The VOI dataset was resized by 2 to reduce the computational burden and reloaded for further processing. The grayscale images were converted into binary images with a threshold of 70 (cell walls converted to white pixels and voids converted to black pixels). The despeckling function was applied to the VOI to reduce background noise from the image, and the final processed image was analyzed in 3D. The cell size was obtained from the structure separation function, and cell wall thickness from the structure thickness function. Void fraction was obtained by the ratio of white voxels (cell walls) to total voxels.

3.2.9 Texture

Mechanical properties of the extrudates were analyzed using a texture analyzer (TA-XT2) and the Texture Expert 1.22 software (both from Stable Micro Systems, United Kingdom). Twenty pieces of each treatment were equilibrated to 3.8 ±0.3% by holding overnight at 40°C. A 38 mm compression plate was used to compress the samples to 80% of their original diameter (test speed of 2.0 mm/s). The area under the curve (S) and the number of peaks (n) were obtained from the force-deformation curves and used to calculate the spatial frequency of ruptures (N_{sr}), the average crushing force (F_{cr}) and crispness work (W_c) (Agbisit et al., 2007; Bouvier et al., 1997).

$$N_{sr} = \frac{n}{d} \qquad (\text{mm}^{-1}) \tag{6}$$

$$F_{cr} = \frac{S}{d} \qquad (\text{N}) \tag{7}$$

$$W_c = \frac{F_{cr}}{N_{sr}} \qquad (\text{N.mm}) \tag{8}$$

where d= probe travel distance

3.3 Results and Discussion

3.3.1 Extrusion processing

The effect of apple pomace and water regimen on SME is presented in Figure 3-2. Apple pomace caused a marked decrease in SME. For instance, under the E water regimen, substitution of 28% pomace for cornmeal caused the SME to fall from 421 to 265 kJ/kg. A firm conclusion for the effect of water addition on SME cannot be drawn due to missing data points for the PE regimen. Comparing E and P, the only marked difference is at 0% pomace (369.8 kJ/kg at P, and

443.1 kJ/kg at E). In the presence of pomace the treatments had a very small difference in motor load (0-1%), resulting in close SME values.

The lower SME for P at 0%AP may be a result of increased plasticization promoted by the longer hydration period. In the case of the blends with pomace the low SME may be due to the high sugar content of apple pomace. The combined amount of sucrose, glucose and fructose in the dry pomace was 15.8% (as quantified by HPLC), resulting in sugar levels of 2.6-4.4% in the blends with pomace. Low molecular weight carbohydrates are effective plasticizers and reduce the melt viscosity, limiting mechanical energy input to the melt. Previous studies have reported reduced SME at sucrose levels of 3-6% (Agbisit, 2007; Jin et al., 1994; Ortiz et al., 2010).

Lower SME and reduced melt viscosity agree with lower die pressure and temperature in the presence of pomace (Figure 3-3). While temperature had a clear reduction with each increase in pomace level, die pressure decreased only slightly or not at all (under E). Viscosity is temperature-dependant, as the melt gets cooler viscosity increases. This increase could have been sufficient to affect localized die pressure. Reduction in temperature can also decrease the extent of starch gelatinization, leading to increased viscosity.

As addition of water in the preconditioner increased (E<PE<P), so did the die pressure (Figure 3-3). One reason can be that addition of water directly into the extruder reduced the opportunity for hydration, leaving an amount of unabsorbed water. The unabsorbed water would reduce the viscosity of the plasticized material, reducing friction (thus, material pumping and pressure build-up). Product temperature at the die followed the same trend and can be a direct result of lubrication, with reduction in heat generated by friction. Overall, the addition of the full

amount of water into the extruder was comparable to increasing in-barrel moisture, despite equal in-barrel moisture contents between the regimens.

3.3.2 Extent of gelatinization

DSC showed little evidence of residual gelatinization enthalpy. Thus, the limited amount of native starch in the samples gave an endothermic peak at or below the sensitivity threshold of the equipment (0.2mW). It is interesting to note that apple pomace before extrusion had an endothermic peak at ~59°C (Figure 3-4). The presence of starch in unripe or early season apples is well known in the apple processing industry, and the peak gelatinization temperature of isolated apple starch has been reported as 57.1-59.1°C (Singh et al, 2005). In the few scans with residual gelatinization peaks, none were in the temperature range for pomace, rather they all appeared at higher temperatures, related to cornmeal (75-80°C, Figure 4). According to Singh et al. (2005), apple starch has lower crystallinity compared to corn starch, which may facilitate melting of the former during extrusion processing.

Microscopic examination of the extrudates under polarized light showed very clear evidence of native starch granules (maltese cross) in all treatments, with the exception of 0% AP under the P water regimen. In fact, native starch granules were scarce for the other treatments at 0% AP. For the treatments with apple pomace native granule identification was highest under the E regimen, with several granules appearing in the same field of observation. The count was clearly reduced under P and PE. 22%AP under the three water regimens is shown as an example (Figure 3-5).

The more complete gelatinization in the treatments with 0% AP is consistent with higher SME and product temperature, as compared to the treatments with pomace. In extrusion starch transformation is achieved by both mechanical and thermal energy, and an increase in both is expected to promote higher loss of granular structure. Additionally, at 0% AP the limited amounts of fiber and sugars resulted in greater water availability for starch alone (which also favors complete gelatinization).

Among the treatments with pomace, the E regimen, with more intact granules, also had lower die pressure and temperature. This supports the idea that although this regimen provided the same total water as the other two, injection in the extruder reduced the opportunity for hydration. The starch granules were allowed less time in contact with water, compared to PE and P, thus gelatinization was reduced. In a system where several components are competing for a limited amount of water, increasing the contact by even a few minutes appears to play an important role.

3.3.3 Moisture loss

Moisture loss at the die is dependant on vapor pressure inside the air cells, as well as matrix characteristics such as extensibility and water binding. It reflects the degree of starch transformation: ungelatinized starch has poor film forming ability, its presence reduces extensibility and residual water is trapped inside the structure rather than escaping as vapor flash-off. Any other poorly extensible biopolymer may have the same effect on moisture loss (such as insoluble fibers and protein).

Overall, highest moisture loss was found at 0%AP and under the P treatment (Figure 3-6). This agrees with the previous results, as 0%AP had higher SME, temperature, and die pressure, along with a scarce amount of native starch granules. Thus, all were favorable conditions for development of good extensibility and vapor flash-off. Conversely, pomace addition created less favorable conditions, and more moisture was retained. There were no clear differences among the 3 pomace levels.

The effect of the different water regimens on moisture loss is also supported by the previous results. The E regimen had lower die pressure and temperature for almost all treatments, which is consistent with a lower vapor flash off (thus, moisture retention in the matrix). This affected even 0%AP, so temperature and pressure at the die were more important than degree of starch conversion.

3.3.4 WAI/WSI

Overall, 0%AP had higher WAI than the treatments with pomace (Figure 3-7). 0%AP under P had a markedly lower WAI compared to E and PE. Since this was the treatment with no indication of native starch granules, the result suggests that starch has been depolymerized to some extent, thus losing water absorption capacity. Although this treatment had lower SME than PE and E, water was added early in the process. Pregelatinized starch readily swells, and swollen granules are more susceptible to rupture under shear (Xie et al., 2006). Delay in adding water may have restricted swelling, thus preventing granule rupture under PE and E. While this explains the differences seen at 0%AP, the treatments with pomace did not follow a clear trend

in terms of the effect of water addition. These treatments did show lower WAI than 0%AP, probably due to reduced starch gelatinization, as discussed earlier.

The presence of apple pomace caused less solubilization of matrix components during extrusion, with decreased WSI as pomace level increased (Figure 3-7). Along with the data for temperature, die pressure and SME, this result supports that the addition of apple pomace causes extrusion conditions to become less drastic. Although the results for WSI do not indicate which component is responsible for solubility, processing only cornmeal and pregelatinized starch caused the solubility to increase from 1.67% (unextruded cornmeal) to around 50%. If apple pomace creates a less drastic process, it is logical to believe that the reduced WSI in the presence of pomace was due to less starch damage. The WSI results agree with the indications of depolymerization of 0%AP under P, as solubility was the highest for this treatment.

3.3.5 In vitro starch digestibility

Both pomace and water regimens impacted the in vitro digestibility of the extrudates (Figure 3-8). Slightly negative RS values are due to experimental variation (not uncommon in digestion analysis) and can be considered zero (Dust et al., 2004).

Overall, as pomace level increased there was a decrease in total available starch (RDS+SDS), with an increase in RS. Thus, replacement of cornmeal with pomace not only decreased the total starch content, but also decreased the susceptibility of the remaining starch to enzymatic activity. This is likely due to reduced starch gelatinization as a result of the effect of pomace on extrusion parameters (SME, die temperature and pressure), and water availability for starch transformation. The positive relationship between starch gelatinization and digestibility is

well described for extruded products (Altan et al., 2009; Yagci and Gogus, 2008). In addition, there may be an effect of pomace fibers hindering the access of enzymes to starch in the hydrolysis medium (Brennan et al., 2008), or even binding to alpha-amylase, inhibiting enzymatic activity (Slaughter et al., 2002), as has been described for other types of fiber.

The P water regimen had the overall highest RDS and highest available starch. This is consistent with the findings of higher starch conversion under this regimen. The markedly higher RDS content of 0%AP under P is an additional evidence of depolymerization of this treatment. Since it had no intact granules and highest WSI, it was expected that the starch would be highly susceptible to enzymatic activity.

Although the previous findings suggested that the E regimen would have the lowest digestibility, this was not observed. Rather, PE tended to have higher RS content, suggesting that the RS fraction might not be solely ungelatinized granules. Other possibilities are retrograded starch, complex formation or physical entrapment of starch in the matrix. Analysis of the DSC curves revealed no consistent indication of amylose:lipid complex (90-100°C) or retrograded amylose (120-170°C) (Chanvrier et al., 2007; Kim and Kwak, 2009). Although these peaks were indentified for a few samples, they did not help explain the digestibility pattern. For example, 22%AP under P and 28%AP under E clearly showed no thermal events. However, the RS content of these treatments was 11.7 and 18.0 g/100g starch, respectively.

Since retrograded amylose and complexation with lipids appear not to be responsible for the totality of the RS fraction, it is likely that resistance was not caused by properties of the starch, but by properties of the matrix. Although physical entrapment of starch generally applies to intact cell walls, entrapment of gelatinized starch in a matrix has been described. According to Brennan and Tudorica (2007), due to the thermodynamic incompatibility between amylose and

71

amylopectin, a thin layer of leached amylose may aggregate and encapsulate the swollen granule, resulting in resistant starch. If this is the case, the PE regimen may have provided enough water in the preconditioner for the initial leaching of amylose and its aggregation on the granule surface. On the other hand the other regimens provided the full amount of water at once, which may have allowed for more complete amylose leaching (in the case of P) or insufficient time for amylose to aggregate before intense shearing (in the case of E). In accordance with the present results, Brennan and Tudorica (2007) found no evidence of ungelatinized granules using DSC.

3.3.6 Macrostructure

Radial expansion ratio was markedly higher in the absence of apple pomace and decreased with increasing pomace levels (Figure 3-9). This very likely reflects the effect of sugar in reducing viscosity and promoting collapse of the expanded structure, along with reduced starch conversion. The presence of fiber and the relative absence of starch is a further hindrance to expansion and likely limited extensibility of the matrix.

Piece density of the extrudates was the inverse of radial expansion, with a sharp increase in density as pomace level increased (Figure 3-9). Specific length was only slightly affected by pomace level and water regimen. The average specific length was lower under the E regimen (44.8 mm/g, versus 50.6 mm/g under PE, and 50.0 mm/g under P). As for pomace level, the average specific length decreased as pomace increased (52.6, 49.0, 46.4 and 45.9 mm/g for 0%, 17%, 22% and 28% AP, respectively). Thus, with higher pomace levels density increased by limiting primarily radial expansion, but also longitudinal expansion. Increased longitudinal expansion is often reported in high-fiber extrudates (Jin et al., 1994; Lue et al., 1991). In fact,

previous studies with apple pomace and corn flour showed that pomace significantly increased

longitudinal expansion (Karkle et al., 2010). The difference in results can be explained by the

difference in sugar content between the pomace samples (2.3% in the previous work versus

15.8% in the present work). It is possible that collapse caused by reduced viscosity was more

important under high sugar content, overcoming any change in expansion direction.

The effect of water addition on macrostructure varied depending on the presence of

pomace. At 0%AP highest expansion was obtained under E. It was surprising that expansion was

also high under P, since this treatment had clear evidence of depolymerization. Perhaps the level

of depolymerization was not extensive enough to reduce matrix extensibility. Chinnaswamy and

Hanna (1991) state that a certain level of starch degradation may adjust viscosity so it becomes

more favorable to expansion. The higher radial expansion under E was compensated by a slightly

lower longitudinal expansion, and 0% under all three water regimens had comparable density.

In the presence of pomace, lower radial expansion combined with a slightly lower

longitudinal expansion resulted in extremely high piece density, up to 9 times higher than the

treatments with 0%AP. The E regimen was the least expanded under the 3 pomace levels. With

lower die temperature as compared to the other water regimens, the driving force for expansion

was decreased, thus lower expansion was expected. The higher evidence of intact granules also

supports lower expansion for the treatments under E.

3.3.7 Microstructure

Typical XMT images are given in Figure 3-10. Microstructure of the extrudates was

described in terms of void fraction (VF), average cell size (CS) and average cell wall thickness

(CWT) (Table 3-1). VF reduced as pomace level increased (up to 50% reduction). In accordance with piece density and expansion ratio data, the E regimen had the lowest VF at all pomace levels. This can be structurally explained by the higher CWT under E, which increased with pomace level. CS tended to be slightly higher for the treatments under E, however this did not overcome the effect of CWT on lowering the VF.

Figure 3-11 shows the volumetric distribution curves for CS. The spread followed E>PE>P for all the treatments, which suggests an effect of water addition on vapor diffusion. Early addition of water may allow for better mixing, with even distribution of water in the material. This would create a more homogeneous movement of vapor into nuclei, thus a narrower CS distribution. On the other hand, late water addition might lead to unequal hydration, creating regions with different vapor pressure and availability of nucleation points, leading to a less uniform size distribution (see proposed schematic, Figure 3-13).

There was a clear increase in CWT as pomace level increased, and the E regimen had a broader spread as compared to P and PE (Figure 3-12). A positive relationship between CWT and CS has been reported by other authors (Babin et al., 2007; Trater et al., 2005). Trater et al. (2005) explain that thicker walls result from merging and coalescence of walls as the cells expand. Our current findings provide reason to believe that thicker walls were a result of poor film forming ability, causing premature coalescence and merging. The E regimen showed a series of conditions that are unfavorable to expansion, such as low die pressure, low die temperature, and incomplete gelatinization. It also showed a tendency toward lower moisture loss, indicating less vapor flash off.

Microstructure data were analyzed against digestibility and a high inverse correlation was found between available starch and the ratio of CWT to CS (r^2=0.909; Figure 14). CWT alone

had only a moderate correlation (r^2=0.522), indicating that the overall microstructure better dictates enzyme access to the matrix. The CWT/CS ratio increased with pomace level but followed no trend for hydration regimen. Although the E regimen had lower VF, the CWT/CS ratio was comparable to the other two for each pomace level.

It is interesting to note that as definition of structural features increased, so did the correlation with digestibility. Piece density is an easy to determine macro feature, and correlation with RDS+SDS gave $r^2 = 0.758$. VF provides more information on internal cellular structure, and its analysis is not subject to human error as incurred in measuring and weighing to obtain piece density. The correlation with RDS+SDS was slightly improved, $r^2 = 0.842$. Characterization of the microstructure in terms of CWT/CS brings greater detail into the analysis of the structure, and proves the influence of microstructure on digestibility of extruded products, as has been suggested by Chanvrier et al. (2007).

3.3.8 Texture-Structure relationships

Textural parameters obtained in compression are presented in Table 3-1. Overall, highest crushing force was found under the P water regimen and increased with pomace level, while the lowest force was under E. Wc followed the same trend as F_{cr}, being the lowest under E. Nsr was similar for all regimens, being always lower for P.

The effect of apple pomace in increasing F_{cr} can be explained by a denser structure, with smaller CS and thicker walls. Nevertheless, when analyzing the effect of the water regimens, the relationship between microstructure and texture become more complex. Although treatments under the E regimen had higher CS, which supports a weaker structure (Trater et al., 2005), they

75

also had the lowest VF and very high piece density as compared to the other regimens. In fact, only weak correlations were found between structure and texture parameters, which is a strong indication that the properties of the cell wall material are also critical in determining texture. As has been shown by the previous results, processing under three different water regimens causes unique changes and interactions within the matrix and it can be expected that this would lead to differences in texture, even if similar microstructures were formed.

The fact that the E regimen had lower F_{cr} is likely a reflection of incomplete gelatinization of starch, thus a continuous matrix of amorphous starch was not created during processing. The native granules are discontinuities that act as weak points where fracture is more likely to occur. The concept of poor mixing and creation of heterogeneous distribution of nuclei also supports a weaker structure. Heterogeneous distribution would lead to a large spread in CS and CWT, which was in fact the case for treatments under E. This is supported by the findings of Babin et al. (2007), who found that mechanical resistance is inversely related to the spread in CS and CWT distribution, with thickness having the more important contribution.

3.4 Conclusions

Overall the results support that small changes in the opportunity for hydration cause an important impact in the degree of starch transformation and extrudate properties in both cornmeal alone and in cornmeal/apple pomace blends. The results support that addition of water into the extruder barrel allows for insufficient time for water incorporation in high fiber systems. While the plasticizing effect of sugars seemed to be a dominating event caused by pomace, when comparing within the same pomace level there was a clear impact of hydration on structure

formation. Therefore, water addition regimen may be used as a tool to achieve a desired microstructure and/or texture. This work also presents preconditioning as a viable way of altering starch digestibility patterns within the same formulation, with reduced opportunity for hydration limiting starch digestibility. Apple pomace was found to limit starch digestibility by reducing starch transformation and creating a more compact structure.

References

AACC International. Methods of Analysis, 11th Ed. Method 44-19.01. Moisture- Air oven method, drying at 135°. Approved November 3, 1999. AACC International, St. Paul, MN, U.S.A. doi: 10.1094/AACCIntMethod-44-19.01.

Agbisit R. (2007). *Relationships between material properties and microstructure-mechanical attributes of extruded biopolymeric foams.* PhD dissertation. Department of Grain Science and Industry, College of Agriculture, Kansas State University, Manhattan, KS. pp. 38-71.

Agbisit, R., Alavi, S., Cheng, E. Z., Herald, T., & Trater, A. (2007). Relationships between microstructure and mechanical properties of cellular cornstarch extrudates. *Journal of Texture Studies, 38*(2), 199-219.

Altan, A., McCarthy, K. L., & Maskan, M. (2008). Twin-screw extrusion of barley-grape pomace blends: Extrudate characteristics and determination of optimum processing conditions. *Journal of Food Engineering, 89*(1), 24-32.

Altan, A., McCarthy, K. L., & Maskan, M. (2009). Effect of extrusion cooking of functional properties and in vitro starch digestibility of barley-based extrudates from fruit and vegetable by-products. *Journal of Food Science, 74*(2), E77-E86.

Anderson, R.A., Conway, H.F., Pfeifer, V.F. & Griffin, E.L. (1969). Gelatinization of corn grits by roll and extrusion cooking. *Cereal Science Today*, 14, 4-12.

Babin, P., Della Valle, G., Dendievel, R., Lourdin, D., & Salvo, L. (2007). X-ray tomography study of the cellular structure of extruded starches and its relations with expansion phenomenon and foam mechanical properties. *Carbohydrate Polymers, 68*(2), 329-340.

Björck, I. & Elmstahl, H.L. (2003). The glycaemic index: importance of dietary fibre and other food properties. *Proceedings of the Nutrition Society*, 62, 201-206.

Bouvier, J. M., Bonneville, R., & Goullieux, A. (1997). Instrumental methods for the measurement of extrudate crispness. *Agro Food Industry Hi-Tech, 8*(1), 16-19.

Brennan, M.A., Merts, I., Monro, J., Woolnough, J. & Brennan, C.S. (2008). Impact of guar gum and wheat bran on the physical and nutritional quality of extruded breakfast cereals. *Starch/Stärke*, 60, 248-256.

Brennan, C.S. & Tudorica, C.M. (2007). Fresh pasta quality as affected by enrichment of nonstarch polysaccharides. *Journal of Food Science*, 72(9), S659-S665.

Camire, M.E., King, C.C. & Bittner, D.R. (1991). Characteristics of extruded mixtures of cornmeal and glandless cottonseed flour. *Cereal Chemistry*, 68(4), 419-424.

Chanvrier, H., Appelqvist, I. A. M., Bird, A. R., Gilbertt, E., Htoon, A., Li, Z., Lillford, P. J., Lopez-Rubio, A., Morell, M. K., & Topping, D. L. (2007). Processing of novel elevated amylose wheats: Functional properties and starch digestibility of extruded products. *Journal of Agricultural and Food Chemistry, 55*(25), 10248-10257.

Chinnaswamy, R. & Hanna, M.A. (1991). Physicochemical and macromolecular properties of starch-cellulose fiber extrudates. *Food Structure, 10*, 229-239.

Dust, J.M., Gajda, A.M., Flickinger, E.A., Burkhalter, T.M., Merchen, N.R. & Fahey Jr., G.C. (2004). Extrusion conditions affect chemical composition and in vitro digestion of select food ingredients. *Journal of Agricultural and Food Chemistry*, 52, 2989-2996.

Englyst, H.N., Kingman, S.M. & Cummings, J.H. (1992). Classification and measurement of nutritionally important starch fractions. *European Journal of Clinical Nutrition*, 46(S2), S33-S50.

Englyst, K.N., Englyst, H.N., Hudson, G.J., Cole, T.J. & Cummings, J.H. (1999). Rapidly available glucose in foods: an in vitro measurement that reflects the glycemic response. *American Journal of Clinical Nutrition*, 69, 448-454.

Gonera, A. & Cornillon, P. (2002). Gelatinization of starch/gum/sugar systems studied by using DSC, NMR, and CSLM. *Starch/Stärke*, 54(11), 508-516.

Jalabert-Malbos, M-L., Mishellany-Dutour, A., Woda, A. & Peyron, M-A. (2007). Particle size distribution in the food bolus after mastication of natural foods. *Food Quality and Preference*, 18(5), 803-812.

Jin, Z., Hsieh, F. & Huff, H.E. (1994). Extrusion cooking of corn meal with soy fiber, salt and sugar. *Cereal Chemistry, 71*(3), 227-234.

Karkle, E.L., Alavi, S., Dogan, H., Shi, Y.C., Keller, L. & Haub, M. (2010). Role of cellular architecture and solid matrix properties on texture of high fiber expanded products. AACC Intl Annual Meeting, oral presentation. October 24-27, Savannah, GA.

Kim, S-K. & Kwak, J-E. (2009). Formation of resistant starch in corn starch and estimation of its content from physicochemical properties. *Starch/Stärke*, 61(9), 514-519.

Liu, H., Xie, F., Yu, L., Chen, L. & Li, L. (2009). Thermal processing of starch-based polymers. *Progress in Polymer Science*, 34, 1348-1368.

Lue, S., Hsieh, F., & Huff, H. E. (1991). Extrusion Cooking of Corn Meal and Sugar-Beet Fiber - Effects on Expansion Properties, Starch Gelatinization, and Dietary Fiber Content. *Cereal Chemistry, 68*(3), 227-234.

Mathew, J.M., Hoseney, R.C. & Faubion, J.M. Effect of corn moisture on the properties of pet food extrudates. *Cereal Chemistry*, 76(6), 953-956.

Ortiz, J.A.R., Carvalho, C.W.P. de, Aschieri, D.P.R., Aschieri, J.L.R. & Andrade, C.T. de. (2010). Effect of sugar and water contents on non-expanded cassava flour extrudates. *Ciencia e Tecnologia de Alimentos*, 30(1), 205-212.

Ryu, G.H. & Ng, P.K.W. (2001). Effects of selected process parameters on expansion and mechanical properties of wheat flour and whole cornmeal extrudates. *Starch/Stärke*, 53, 147-154.

Silvester, K.R., Englyst, H.N. & Cummings, J.H. (1995). Ileal recovery of starch from whole diets containing resistant starch measured in-vitro and fermentation of ileal effluent. *American Journal of Clinical Nutrition*, 62(2), 403-411.

Singh, J., Dartois, A. & Kaur, L. (2010) Starch digestibility in food matrix: a review. *Trends in Food Science and Technology*, 21, 168-180.

Singh, N., Inouchi, N. & Nishinari, K. (2005). Morphological, structural, thermal, and rheological characteristics of starches separated from apples of different cultivars. *Journal of Agricultural and Food Chemistry*, 53(26), 10193-10199.

Slaughter, S.L., Ellis, P.R., Jackson, E.C. & Butterworth, P.J. (2002). The effect of guar galactomannan and water availability during hydrothermal processing on the hydrolysis of starch catalysed by pancreatic aplpha-amylase. *Biochimica et Biophysica Acta*, 1571(1), 55-63.

Stojceska, V., Ainsworth, P., Plunkett, A. & Ibanoglu, S. (2009). The effect of extrusion cooking using different water feed rates on the quality of ready-to-eat snacks made from food by-products. *Food Chemistry, 114*, 226-232.

Tester, R.F & Sommerville, M.D. (2003). The effects of non-starch polysaccharides on the extent of gelatinization, swelling and alpha-amylase hydrolysis of maize and wheat starches. *Food Hydrocolloids*, 17, 41-54.

Trater, A. M., Alavi, S., & Rizvi, S. S. H. (2005). Use of non-invasive X-ray microtomography for characterizing microstructure of extruded biopolymer foams. *Food Research International, 38*(6), 709-719.

Xie, F., Liu, H., Chen, P., Xue, T., Chen, L., Yu, L. & Corrigan, P. (2006). Starch gelatinization under shearless and shear conditions. *International Journal of Food Engineering*, 2(5), 1-29.

Wen, L.F., Rodia, P. & Wasserman, B.P. (1990). Starch fragmentation and protein insolubilization during twin-screw extrusion of corn meal. *Cereal Chemistry*, 67, 268-275.

Yagci, S., & Gogus, F. (2008). Response surface methodology for evaluation of physical and functional properties of extruded snack foods developed from food-by-products. *Journal of Food Engineering, 86*(1), 122-132.

Yagci, S. & Gogus, F. (2010). Effect of incorporation of various food by-products on some nutritional properties of rice-based extruded foods. *Food Science and Technology International*, 15(6), 571-581.

Zhang, W. & Hoseney, R.C. (1998). Factors affecting expansion of corn meals with poor and good expansion properties. *Cereal Chemistry*, 75(5), 639-643.

Figures and Table

Inlet	75℃	75℃	75℃	90℃	110℃

3/4pitch, 78 mm

3/4pitch, 78 mm

Full pitch, 78 mm

Full pitch, 78 mm

7x 90° kneading block, 8.7mm (total 60.9mm)

3/4pitch, 78 mm

3/4pitch, 78 mm

3/4pitch, 78 mm

1/2pitch, 52 mm

2x 90° kneading block, 8.7mm (total17.4mm)
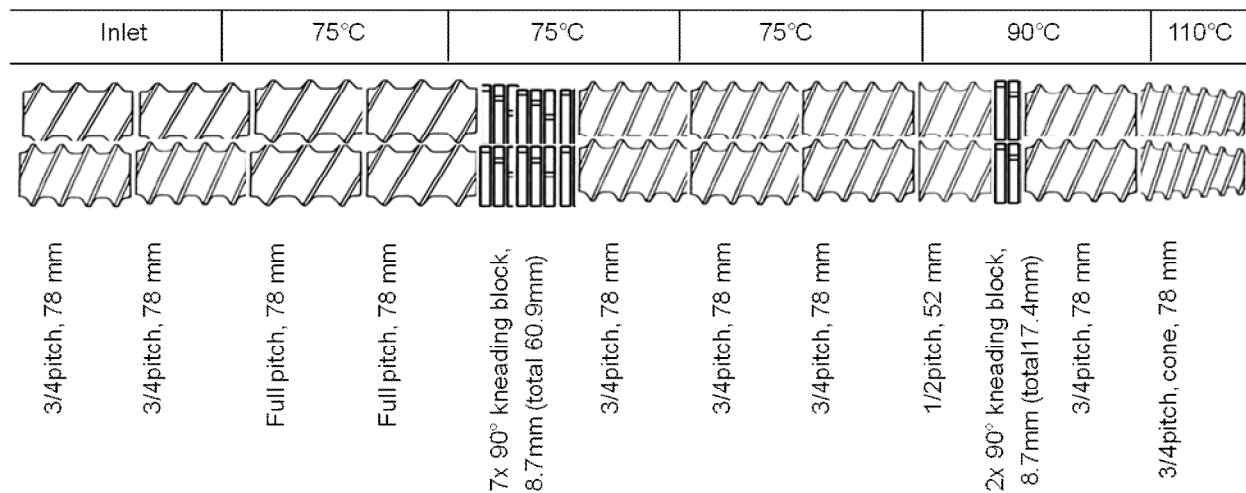
3/4pitch, 78 mm

3/4pitch, cone, 78 mm

Figure 3-1 Screw configuration and temperature profile. All elements double flighted, except for first two elements on right shaft (single flight).
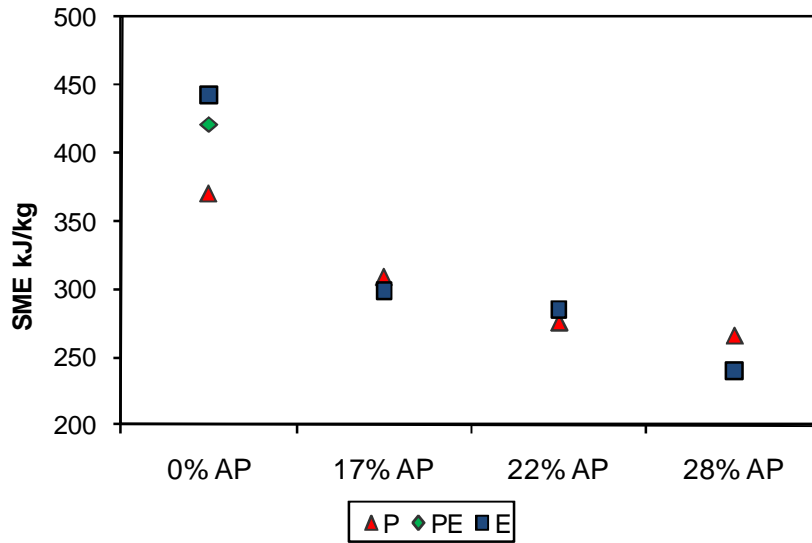
Figure 3-2 Specific mechanical energy (SME). AP: apple pomace; PE, P and E refer to water addition regimen (see text).
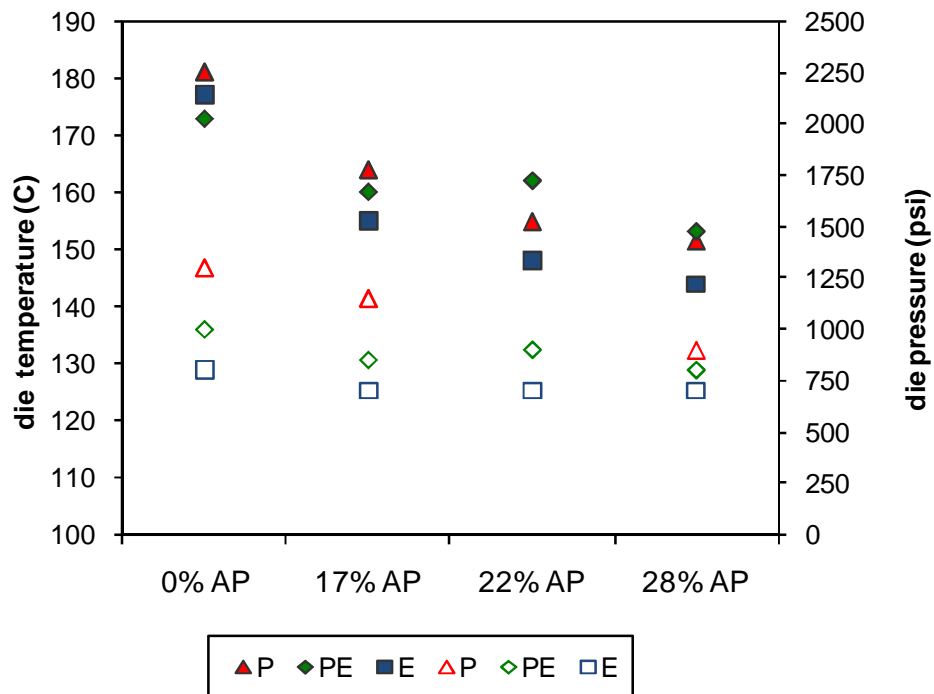
Figure 3-3 Product temperature (left axis; solid symbols) and die pressure (right axis; open symbols). AP: apple pomace; PE, P and E refer to water addition regimen (see text).
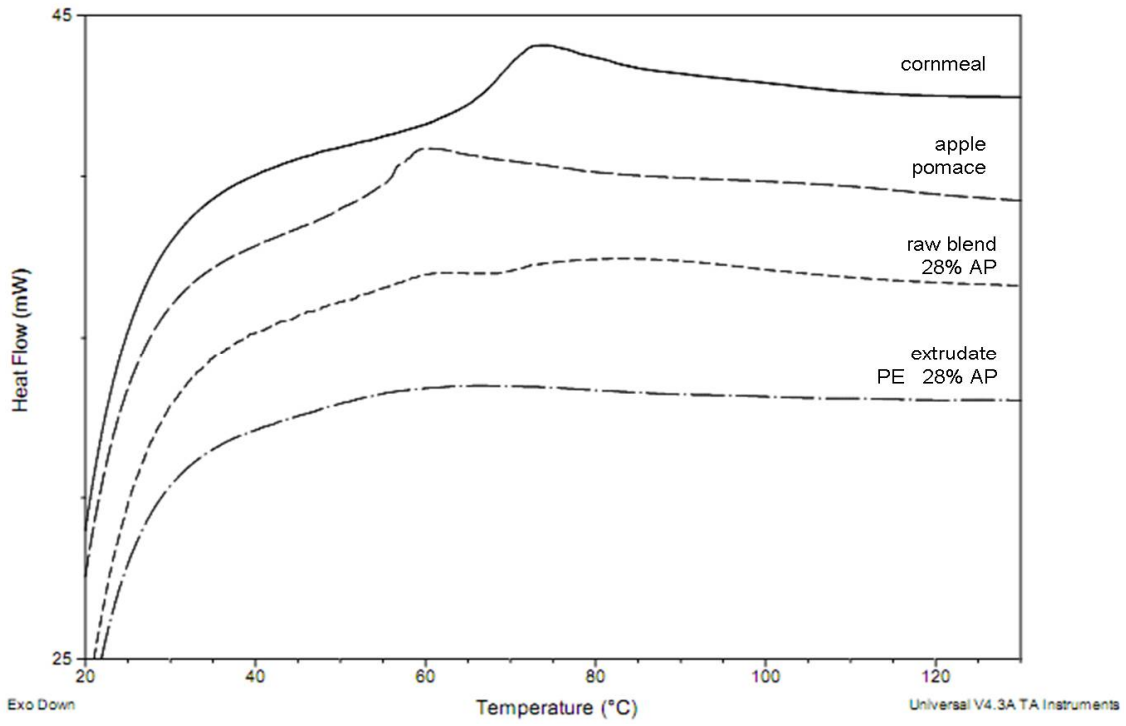
Figure 3-4 DSC thermogram for raw materials, raw blend and extruded product (shown for 28% apple pomace addition). PE refers to water addition regimen (see text).
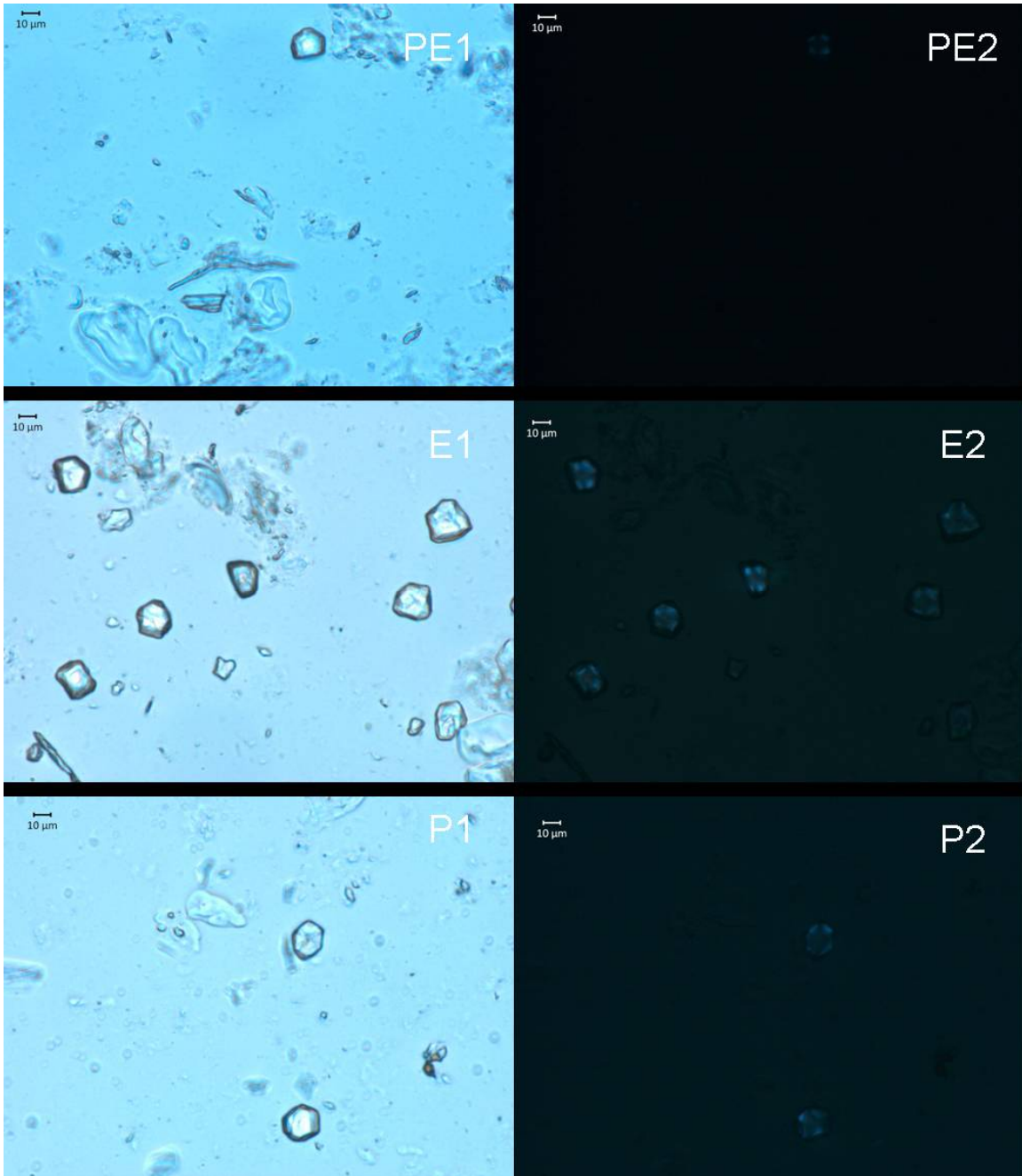
Figure 3-5 Extrudates with 22% apple pomace viewed under bright field (1) and polarized light (2). PE, P and E refer to water addition regimen (see text).
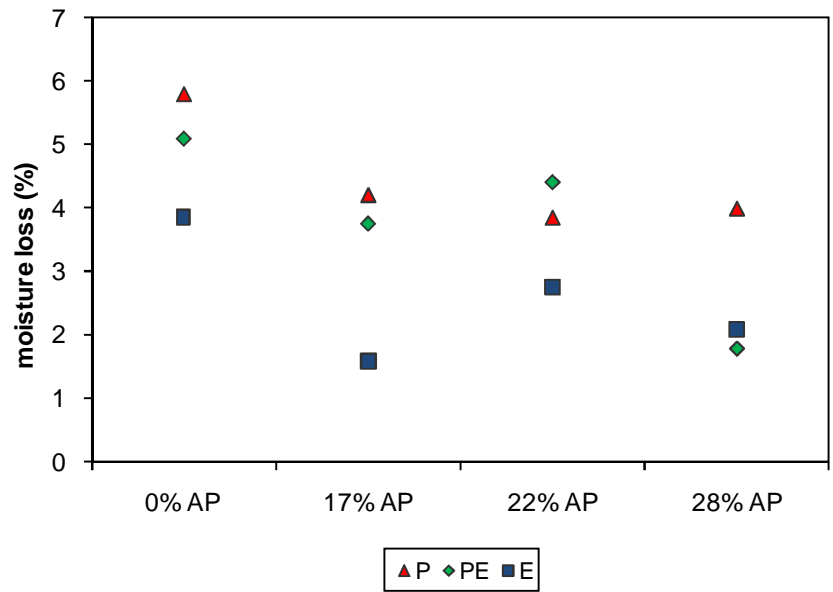
Figure 3-6 Moisture loss at the die. AP: apple pomace; PE, P and E refer to water addition regimen (see text).

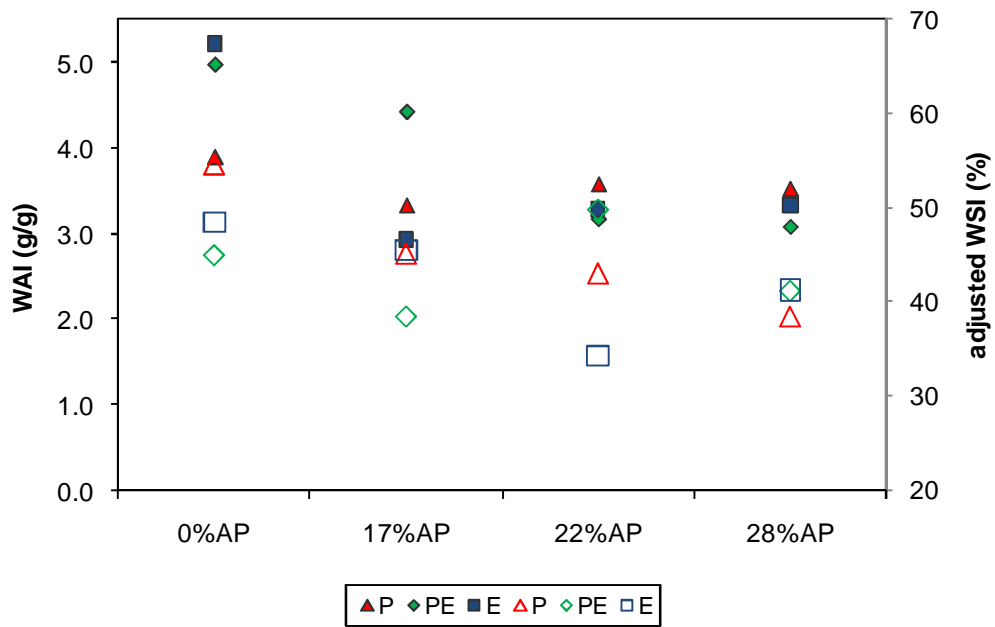Figure 3-7 Water absorption index (WAI, left axis, solid symbols) and adjusted water solubility index (WSI, right axis, open symbols). AP: apple pomace; PE, P and E refer to water addition regimen (see text).
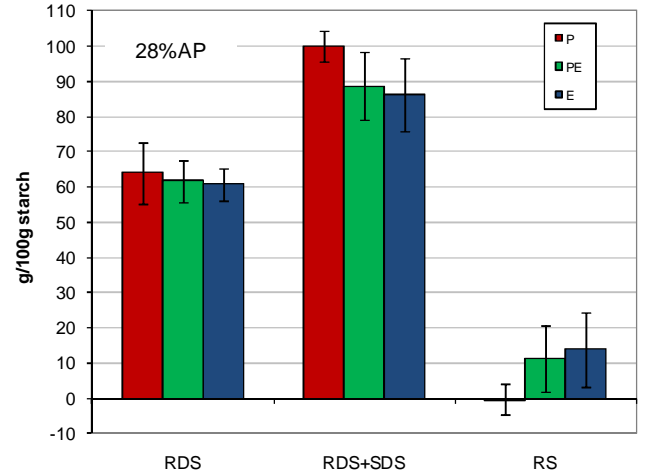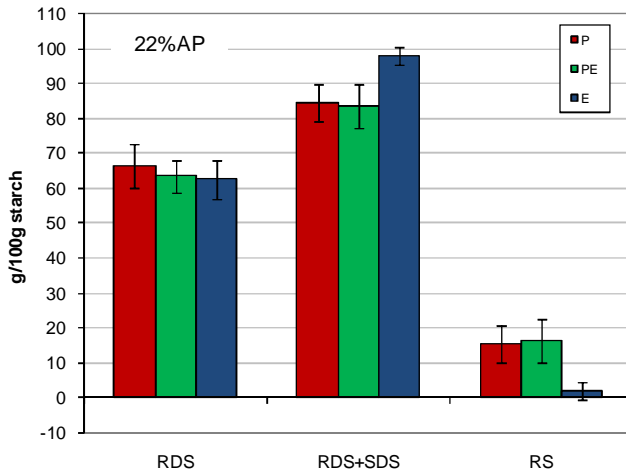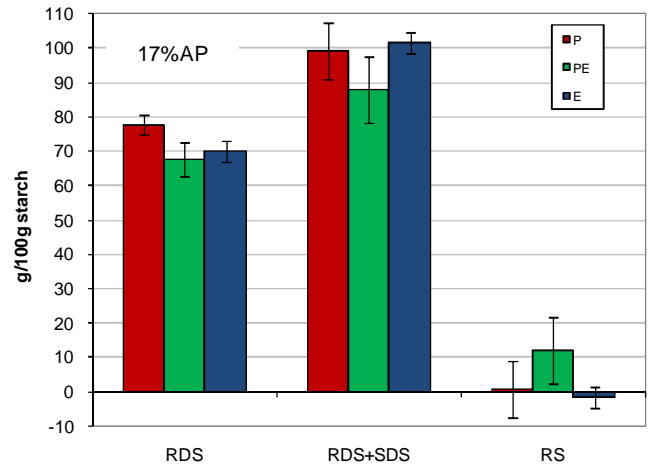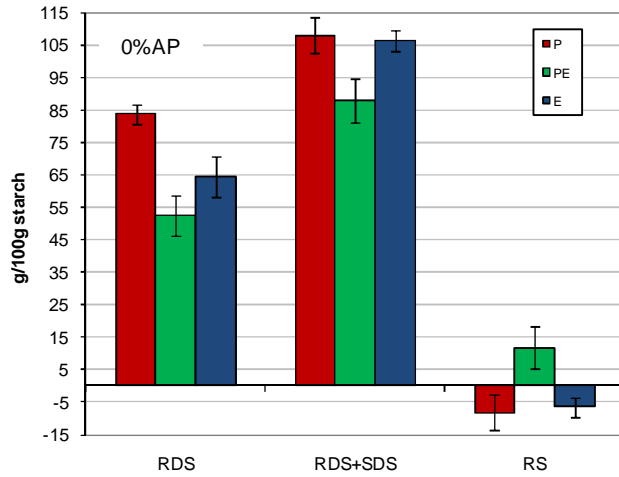
Figure 3-8 In vitro digestibility. RDS: rapidly digestible starch; SDS: slowly digestible starch; RS: resistant starch; AP: apple pomace; PE, P and E refer to water addition regimen (see text).
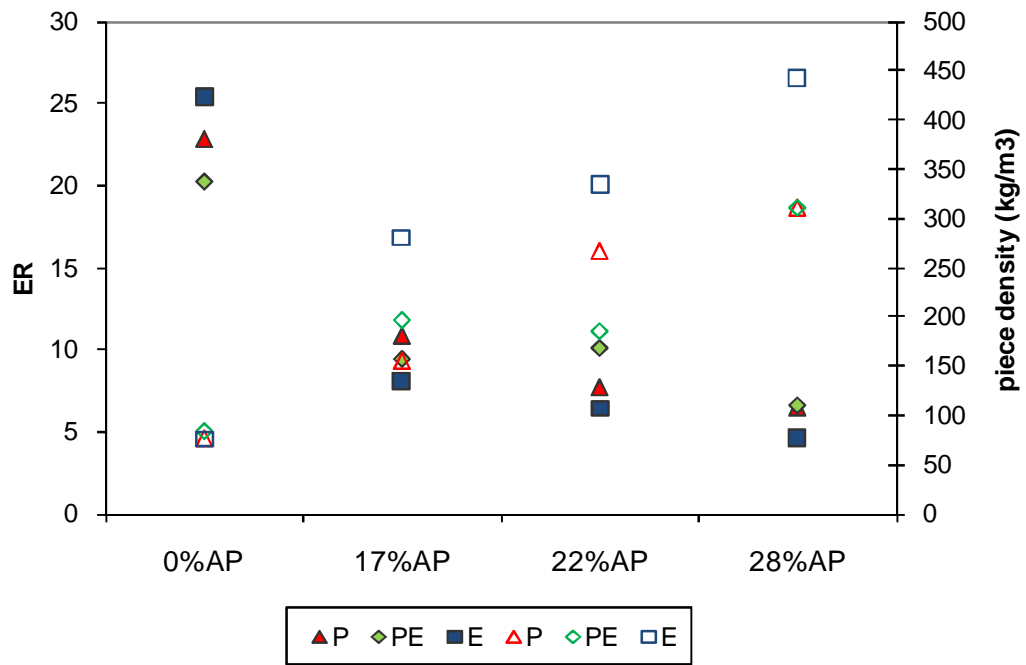
Figure 3-9 Expansion ratio –ER (solid symbols) and piece density (open symbols) of extrudates. AP: apple pomace; PE, P and E refer to water addition regimen (see text).

	0% AP	17% AP	22% AP	28% AP
P				10 mm
PE				
E				
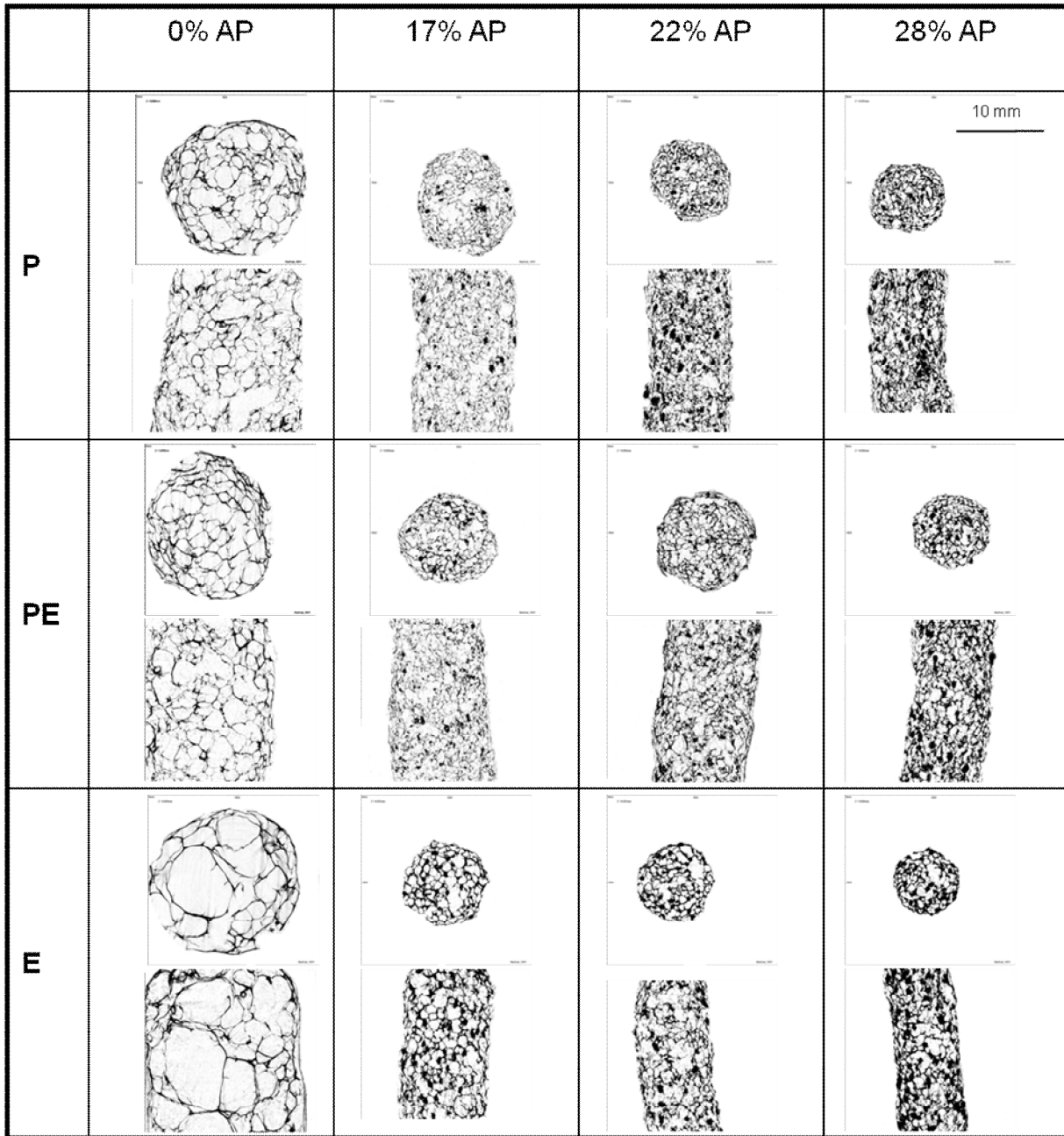
Figure 3-10 Representative XMT images of samples in radial (top) and longitudinal views (bottom).
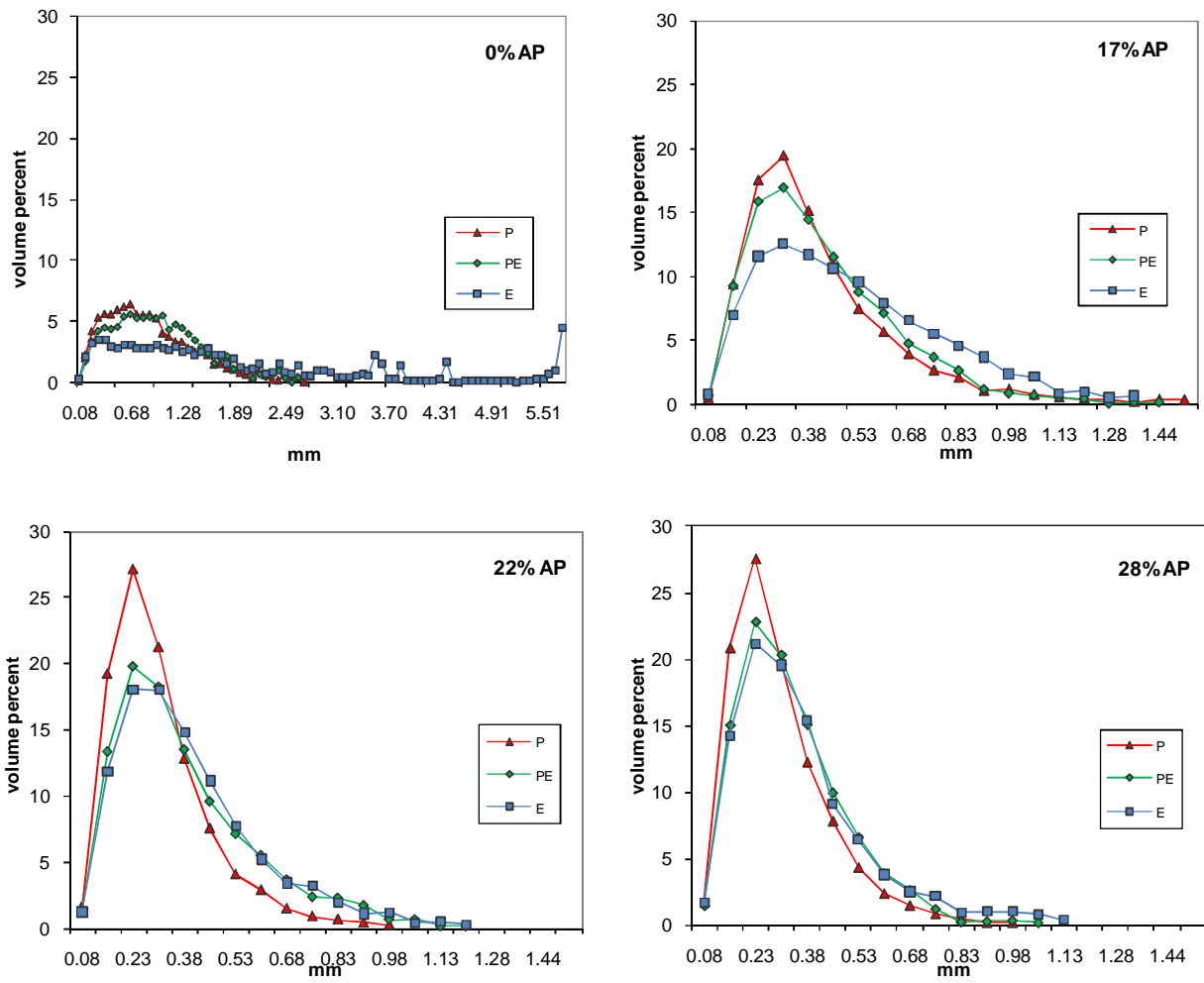
Figure 3-11 Cell size - volumetric distribution. Note difference in scale for 0% AP (x axis). AP: apple pomace; PE, P and E refer to water addition regimen (see text).
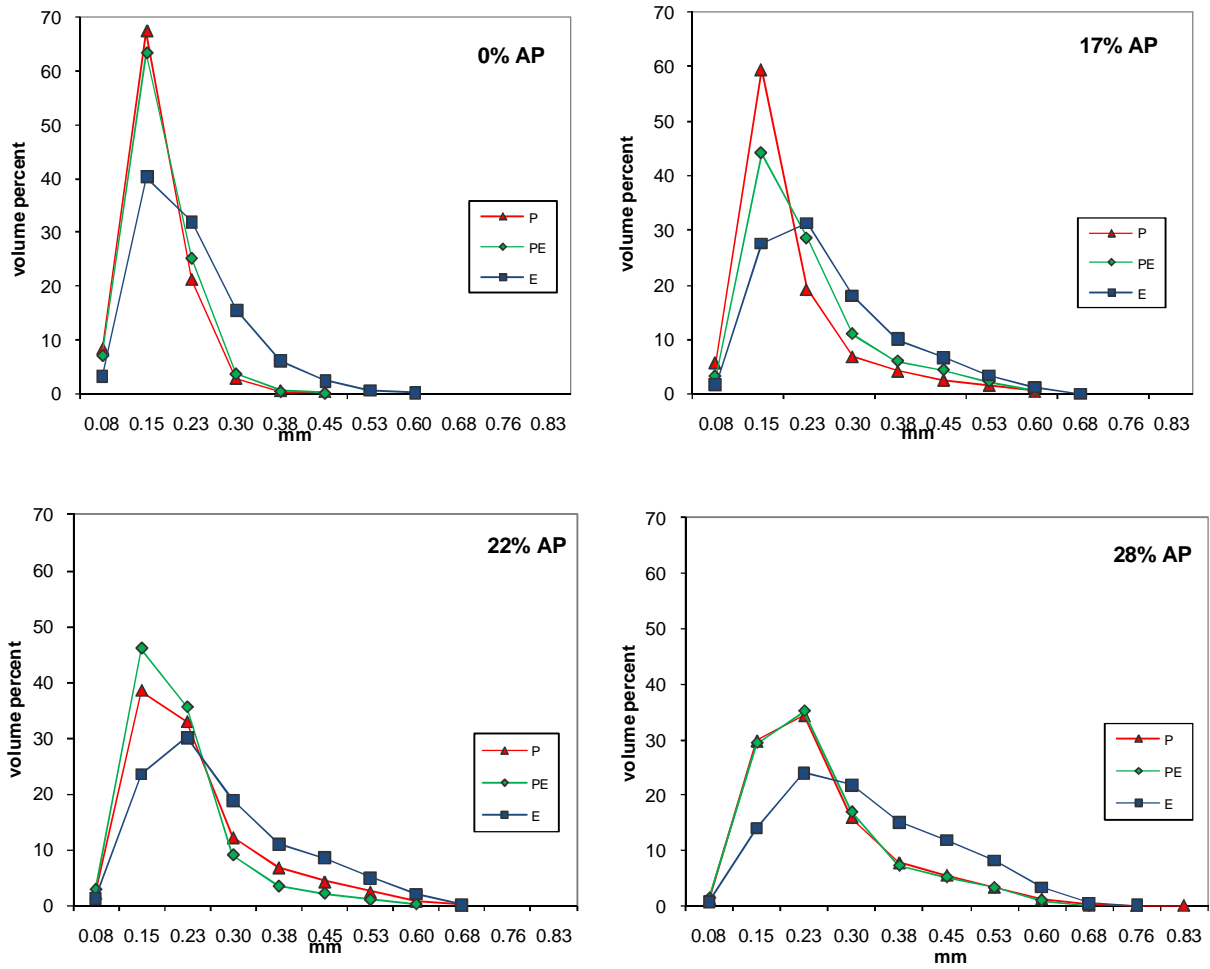
Figure 3-12 Cell wall thickness - volumetric distribution. AP: apple pomace; PE, P and E refer to water addition regimen (see text).
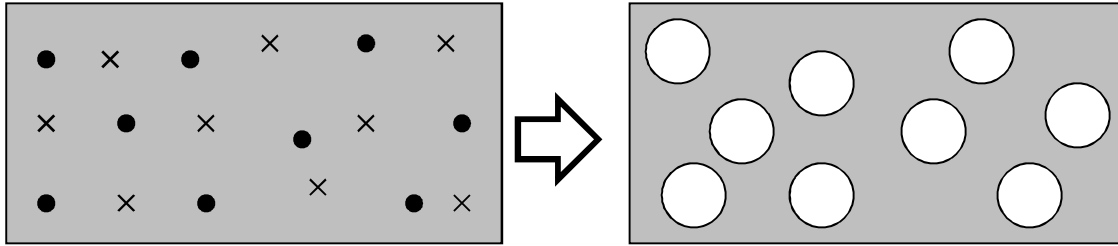
a. Even mixing of water in matrix promotes homogeneous movement of vapor into nuclei, resulting in even cell size distribution
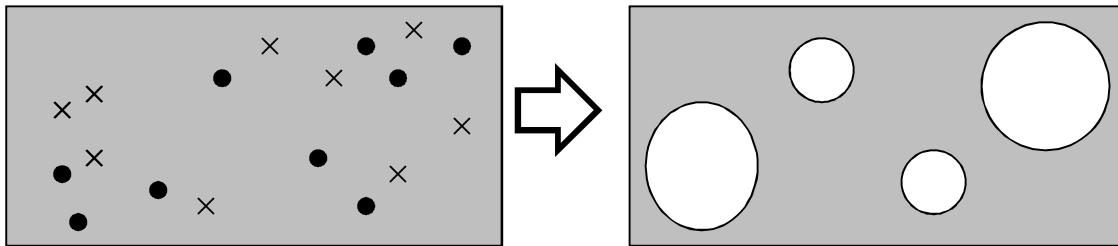
b. Poor hydration promotes heterogeneous movement of vapor . Nearby cells merge, isolated cells remain small, resulting in broad cell size distribution

Figure 3-13 Schematic of effect of hydration on microstructure. Black circles indicate nuclei, black crosses indicate water and white symbols indicate air cells.
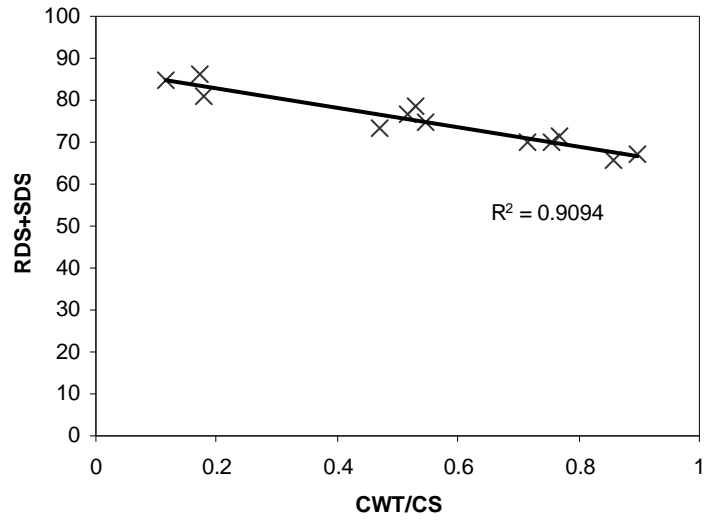
Figure 3-14 Available starch (RDS+SDS) versus ratio of cell wall thickness to cell size (CWT/CS).

Table 3-1 Microstructural and textural parameters of extrudates.

Water addition regimen	Apple pomace level (%)	VF (%)	CS (mm)	CWT (mm)	F_{cr} (N)	N_{sr} (mm^{-1})	W_c (N.mm)
PE	0	86.36	1.01	0.17	66.6	0.85	81.6
	17	65.68	0.43	0.22	101.9	0.68	146.6
	22	58.54	0.38	0.21	122.2	0.86	146.5
	28	50.59	0.33	0.25	127.7	0.82	159.9
E	0	83.05	1.88	0.22	30.9	0.88	35.5
	17	59.58	0.51	0.26	79.5	1.02	79.8
	22	51.42	0.39	0.28	106.6	0.85	128.5
	28	41.01	0.36	0.32	114.4	0.89	138.8
P	0	85.81	0.94	0.17	73.6	0.85	87.1
	17	72.75	0.42	0.20	152.6	0.67	238.0
	22	52.91	0.31	0.23	142.3	0.74	206.5
	28	47.22	0.30	0.26	142.5	0.75	198.1

VF: void fraction; CS: average cell size; CWT: average cell wall thickness; F_{cr}: average crushing force; N_{sr}: frequency of spatial ruptures; W_c: crispness work. PE, P and E refer to water addition regimen (see text).

CHAPTER 4 - Interactions and functionality of fiber components in a directly expanded starch matrix

Abstract

The objective of this work was to determine the effect of cellulose, hemicellulose, pectin, and lignin on the properties of a directly expanded starch-based matrix as well as their interactions with the matrix. Fibers were blended with cornstarch and the impact on gelatinization parameters and softening and flow temperatures of the blends was measured. Blends were extruded on a twin-screw extruder under typical conditions for directly expanded products. Macrostructure of the extrudates was evaluated for sectional expansion, piece density, and specific length. Microstructure was evaluated using X-ray microtomography to obtain void fraction, average cell size, and cell wall thickness. Mechanical properties of the expanded extrudates were measured in compression and films cast from ground extrudates were used for tensile testing. The soluble fibers were found to increase gelatinization temperatures, indicating competition for water. The radial expansion of treatments with pectin (24.7-27.8), xyloglucan (22.4-25.5), and lignin (23.5-23.6) was equal or higher than the starch-only control (22.7). Overall expansion with cellulose was decreased, as indicated by reduced void fraction and expansion ratio. Crushing force was related to cell size. Tensile strength and percentage elongation decreased for cellulose, but was equal to or higher than the control for the other fibers, indicating their compatibility with the starch matrix. Compatibility was related to the availability of groups to interact with starch, but not solubility of the dietary fiber component.

4.1 Introduction

Interest in the incorporation of fruit and vegetable by-products into extruded snacks and breakfast cereals is growing. Several authors have demonstrated that this results in increased dietary fiber and antioxidant content, along with more desirable starch digestibility patterns (Karkle et al, 2011; Yagci and Gogus, 2010; Altan et al., 2009; Stojceska et al., 2009). However, the reports also show that the fruit and vegetable fibers cause marked structural and textural changes when compared to the typical refined grain formulation.

Dietary fibers found in the plant cell wall are the main constituents of fruit and vegetable pomace; they include cellulose, hemicellulose, lignin, and pectin. Although vast literature concerns the incorporation of different fiber sources into directly expanded products, few studies use each type of fiber as an individual component. Cellulose is the isolated fiber component that has received the most attention; its effect on expansion in terms of macrostructure is well established. Chinnaswamy and Hanna (1991) reported that cellulose levels greater than 2% decreased expansion due to changes in starch fragmentation and dilution of starch content. Camire and King (1991) attributed reduced expansion to the water-binding capacity of cellulose, finding it responsible for reducing starch gelatinization and therefore its capacity to form film.

The study by Yanniotis et al. (2007) confirmed the previous data for cellulose but showed a very different effect for pectin. The authors reported that the addition of 10% pectin had no impact on the microstructure of extrudates. Furthermore, pectin increased porosity of the samples and decreased hardness compared to a cornstarch control. According to the authors, pectin increased the extensibility of the extrudate cell walls, although this conclusion was based on expansion characteristics rather than direct testing of the matrix.

Along these same lines, other authors have found that highly soluble and branched plant fibers did not reduce expansion, but expanded comparably to the flour or starch control (Pai et al., 2009; Brennan et al., 2008; Adamu and Jin, 2002). This suggests that such structure may allow for dispersion of the fiber in the starch matrix, thus forming a composite material with good extensibility. On the other hand, linear and insoluble fibers act as dispersed fillers, promoting discontinuities in the matrix and reducing extensibility (Jain et al., 2011; Moraru and Kokini, 2003).

Therefore, the objective of this work was to determine the effect of cellulose, hemicellulose, pectin, and lignin on the properties of a directly expanded starch-based matrix and their interactions with the matrix. The microstructure and texture resulting from the individual fiber component also was studied. A better understanding of the impact of the individual fiber component on expansion and structure formation would provide a strong basis for selecting fruit and vegetable by-products with better functionality. With this in mind, the fibers were used in concentrations consistent with their natural occurrence in fruit and vegetable pomaces, as well as acceptable inclusion levels in directly expanded products.

4.2 Materials and methods

4.2.1 Materials and blend formulation

Normal cornstarch was obtained from Cargill (Wayzata, MN). The following plant fibers were used: cellulose (pure bamboo fiber - BF200, International Fiber Corp., North Tonawanda,

NY), pectin (high methoxyl, Obipektin, Naturex, South Hackensack, NJ), lignin (kraft lignin, Indulin AT, MeadWestvaco, Richmond, VA) and hemicellulose (xyloglucan from tamarind, Shaanxi Top Pharm Chemical, Xi'an, China). Particle size of each material was determined by laser diffraction (LS 13320 Laser Diffraction PS Analyzer, Beckman Coulter, Brea, CA).

Fibers were analyzed for neutral detergent fiber, acid detergent fiber, and acid detergent lignin to obtain cellulose, hemicellulose, and lignin contents. Insoluble and soluble dietary fiber were determined using the Megazyme Total Dietary Fiber Assay Procedure (K-TDFR 06/07), which is based on AACC method 32-07. Briefly, the sample was hydrolyzed with α-amylase, protease, and amyloglucosidase. The solution was filtered and the residue collected as the insoluble fiber portion. Soluble fiber in the filtrate was precipitated out with ethanol and collected by filtration. Soluble and insoluble fiber content was corrected for protein and ash in the residues.

Blends of individual fibers at different levels and starch were prepared, along with mixes of the four fibers (levels given in Table 4-1). The levels of addition were chosen to reflect the amount of each component upon the addition of fruit and vegetable pomace to obtain high-fiber snacks (>10% daily value of fiber in 30 g). Average pomace composition was obtained from literature and previous experiments (Karkle et al., 2010; Nawirska and Kwasniewska, 2005). Fiber components and starch were blended in a ribbon mixer for 8 min (model HR2SSS-0106; Hayes and Stolz Ind. Mfg. Co. Ltd., Fort Worth, TX).

4.2.2 Phase transition analysis (PTA)

The blends were analyzed on a Phase Transition Analyzer^{TM} (PTA; Wenger, Sabetha, KS), to determine the softening and flow temperatures. These are analogous to glass transition and melt temperatures, respectively; however, they are a measure of deformation and flow behavior of the material upon heating under constant pressure (Liu et al., 2010; Bengoechea et al., 2007). The blends were hydrated to 19% moisture to reflect the in-barrel moisture during extrusion. A 2-g sample was loaded in the chamber with a closed die underneath, and an initial compression of 12 MPa was applied for 15 s. The pressure was then fixed at 10MPa and the sample was heated at 8 °C/min, with a starting temperature of 1 °C. Softening temperature was obtained from the midpoint between onset and end of softening (identified by chamber displacement over the threshold of 0.0106 mm/°C). After the softening period, the closed die was replaced by a 2-mm capillary die and heating continued at the same rate and operating pressure. The flow temperature was obtained from the temperature at which the material started to flow through the capillary (identified by a steep increase in displacement).

4.2.3 Differential scanning calorimetry (DSC)

The effect of the fibers on starch gelatinization was studied using DSC. Preliminary experiments showed that gelatinization was unchanged when testing at excess moisture (>66%), whereas at the in-barrel moisture (19%) no endotherm could be detected. Using a moisture content of 55% ensured that most of the starch would gelatinize, water would remain limited, and interference of the fibers could be detected. The blends were weighed into high-volume

stainless steel pans, the required amount of water was added, and pans were sealed and allowed to hydrate overnight at room temperature. The samples were scanned against an empty pan at a heating rate of 10 °C/min, from 10 to 140 °C (Q100, TA Instruments, New Castle, DE).

4.2.4 Extrusion processing

Extrusion processing was carried out on a pilot-scale twin-screw extruder (TX-52, Wenger Manufacturing, Sabetha, KS) equipped with a differential diameter cylinder preconditioner. The dry blend was fed at 50kg/h and water addition was distributed between the preconditioner (3.2 kg/h) and extruder (2.5 kg/h), for an in-barrel moisture of 19.1 ±0.5% wet basis. The extruder setup consisted of a screw profile typical for directly expanded snacks (Figure 4-1). Screw diameter was 52 mm and L/D ratio was 16. The screw speed was fixed at 300 rpm for all treatments. A one-opening circular die of 3.6 mm was used. Product was cut at the die exit and conveyed to a dual pass dryer (4800, Wenger Manufacturing, Sabetha, KS) at 115 °C for 18 min, followed by a 7-min cooling step. Samples were immediately transferred to thick polyethylene bags and stored at room temperature until analysis.

The specific mechanical energy (SME) for each treatment was calculated using

$$SME = \frac{\frac{(T - T_0)}{100} \times \frac{N}{N_r} \times P_r}{\overset{\bullet}{m}} \quad \text{(kJ/kg)} \tag{1}$$

where N = screw speed, N_r = rated screw speed (508rpm), T = torque, T_0 = no-load torque (5%),

P_r = rated motor power (37.9 kW), and $\dot{m}$ = mass flow rate (kg/s).

4.2.5 Macrostructure

The length (l_e), diameter (D_e), and weight (m_e) were measured for 20 pieces of dried product from each treatment, and were used to obtain the radial expansion ratio (ER), specific length (l_{sp}), and piece density (ρ).

$$ER = \frac{D_e{}^2}{D_d{}^2} \tag{2}$$

$$l_{sp} = \frac{l_e}{m_e} \qquad \text{(mm/g)} \tag{3}$$

$$\rho = \frac{m_e}{\left[3.14 * \left(\dfrac{D_e}{2}\right)^2 * l_e\right]} \qquad \text{(kg/m}^3) \tag{4}$$

where D_d = die diameter.

4.2.6 Microstructure

Microstructural features of the extrudates were analyzed using X-ray microtomography (XMT). One piece of each treatment was scanned. To ensure that the samples were representative, the diameter of the scanned piece matched the average diameter for that treatment. Samples were scanned on an XMT system (Model 1072, Skyscan, Belgium) under the following settings: voltage 40 kV, current 244 µA, exposure time 1.2 s, rotation step 0.9°, sample rotation 180°, and magnification 14.48x. Shadow images were reconstructed into a 3D object (software NRecon v. 1.6.1, Skyscan, Belgium) that was virtually sliced into 500 cross-sections and analyzed (CTAn 1.9.1, Skyscan, Belgium). For analysis, a volume of interest (VOI) was determined by setting a region of interest tightly around the perimeter of each cross-section and interpolating for the dataset. The grayscale images within the VOI were converted into binary images with a threshold of 32 (cell walls converted to white pixels and voids converted to black pixels). The despeckling function was applied to the VOI to reduce background noise from the image, and the final processed image was analyzed in 3D. The cell size was obtained from the structure separation function, and cell wall thickness from the structure thickness function. Void fraction was obtained by the ratio of white voxels (cell walls) to total voxels.

4.2.7 Mechanical properties

4.2.7.1 Expanded extrudates

Mechanical properties of the extrudates were analyzed using a texture analyzer (TA-XT2) and the Texture Exponent 5,0,7,0 software (both from Stable Micro Systems, United Kingdom). Twenty pieces of each treatment were equilibrated to moisture content of 4.3 ±0.3% by holding 15 h at 52 °C. A 38-mm compression plate was used to compress the samples to 70% of their original diameter (test speed of 2.0 mm/s). The area under the curve (S) and the number of peaks (n) were obtained from the force-deformation curves and used to calculate the spatial frequency of ruptures (N_{sr}), the average crushing force (F_{cr}), and crispness work (W_c) (Agbisit et al., 2007; Bouvier et al., 1997).

$$N_{sr} = \frac{n}{d} \qquad (\text{mm}^{-1}) \tag{6}$$

$$F_{cr} = \frac{S}{d} \qquad (\text{N}) \tag{7}$$

$$W_c = \frac{F_{cr}}{N_{sr}} \qquad (\text{N.mm}) \tag{8}$$

where d= probe travel distance

4.2.7.2 Films of ground extrudates

To study the effect of fibers on the properties of the starch matrix, films were cast and subjected to tensile testing. Extrudates at the high level of each fiber and the control were ground and suspended in water (4g/100mL) with 15% glycerol (solid base). The addition of glycerol was required to reduce brittleness of the films and enable specimen cutting and testing. The suspension was heated to 95 °C under constant stirring. The temperature was maintained for 10 minutes, then cooled to 65 °C. Solution (20mL) was pipetted into petri dishes and allowed to dry at room temperature for 12 h. The films were conditioned in an environmental chamber at 80% relative humidity for 3 d and cut into strips (15 mm wide and 80 mm long). Tensile strength (TS) and percent elongation (%E) were tested using a texture analyzer (TA-XT2, Stable Micro Systems, United Kingdom), according to the standard method ASTM D882-10 for tensile properties of thin plastic sheeting (ASTM, 2010). Test speed was 1mm/min and gauge length 40 mm. Tensile data was averaged over 3 specimens for each data point (5 per treatment). TS and %E were calculated using the following equations:

$$TS = \frac{L_p}{a} \quad \text{(MPa)} \tag{9}$$

$$\%E = \frac{\Delta l}{l} \times 100 \tag{10}$$

where L_p = peak load (N), a = cross-sectional area of samples (mm^2), Δl = increase in length at breaking point (mm), and l = original length (mm).

4.2.8 Experiment design and statistical analysis

Extrusion processing followed a one-way treatment structure in a randomized complete block design. The blocks were the day of processing (2 d), with one block containing all 16 treatments and the other block a replicate of 12 treatments. For raw blends, the analysis followed a one-way treatment structure in a completely randomized design. All raw blend and extrudate analyses were conducted at least in duplicate.

The analysis was conducted in the ANOVA framework, with the null hypothesis of no difference between treatments. The contrast of the control versus the average of each fiber at the 3 levels was tested for significance. Pairwise comparisons were made using least significant means. Significance was established at $\alpha \leq 0.05$.

4.3 Results and Discussion

4.3.1 Material characterization

Ingredient composition analysis (Table 4-2) revealed how the isolated forms of the fiber differ from less processed forms. For instance, no acid detergent lignin was found in the isolated lignin sample, which indicates that the structure is highly modified during the kraft pulping

process. This process uses alkali to dissolve the lignin and separate it from cellulose, to which is it tightly bound in unprocessed plant cell walls (Kaewtatip et al., 2010). The molecular weight of the polymer is reduced, so changes in analytical and functional characteristics are expected. Nevertheless, this is the only form of lignin commercially available in sufficient quantities to allow for a pilot-scale extrusion experiment (personal communication from the supplier).

Results from analysis of dietary fiber were more consistent with the characteristics of each component in less processed materials, such as pomace. The fiber fraction in cellulose and lignin was mostly insoluble, whereas pectin and xyloglucan had mostly soluble fiber.

The fibers had varying particle sizes (Figure 4-2); pectin was the highest (111.2 μm), and xyloglucan was the lowest (15.7 μm). In cellulose, an increase in particle size (from 20 to 110 μm) has been shown to be detrimental to starch extrudate expansion (Chinnaswamy and Hanna, 1991). The authors reported that as the particle size increased, so did starch degradation. Smaller particles would not disturb the shear field in the extruder as much, thus minimizing degradation. Although this is valid for insoluble cellulose, the effect of soluble fibers cannot be inferred by particle size, but rather through compatibility with the starch matrix.

4.3.2 Phase transition analysis

Softening and flow temperatures (Figure 4-3) are a good indication of the behavior of the blends under extrusion because they are related to polymer interactions and rheological properties of the material (Agbisit, 2007). The T_s of the control was 58.7 ˚C, and addition of fibers to starch caused the T_s to decrease overall. The reduction was significant for lignin, xyloglucan, and the mix. Reduced T_s can be due to the reduction in starch content. The native

starch granule has a highly ordered structure, with crystalline and amorphous regions that require moisture and heat to be plasticized. The moisture content used for the phase transition experiments (19%) is insufficient to allow for complete granule hydration, thus strong interactions between starch molecules remain. When starch is replaced with fibers, these interactions are reduced and the material is more easily compacted.

T_f of the blends varied from 129 to 154 ˚C (Figure 3). The effect of lignin, xyloglucan and the mix was not significant, but across the three levels cellulose and pectin caused an increase in T_f. The higher T_f for pectin is likely due to the viscosity-building properties of this fiber. In the case of cellulose, the increase in T_f reflects the fiber's resistance to flow. T_f as it relates to processing and structure formation is discussed in more detail in sections 3.4 and 3.5.

4.3.3 DSC

DSC revealed the effect of fiber in restricting starch gelatinization (Table 4-3). Pectin, xyloglucan, and the mix caused the most restriction, as evidenced by an increase in peak and end temperatures. Pectin and xyloglucan are highly soluble and readily absorb water. Less water becomes available for starch, which then requires higher temperature to gelatinize (Santos et al., 2008; Khanna and Tester, 2006). In the mix both pectin and xyloglucan were present, thus increasing competition for water, even with lower starch content. The enthalpy of gelatinization was not significantly decreased by any fiber, so complete gelatinization was achieved (or the maximum possible at that particular moisture content).

All blends with pectin showed a trailing shoulder on the main gelatinization peak (Figure 4-4). This has been observed by various authors and is referred to as the M endotherm (Goldstein

et al., 2010; Khanna and Tester, 2006; Wang and Kim, 1998). The M endotherm indicates that water is limited; therefore, crystallite dissociation assumes a bimodal configuration, less perfect crystals dissociate at lower temperatures, and a group of more ordered crystallites requires further heating.

4.3.4 SME

The fibers caused a slight but non-significant reduction in SME (p=0.2573; Figure 4-5). Reduced energy input is related to the lower T_s for some blends. Materials with lower softening temperatures can be easier to plasticize during extrusion and can provide less restriction to the shearing action of the screws. All levels of the mix caused unstable feeding because of fluctuations in the feed rate and motor load, which may be a contributing factor to lower SME.

Pectin and cellulose had significantly higher T_f compared to the control, but this was not reflected in higher SME as expected. Although both SME and T_f give indications of viscosity, the shear in the extruder is the main difference between both systems. Pectin may have developed viscosity in the PTA, but under shear the polymers can be cleaved (Hwang et al., 1997). Starch also can be cleaved, and Chinnaswamy and Hanna (1991) found that cellulose increased starch depolymerization during extrusion. Therefore, both pectin and cellulose potentially increase the resistance to flow when blended with starch, but polymer transformations during extrusion may have prevented this from being reflected in higher mechanical energy input.

4.3.5 Macrostructure

Overall, the effect of the fibers on expansion ratio was insignificant at the low level, but became important at the higher levels (Figure 4-6). Pectin caused a substantial increase in radial expansion (34%). Lignin and xyloglucan were equal to the control (p=0.6153 and p=0.0726, respectively), and cellulose and the mixes caused a sharp decrease. Such effects are the result of several mechanisms. The driving force for expansion is the difference in vapor pressure inside the nucleated cells and outside the die (Moraru and Kokini, 2003). Whether the driving force will translate into expansion depends on the viscosity of the melt and its extensibility. These determine the resistance to expansion of the cells as the material exits the die. At low viscosity the melt will initially expand, but the lack of resistance will cause some bubbles to rupture and the structure will collapse during cooling. At an ideal viscosity the structure is fluid enough to expand during vapor flash-off, but viscous enough to hold the structure of the expanded bubbles until the material has cooled past its glass transition temperature, thus minimizing collapse. If the material has a high viscosity it will resist bubble growth, limiting expansion. The T_f can be used to assess the potential of the blend for expansion. High T_f reflects high viscosity-building ability, thus the ability to increase pressure and the driving force for expansion. In the case of an extensible matrix (starch with pectin), this will result in high expansion. For a poorly extensible matrix (starch with cellulose), the increased driving force will change the expansion dynamics. Cellulose is linear, highly crystalline, and insoluble, even upon heating and shearing (Harris and Smith, 2006; BeMiller, 2007). Cellulose is believed to align in the shear field in the extruder and provide resistance to radial expansion (Moraru and Kokini, 2003). Because the driving force was

increased but radial expansion encountered resistance, the vapor was released in the longitudinal

direction, as can be verified by the increase in specific length (Figure 4-6).

With the exception of lignin, all fibers caused a significant reduction in piece density

($p<0.0017$). This was mainly promoted by increased longitudinal expansion compared with the

control. Lignin was equal to the control for radial expansion, specific length, and piece density,

and did not show any changes as the levels of addition increased. The lignin used for this study

was highly compatible with starch and formed a matrix that exhibited comparable viscosity and

extensibility. Kraft lignin has several phenolic and aliphatic hydroxyl groups that have been

described as plasticizing wheat gluten through the formation of hydrogen bonds (Kaewtatip et

al., 2010). The same mechanism likely occurs with starch. One piece of evidence supporting

plasticization is the reduced T_s of the blends with lignin ($p=0.029$, contrast of all levels versus

control).

4.3.6 Microstructure

Representative XMT images of the internal structure of the extrudates are presented in

Figure 4-7. Although large cells are observed for the control, pectin, lignin, and xyloglucan,

cellulose and the mix clearly have a more compact structure. The visual observation is confirmed

by the void fraction values. Overall, cellulose and the mix caused a reduction in void fraction,

whereas lignin, pectin, and xyloglucan caused it to increase (Table 4-4). Although these results

agree with radial expansion, they do not support the lower piece density found for all treatments

with fibers. Therefore, the large increase in longitudinal expansion of the treatments with

cellulose and mix did not fully account for the reduction in radial expansion. Given the low

density of purified cellulose, the decrease in piece density may have been a result of decreased density of the matrix itself. In previous experiments (Karkle et al., 2010), an increase in porosity promoted by longitudinal expansion has been confirmed by void fraction. This difference in results draws attention to the difference between using intact cell wall structures versus isolated components.

Cell size varied from 343 to 2395 μm (mix 25% and lignin 5%, respectively). Despite the high void fraction of the extrudate with xyloglucan, cell size was reduced by close to 50% compared to the control. Visual examination of the cross-sections reveals a higher cell density (Figure 4-7). With the exception of the treatment with lignin, cell wall thickness decreased compared to the control. Thinner walls and smaller cells in the presence of cellulose may reflect the effect of a high driving force for expansion (high T_f) but low extensibility. Intense nucleation occurred, but the matrix was not able to expand. Expansion in highly extensible matrices leads to merging of neighboring cells, which results in large cells and thick walls, as seen for lignin (Trater et al., 2005; Babin et al., 2007).

4.3.7 Mechanical resistance

The fibers caused marked differences in the mechanical resistance of the extrudates (Figure 4-8). Crushing force (Fcr) was increased as much as 9 times when comparing the control with cellulose at 10%. The impact caused by pectin and xyloglucan was more modest (up to 3 times higher), albeit significant ($p < 0.0464$). Crispness work followed the same trends, but with an even higher disparity between cellulose and the other fibers due to the sharp decrease in frequency of spatial ruptures (Nsr).

113

In the present study, cellular architecture appeared more important in defining resistance to compression than composition of the solid matrix. Although the discontinuities in the matrix with cellulose may provide fracture points, the large number of smaller cells was more important in providing resistance. This same structural feature (small cells and thin walls) has been described as providing resistance to starch matrices without any fibers (Babin et al., 2007). The larger number of cells also may be the reinforcing factor in the treatments with xyloglucan, despite the high void fraction.

To highlight the effect of structure on mechanical properties, treatments with lignin did not differ from the control either in terms of macrostructure or in any of the mechanical resistance parameters. Notably, specific length and crushing force followed very similar trends. This supports previous experiments (Karkle et al., 2011) that have shown the relationship between direction of expansion and mechanical resistance. Longitudinal expansion is believed to reinforce the structure by providing various shorter cell walls in the direction of compression. In contrast, radial expansion leads to longer walls in the direction of compression, which weakens the structure.

To better understand the interactions between the fibers and starch, the extrudates were ground and cast into films. Although testing the films under room temperature and pressure does not duplicate the deformation conditions encountered by the matrix as it exits the die, such an approach may provide some insight regarding the dispersion of the fibers in the starch matrix. Tensile strength of the films containing cellulose and the mix decreased compared to the control (Figure 4-9). This may be the result of cellulose, as discrete particles in the matrix, providing points of reduced interaction where resistance to tension decreases. Although pectin had a much larger particle size than the cellulose used in this study (111.2 vs. 53.2 μm, respectively), it

114

slightly increased the tensile strength of the films, which is an indication that pectin molecules were well dispersed in the starch matrix, and not found as discrete particles.

As with pectin, xyloglucan slightly increased tensile strength compared to the control. Kochumalayil et al. (2010) reported casting films of xyloglucan from tamarind and found good film forming ability, transparency, and tensile properties. At 5% addition, xyloglucan appeared to be compatible with the starch matrix and formed a continuous matrix, providing some reinforcement to the films.

Lignin caused a significant increase in the tensile strength of the films. Even though it is mainly insoluble, kraft lignin has been shown to contain polar groups that may interact with starch through hydrogen bonding (Baumberger et al., 1998). The same authors tested lignin contents up to 35% in starch-based films and found lower strength values. One reason may be differences in extrusion processing; higher starch degradation would reduce the strength of the films.

Elongation of the films with pectin, lignin, and xyloglucan was not significantly different than the control. However, cellulose and the mix had significantly lower elongation. This supports the idea that the branched and compatible polymers may expand along with the starch matrix, whereas cellulose exists as discrete particles and creates fracture points.

4.4 Conclusions

The results found for cellulose, lignin, xyloglucan, and pectin in a starch matrix confirm the difference in effect according to compatibility with starch. The high expansion found for the treatments with lignin demonstrate that insolubility per se is not the best indicator of compatibility. Rather, the presence of polar groups able to interact with hydroxyl groups in starch appears to be critical for good dispersion in the matrix, and therefore good expansion and structure-forming properties.

Cellulose was clearly the least functional fiber; however, it is the main fiber in most pomaces, and its effect is dominant. This was verified by the mixes following the same trends as the treatments with cellulose, with the additional limitation of reduced starch content. Therefore, when considering the addition of fruit and vegetable pomaces in extruded products, reduced cellulose content is desirable. This need not limit the total fiber content because pectin and hemicellulose showed good functionality in a directly expanded starch matrix.

References

Adamu, A. & Jin, Z.Y. (2002). Effect of chemical agents on physical and rheological properties of starch-guar gum extrudates. *International Journal of Food Properties, 5(2)*, 261–275.

Agbisit, R., Alavi, S., Cheng, E. Z., Herald, T., & Trater, A. (2007). Relationships between microstructure and mechanical properties of cellular cornstarch extrudates. *Journal of Texture Studies, 38*(2), 199–219.

Altan, A., McCarthy, K. L., & Maskan, M. (2009). Effect of extrusion cooking of functional properties and in vitro starch digestibility of barley-based extrudates from fruit and vegetable by-products. *Journal of Food Science, 74*(2), E77–E86.

ASTM Standard D882, 2010. *Standard test method for tensile properties of thin plastic sheeting*. ASTM International, West Conshohocken, PA, 2010, DOI: 10.1520/D0882-10, www.astm.org.

Babin, P., Della Valle, G., Dendievel, R., Lourdin, D., & Salvo, L. (2007). X-ray tomography study of the cellular structure of extruded starches and its relations with expansion phenomenon and foam mechanical properties. *Carbohydrate Polymers, 68*(2), 329–340.

Baumberger, S., Lapierre, C., Monties, B. & Della Valle, G. (1998). Use of kraft lignin as filler for starch films. *Polymer degradation and stability, 59,* 273–277.

BeMiller, J.N. (2007). *Carbohydrate Chemistry for Food Scientists* (2nd ed.). St. Paul, AACC-International Press.

Bengoechea, C., Arrachid, A., Guerrero, A., Hill, S. E., & Mitchell, J. R. (2007). Relationship between the glass transition temperature and the melt flow behavior for gluten, casein and soya. *Journal of Cereal Science, 45*(3), 275–284.

Bouvier, J. M., Bonneville, R., & Goullieux, A. (1997). Instrumental methods for the measurement of extrudate crispness. *Agro Food Industry Hi-Tech, 8*(1), 16–19.

Brennan, M.A., Merts, I., Monro, J., Woolnough, J., & Brennan, C.S. (2008). Impact of guar gum and wheat bran on the physical and nutritional quality of extruded breakfast cereals. *Starch/Stärke*, 60, 248–256.

Camire, M.E. & Clay King, C. (1991). Protein and fiber supplementation effects on extruded cornmeal snack quality. *Journal of Food Science 56*(3), 760–768.

Chinnaswamy, R. & Hanna, M.A. (1991). Physicochemical and macromolecular properties of starch-cellulose fiber extrudates. *Food Structure, 10*, 229–239.

Goldstein, A., Nantanga, K.K.M., & Seetharaman, K. (2010). Molecular Interactions in Starch-Water Systems: Effect of Increasing Starch Concentration. *Cereal Chemistry, 87*(4), 370–375.

Harris, P.J. & Smith, B.G. (2006). Plant cell walls and cell-wall polysaccharides: structures, properties and uses in food products. *International Journal of Food Science and Technology, 41*(2), 129–143.

Hwang, J.K., Choi, J.S., Kim, C.J., & Kim, C.T. (1997). Solubilization of apple pomace by extrusion. *Journal of Food Processing Preservation, 22,* 477–491.

Kaewtatip, K., Menut, P., Auvergne, R., Tanrattanakul, V., Morel, M.H., & Guilbert, S. (2010). Interactions of Kraft Lignin and Wheat Gluten during Biomaterial Processing: Evidence for the Role of Phenolic Groups. *Journal of Agricultural and Food Chemistry, 58,* 4185–4192.

Khanna, S. & Tester, R.F. (2006). Influence of purified konjac glucomannan on the gelatinisation and retrogradation properties of maize and potato starches. *Food Hydrocolloids, 20,* 567–576.

Kochumalayil, J., Sehaqui, H., Zhou, Q., & Berglund, L.A. (2010). Tamarind seed xyloglucan – a thermostable high-performance biopolymer from non-food feedstock. *Journal of Materials Chemistry, 20,* 4321–4327

Karkle, E.L., Keller, L., Dogan, H., Alavi, S. (2011). Extent of matrix transformation in fiber-added extruded products under different hydration regimens and its impact on texture, microstructure and digestibility. *Journal of Food Engineering*, under review.

Liu, S., Alavi, S., & Abughush, M. (2010). Extruded moringa leaf-oat flour snacks: physical, nutritional and sensory properties. *International Journal of Food Properties.* Submitted December 2009. Accepted May 2010.

Moraru CI, & Kokini JL (2003). Nucleation and expansion during extrusion and microwave heating of cereal foods. *Comprehensive Reviews in Food Science and Food Safety, 2*(4), 120–138.

Nawirska, A. & Kwaśniewska, M. (2005). Dietary fibre fractions from fruit and vegetable processing waste. *Food Chemistry, 91*, 221–225.

Pai, D.A., Blake, O.A., Hamaker, B.R., & Campanella, O.H. (2009). Importance of extensional rheological properties of fiber-enriched corn extrudates. *Journal of Cereal Science*, *50*, 227–234.

Santos, E., Rosell, C.M. & Collar, C. (2008). Gelatinization and retrogradation kinetics of high-fibre wheat flour blends: a calorimetric approach. *Cereal Chemistry, 85,* 457–465.

Stojceska, V., Ainsworth, P., Plunkett, A., & Ibanoglu, S. (2009). The effect of extrusion cooking using different water feed rates on the quality of ready-to-eat snacks made from food by-products. *Food Chemistry, 114*, 226–232.

Trater, A.M., Alavi, S., & Rizvi, S. S. H. (2005). Use of non-invasive X-ray microtomography for characterizing microstructure of extruded biopolymer foams. *Food Research International, 38*(6), 709–719.

Wang, S.S. & Kim, Y. (1998). The Effect of Protein and Fiber on the Kinetics of Starch Gelatinization and Melting in Waxy Corn Flour. *Starch/Stärke, 50* (10), 419–423.

Yagci, S. & Gogus, F. (2010). Effect of incorporation of various food by-products on some nutritional properties of rice-based extruded foods. *Food Science and Technology International*, 15(6), 571–581.

Yanniotis, S., Petraki, A., & Soumpasi, E. (2007). Effect of pectin and wheat fibers on quality attributes of extruded cornstarch. *Journal of Food Engineering, 80*(2), 594–599.

Figures and Tables

Inlet	30°C	30°C	80°C	110°C	120°C

¾ pitch, 78mm*
¾ pitch, 78mm*
full pitch, 78mm
full pitch, 78mm
¾ pitch, 78mm
3x90° kneading block 8.7mm (total 26.1mm)
¾ pitch, 78mm
3x90° kneading block 8.7mm (total 26.1mm)
¾ pitch, 78mm
3x90° kneading block 8.7mm (total 26.1mm)
½ pitch, 52mm
¾ pitch, 78mm
¾ pitch, cone, 78mm
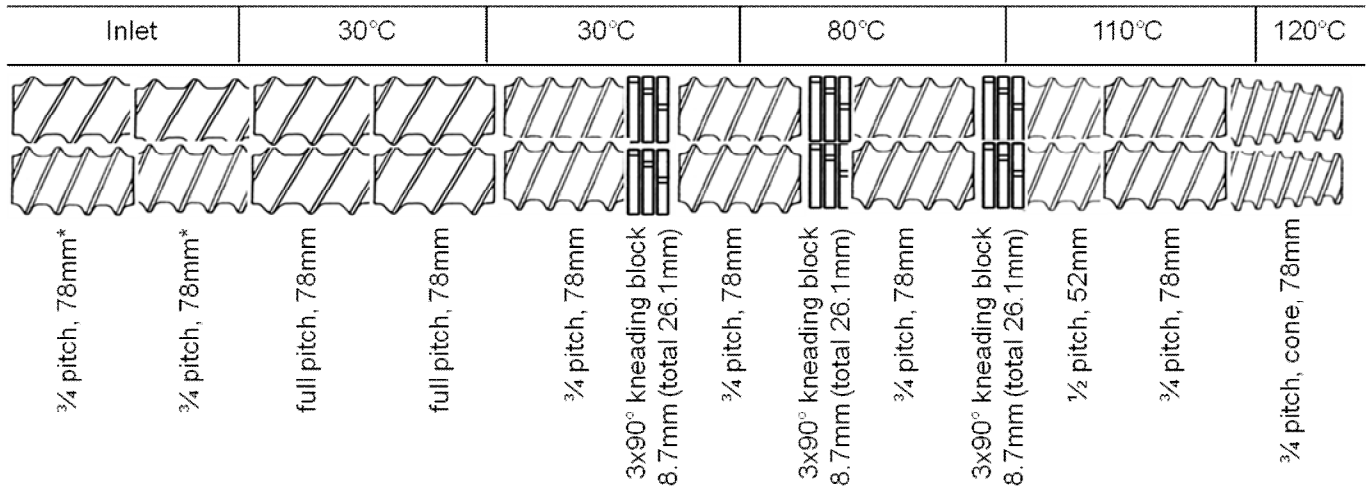
Figure 4-1 Screw configuration and temperature profile.
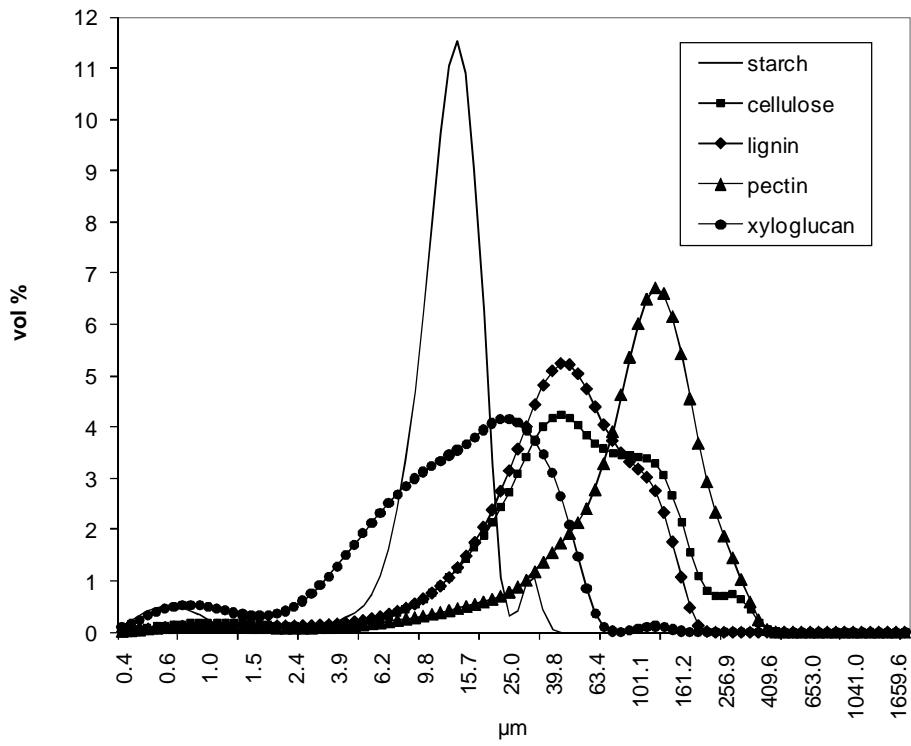
Figure 4-2 Particle size analysis of starch and fibers.
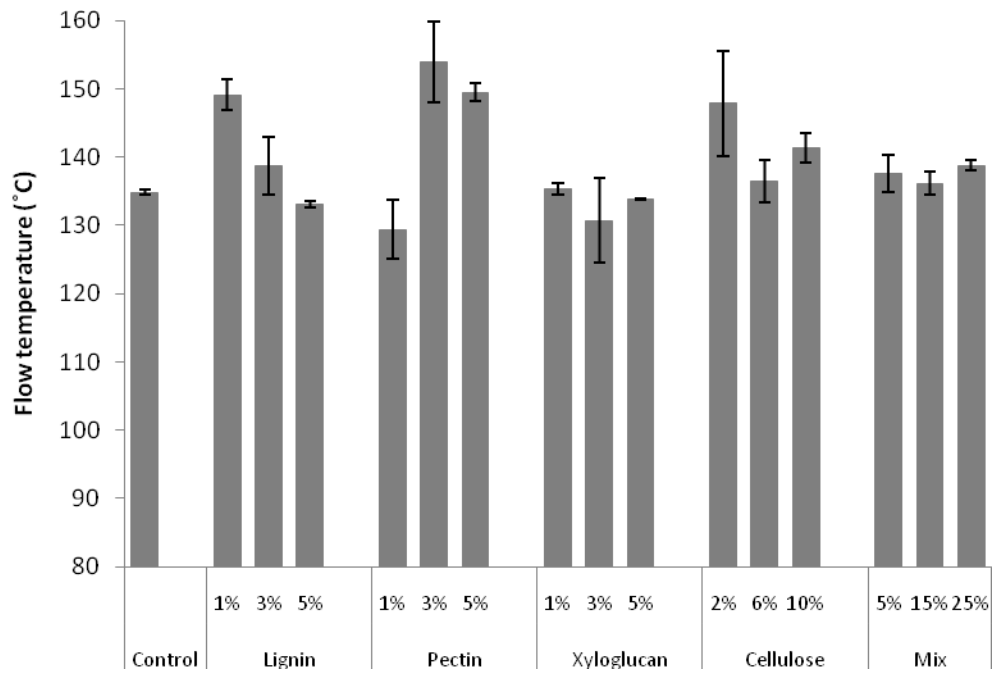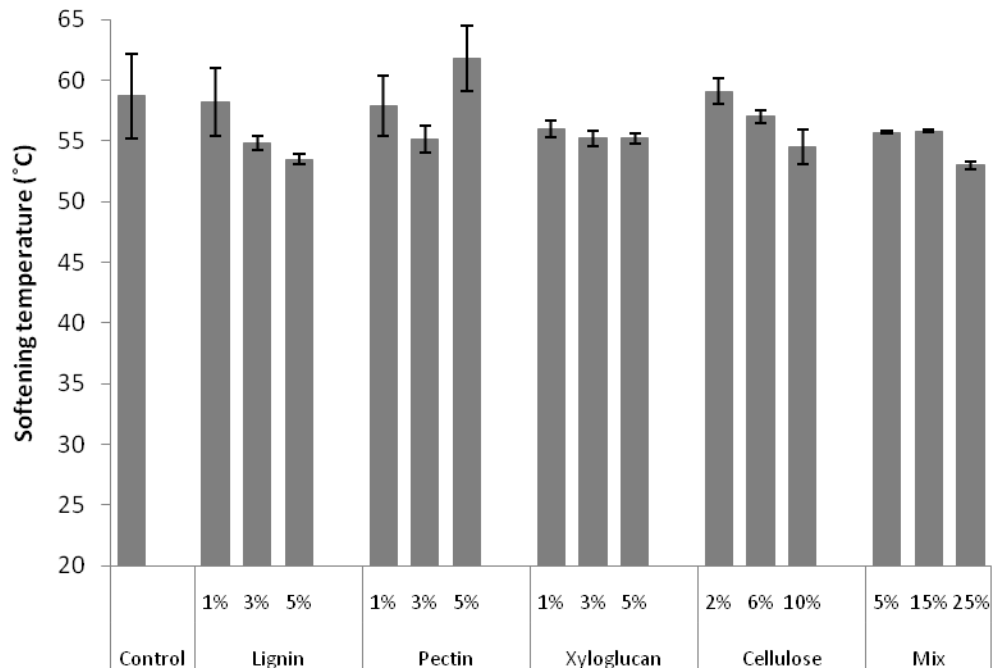
Figure 4-3 Softening and Flow temperatures of blends (19% moisture).
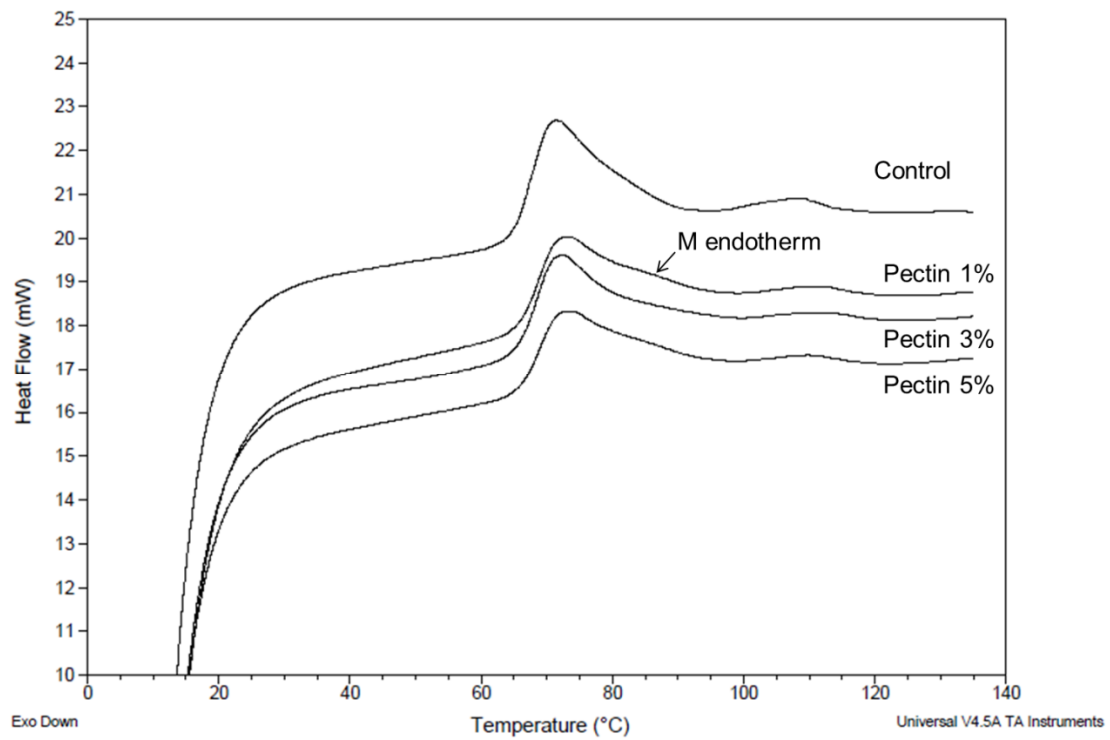
Figure 4-4 Differential scanning calorimetry curves of control and blends with pectin (55% moisture).
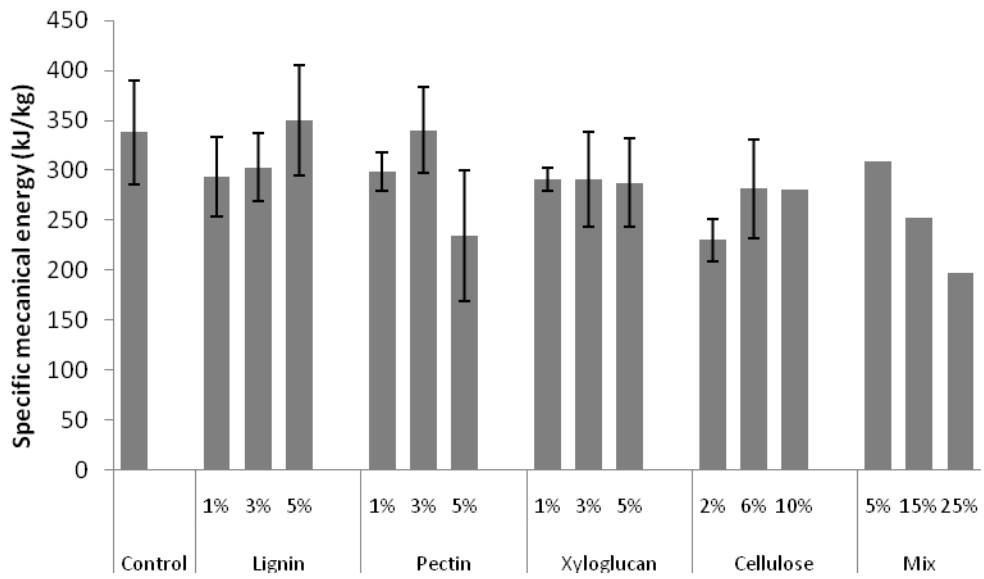
Figure 4-5 Specific mechanical energy (SME) of control and blends with fiber.
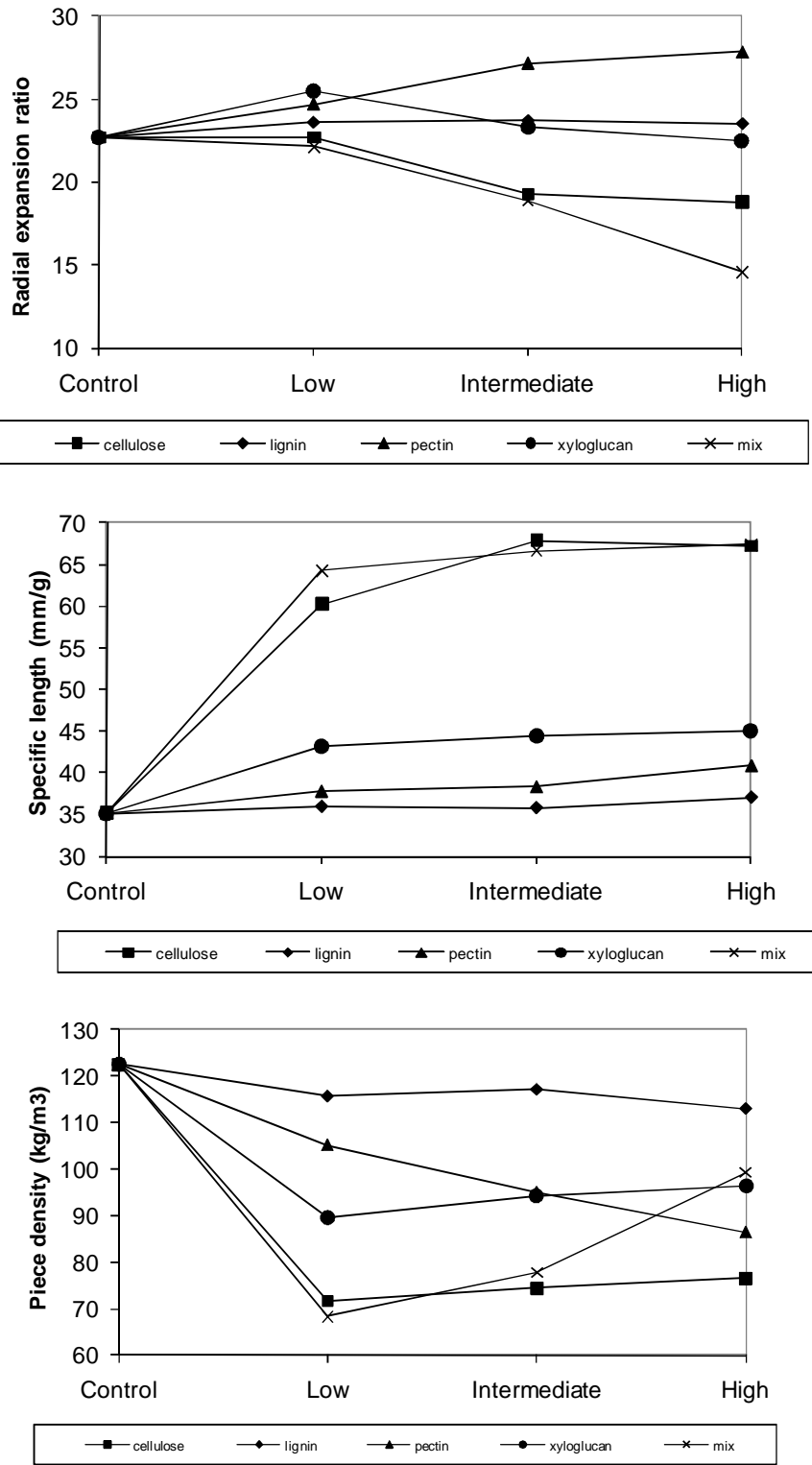
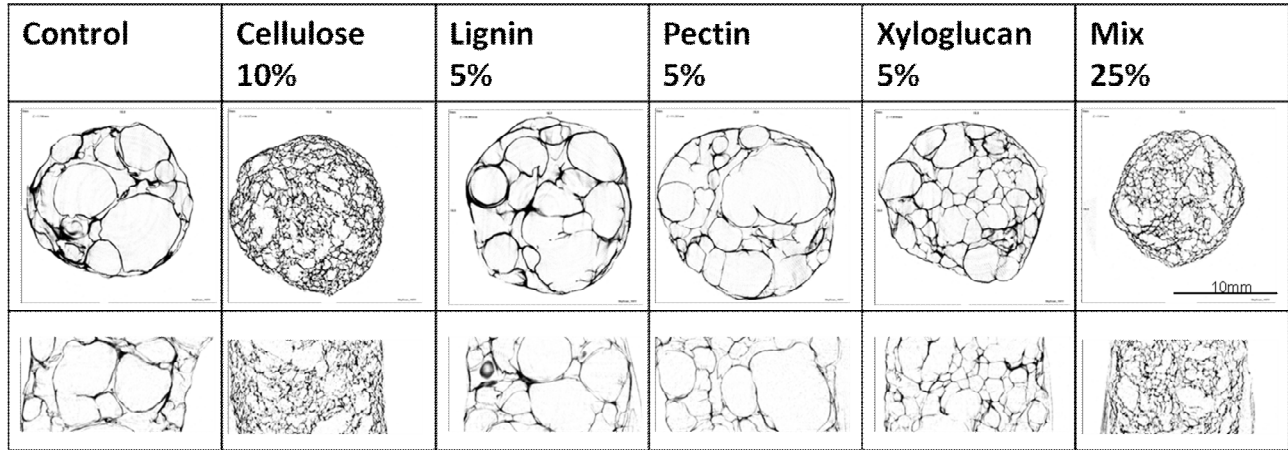Figure 4-6 Macrostructural characteristics of extrudates (see Table 4-1 for fiber levels).

Control	Cellulose 10%	Lignin 5%	Pectin 5%	Xyloglucan 5%	Mix 25%

Figure 4-7 X-ray microtomography images of extrudates at the high level of fiber addition.
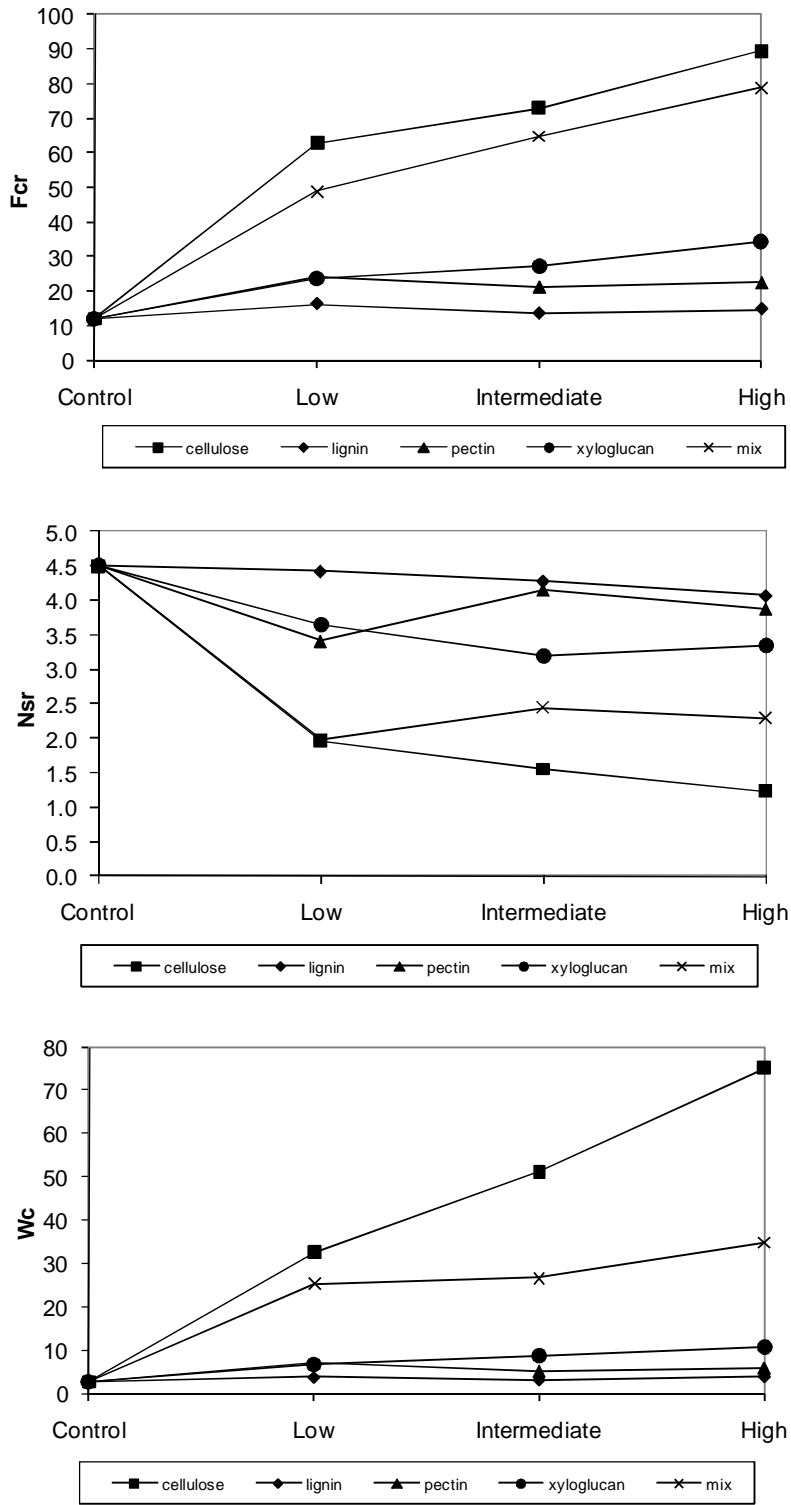
Figure 4-8 Mechanical resistance of extrudates: crushing force (Fc), frequency of spatial ruptures (Nsr), and crispness work (Wc) (see Table 4-1 for fiber levels).
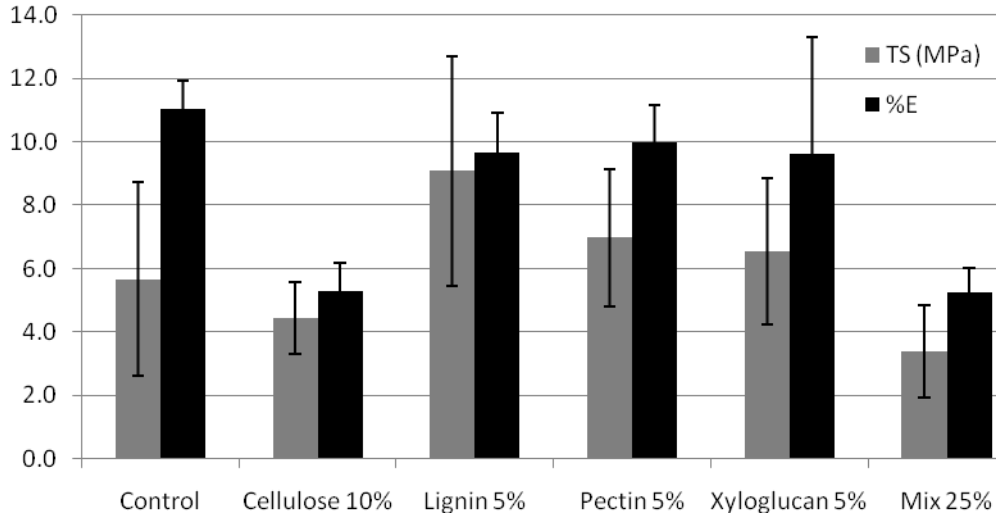
Figure 4-9 Tensile strength (TS) and % elongation (%E) of starch/fiber films.

Table 4-1 Blend formulation

Fiber	Level		
	Low	Intermediate	High
Single fiber blends:			
Cellulose	2%	6%	10%
Lignin	1%	3%	5%
Pectin	1%	3%	5%
Xyloglucan	1%	3%	5%
Mixes:	the above combined (5% total)	the above combined (15% total)	the above combined (25% total)

Table 4-2 Ingredient composition (g/100g dry basis)

	Bamboo cellulose	Kraft lignin (Indulin AT)	High methoxyl pectin	Tamarind xyloglucan
Cellulose[a]	25.7	0.0	0.0	0.0
Hemicellulose[b]	13.8	0.4	0.5	25.9
Lignin[c]	0.0	0.0	0.0	0.0
Protein	0.0	5.2	1.5	21.2
Total dietary fiber	103.2	61.1	90.4	75.9
Insoluble	101.3	60.3	1.1	7.1
Soluble	1.9	0.8	89.3	68.8

[a] Acid detergent fiber minus acid detergent lignin
[b] Neutral detergent fiber minus acid detergent fiber
[c] Acid detergent lignin

Table 4-3. Gelatinization parameters of blends.

	Onset (°C)	Peak (°C)	End (°C)	Enthalpy (J/g)	Enthalpy, starch base (J/g starch)
Control	65.2±0.3 [a*]	71.4±0.3 [a]	94.3±0.8 [acd]	15.6±0.2 [ab]	15.6±0.2 [abc]
Cellulose					
2%	65.7±0.1 [a]	72.0±0.1 [a]	96.6±0.8 [a]	16.3±1.4 [a]	16.7±1.4 [a]
6%	65.3±0.2	71.7±0.6	95.1±0.4	15.0±0.9	15.9±1.0
10%	65.4±0.6	71.9±0.8	93.5±1.4	13.9±0.5	15.4±0.5
Lignin					
1%	65.6±0.0 [a]	71.6±0.0 [a]	94.4±1.4 [a]	15.6±0.8 [a]	15.7±0.8 [a]
3%	65.3±0.2	71.6±0.0	94.9±0.7	16.1±0.7	16.6±0.7
5%	65.9±0.1	71.9±0.2	95.2±0.5	15.8±0.7	16.6±0.7
Pectin					
1%	65.3±0.3 [a]	71.8±0.1 [b]	97.9±0.7 [bc]	15.2±0.4 [bc]	15.4±0.4 [bc]
3%	65.8±0.0	72.5±0.1	97.9±0.7	14.4±0.3	14.8±0.3
5%	66.0±0.1	72.7±0.1	98.5±1.6	14.2±0.0	14.9±0.0
Xyloglucan					
1%	65.6±0.2 [a]	71.4±0.1 [ab]	94.8±0.8 [bd]	15.3±0.4 [ac]	15.5±0.4 [ac]
3%	65.8±0.1	72.2±0.2	99.2±0.5	15.3±0.3	15.7±0.3
5%	65.6±0.0	72.4±0.0	101.2±0.0	15.1±0.0	15.8±0.0
Mix					
5%	65.7±0.2 [b]	72.3±0.6 [c]	96.6±0.4 [b]	14.3±0.0 [b]	15.1±0.0 [b]
15%	66.6±0.5	73.3±0.4	99.7±0.9	12.6±0.9	14.8±1.1
25%	67.2±0.5	74.8±0.0	103.1±8.1	10.7±0.3	14.3±0.4

*Same letters indicate no significant difference in the contrast between each fiber type
(considering all three levels, letters indicated on first row for clarity).

Table 4-4 Microstructural features of extrudates at the high level of fiber addition.

	Void fraction	Average cell size (μm)	Average cell wall thickness (μm)
Control	83.7 ±3.3	2249.0 ±26.5	213.7 ±20.0
Cellulose 10%*	72.1	473.3	118.6
Lignin 5%	87.2 ±2.4	2395.3 ±8.1	220.5 ±52.6
Pectin 5%	89.0 ±0.8	2334.4 ±111.4	162.5 ±16.9
Xyloglucan 5%	86.0 ±0.7	1219.2 ±233.8	142.4 ±6.1
Mix 25%*	64.5	343.5	132.7

*Treatments were not replicated, thus standard deviation is not available.

APPENDIX A – Analysis of variance tables for Chapter 2

Table A-1 Specific mechanical energy

Type 3 Analysis of Variance								
Source	DF	Sum of Squares	Mean Square	Expected Mean Square	Error Term	Error DF	F Value	Pr > F
AP	3	125555	41852	Var(Residual) + Q(AP,AP*MC)	MS(Residual)	11	1.60	0.2457
MC	2	466901	233451	Var(Residual) + Q(MC,AP*MC)	MS(Residual)	11	8.92	0.0050
AP*MC	6	65589	10932	Var(Residual) + Q(AP*MC)	MS(Residual)	11	0.42	0.8525
Blk	1	181221	181221	Var(Residual) + 12 Var(blk)	MS(Residual)	11	6.92	0.0233
Residual	11	287881	26171	Var(Residual)	.	.	.	.

Table A-2 Hydration capacity

Type 3 Analysis of Variance								
Source	DF	Sum of Squares	Mean Square	Expected Mean Square	Error Term	Error DF	F Value	Pr > F
MC	2	3.858072	1.929036	Var(Residual) + Q(MC,MC*AP)	MS(Residual)	11	6.52	0.0136
AP	3	1.812262	0.604087	Var(Residual) + Q(AP,MC*AP)	MS(Residual)	11	2.04	0.1663
MC*AP	6	1.029275	0.171546	Var(Residual) + Q(MC*AP)	MS(Residual)	11	0.58	0.7396
blk	1	12.033650	12.033650	Var(Residual) + 12 Var(blk)	MS(Residual)	11	40.69	<.0001
Residual	11	3.253109	0.295737	Var(Residual)	.	.	.	.

Table A-3 Expansion ratio

Type 3 Analysis of Variance								
Source	DF	Sum of Squares	Mean Square	Expected Mean Square	Error Term	Error DF	F Value	Pr > F
AP	3	66.767917	22.255972	Var(Residual) + Q(AP,AP*MC)	MS(Residual)	11	82.30	<.0001
MC	2	27.563333	13.781667	Var(Residual) + Q(MC,AP*MC)	MS(Residual)	11	50.96	<.0001
AP*MC	6	6.763333	1.127222	Var(Residual) + Q(AP*MC)	MS(Residual)	11	4.17	0.0198
blk	1	1.260417	1.260417	Var(Residual) + 12 Var(blk)	MS(Residual)	11	4.66	0.0538
Residual	11	2.974583	0.270417	Var(Residual)	.	.	.	.

Table A-4 Piece density

Type 3 Analysis of Variance								
Source	DF	Sum of Squares	Mean Square	Expected Mean Square	Error Term	Error DF	F Value	Pr > F
AP	3	5044.605000	1681.535000	Var(Residual) + Q(AP,AP*MC)	MS(Residual)	11	2.85	0.0862
MC	2	280998	140499	Var(Residual) + Q(MC,AP*MC)	MS(Residual)	11	238.10	<.0001
AP*MC	6	5671.697500	945.282917	Var(Residual) + Q(AP*MC)	MS(Residual)	11	1.60	0.2357
blk	1	3870.960000	3870.960000	Var(Residual) + 12 Var(blk)	MS(Residual)	11	6.56	0.0265
Residual	11	6491.020000	590.092727	Var(Residual)	.	.	.	.

Table A-5 Specific length

Type 3 Analysis of Variance								
Source	DF	Sum of Squares	Mean Square	Expected Mean Square	Error Term	Error DF	F Value	Pr > F
AP	3	17690	5896.790000	Var(Residual) + Q(AP,AP*MC)	MS(Residual)	11	21.55	<.0001
MC	2	6486.660833	3243.330417	Var(Residual) + Q(MC,AP*MC)	MS(Residual)	11	11.85	0.0018
AP*MC	6	3469.982500	578.330417	Var(Residual) + Q(AP*MC)	MS(Residual)	11	2.11	0.1337
blk	1	3988.681667	3988.681667	Var(Residual) + 12 Var(blk)	MS(Residual)	11	14.58	0.0029
Residual	11	3009.578333	273.598030	Var(Residual)	.	.	.	.

Table A-6 Average cell size

Type 3 Analysis of Variance								
Source	DF	Sum of Squares	Mean Square	Expected Mean Square	Error Term	Error DF	F Value	Pr > F
AP	3	0.934052	0.311351	Var(Residual) + Q(AP,AP*MC)	MS(Residual)	11	26.39	<.0001
MC	2	0.014914	0.007457	Var(Residual) + Q(MC,AP*MC)	MS(Residual)	11	0.63	0.5498
AP*MC	6	0.078781	0.013130	Var(Residual) + Q(AP*MC)	MS(Residual)	11	1.11	0.4143
blk	1	0.175831	0.175831	Var(Residual) + 12 Var(blk)	MS(Residual)	11	14.90	0.0027
Residual	11	0.129792	0.011799	Var(Residual)	.	.	.	.

Table A-7 Average cell wall thickness

Type 3 Analysis of Variance								
Source	DF	Sum of Squares	Mean Square	Expected Mean Square	Error Term	Error DF	F Value	Pr > F
AP	3	0.038645	0.012882	Var(Residual) + Q(AP,AP*MC)	MS(Residual)	11	13.24	0.0006
MC	2	0.062038	0.031019	Var(Residual) + Q(MC,AP*MC)	MS(Residual)	11	31.88	<.0001
AP*MC	6	0.003237	0.000539	Var(Residual) + Q(AP*MC)	MS(Residual)	11	0.55	0.7578
blk	1	0.004785	0.004785	Var(Residual) + 12 Var(blk)	MS(Residual)	11	4.92	0.0486
Residual	11	0.010704	0.000973	Var(Residual)	.	.	.	.

Table A-8 Void fraction

Type 3 Analysis of Variance								
Source	DF	Sum of Squares	Mean Square	Expected Mean Square	Error Term	Error DF	F Value	Pr > F
AP	3	102.530683	34.176894	Var(Residual) + Q(AP,AP*MC)	MS(Residual)	11	3.22	0.0651
MC	2	1485.841058	742.920529	Var(Residual) + Q(MC,AP*MC)	MS(Residual)	11	70.03	<.0001
AP*MC	6	13.657442	2.276240	Var(Residual) + Q(AP*MC)	MS(Residual)	11	0.21	0.9643
blk	1	192.326817	192.326817	Var(Residual) + 12 Var(blk)	MS(Residual)	11	18.13	0.0013
Residual	11	116.690983	10.608271	Var(Residual)	.	.	.	.

Table A-9 Crushing force

				Type 3 Analysis of Variance				
Source	DF	Sum of Squares	Mean Square	Expected Mean Square	Error Term	Error DF	F Value	Pr > F
AP	3	14072	4690.574444	Var(Residual) + Q(AP,AP*MC)	MS(Residual)	11	22.95	<.0001
MC	2	3739.657500	1869.828750	Var(Residual) + Q(MC,AP*MC)	MS(Residual)	11	9.15	0.0046
AP*MC	6	1769.659167	294.943194	Var(Residual) + Q(AP*MC)	MS(Residual)	11	1.44	0.2827
blk	1	68.681667	68.681667	Var(Residual) + 12 Var(blk)	MS(Residual)	11	0.34	0.5738
Residual	11	2247.958333	204.359848	Var(Residual)	.	.	.	.

Table A-10 Crispness work

				Type 3 Analysis of Variance				
Source	DF	Sum of Squares	Mean Square	Expected Mean Square	Error Term	Error DF	F Value	Pr > F
AP	3	7932.315000	2644.105000	Var(Residual) + Q(AP,AP*MC)	MS(Residual)	11	13.40	0.0005
MC	2	1037.890833	518.945417	Var(Residual) + Q(MC,AP*MC)	MS(Residual)	11	2.63	0.1165
AP*MC	6	1433.542500	238.923750	Var(Residual) + Q(AP*MC)	MS(Residual)	11	1.21	0.3697
blk	1	115.281667	115.281667	Var(Residual) + 12 Var(blk)	MS(Residual)	11	0.58	0.4607
Residual	11	2169.948333	197.268030	Var(Residual)	.	.	.	.

Table A-11 Frequency of spatial ruptures

Type 3 Analysis of Variance								
Source	DF	Sum of Squares	Mean Square	Expected Mean Square	Error Term	Error DF	F Value	Pr > F
AP	3	13.731250	4.577083	Var(Residual) + Q(AP,AP*MC)	MS(Residual)	11	12.37	0.0008
MC	2	0.292500	0.146250	Var(Residual) + Q(MC,AP*MC)	MS(Residual)	11	0.40	0.6828
AP*MC	6	1.667500	0.277917	Var(Residual) + Q(AP*MC)	MS(Residual)	11	0.75	0.6217
blk	1	0.003750	0.003750	Var(Residual) + 12 Var(blk)	MS(Residual)	11	0.01	0.9216
Residual	11	4.071250	0.370114	Var(Residual)	.	.	.	.

APPENDIX B – Analysis of variance tables and contrasts for Chapter 4

Table B-1 Onset temperature

Source	DF	Sum of Squares	Mean Square	F Value	Pr > F
Model	15	8.09444355	0.53962957	6.12	0.0006
Error	15	1.32295000	0.08819667		
Corrected Total	30	9.41739355			

Table B-2 Peak temperature

Source	DF	Sum of Squares	Mean Square	F Value	Pr > F
Model	15	22.00888548	1.46725903	13.22	<.0001
Error	15	1.66445000	0.11096333		
Corrected Total	30	23.67333548			

Table B-3 End temperature

Source	DF	Sum of Squares	Mean Square	F Value	Pr > F
Model	15	207.8489355	13.8565957	2.69	0.0320
Error	15	77.1434000	5.1428933		
Corrected Total	30	284.9923355			

Table B-4 Enthalpy

Source	DF	Sum of Squares	Mean Square	F Value	Pr > F
Model	15	14.16460590	0.94430706	2.23	0.0654
Error	15	6.34091379	0.42272759		
Corrected Total	30	20.50551968			

Table B-5 Softening temperature

Source	DF	Sum of Squares	Mean Square	F Value	Pr > F
Model	15	153.1448387	10.2096559	3.96	0.0057
Error	15	38.6900000	2.5793333		
Corrected Total	30	191.8348387			

Table B-6 Flow temperature

Source	DF	Sum of Squares	Mean Square	F Value	Pr > F
Model	15	1567.819677	104.521312	7.14	0.0002
Error	15	219.610000	14.640667		
Corrected Total	30	1787.429677			

Table B-7 Contrast between extrudate parameters

Label	PD	ER	SL	Fc	Nsr	Wc	SME
treatment	0.0007	0.0439	<0.0001	<0.0001	0.0007	<0.0001	0.2573
control vs average of L1, L3, L5	0.2977	0.6153	0.7087	0.5636	0.5665	0.8541	0.5312
control vs average of P1, P3, P5	0.0017	0.4773	0.0230	0.0464	0.1168	0.4667	0.2091
control vs average of X1, X3, X5	0.0010	0.0726	0.0768	0.0054	0.0194	0.1955	0.1954
control vs average of C2, C6, C10	<.0001	0.2202	<.0001	<.0001	<.0001	<.0001	0.0690
control vs average of M1, M2, M3	0.0002	0.0646	<.0001	<.0001	0.0004	0.0002	0.0525
average of M vs average of L	0.0001	0.0078	<.0001	<.0001	0.0001	<.0001	0.0640
average of M vs average of P	0.0349	0.0050	<.0001	<.0001	0.0008	<.0001	0.2320
average of M vs average of X	0.0654	0.0004	<.0001	<.0001	0.0064	0.0002	0.2503
average of M vs average of C	0.2287	0.3236	0.7077	0.0487	0.1015	0.0001	0.7230
average of P vs average of L	0.0013	0.7630	0.0086	0.0398	0.1444	0.4405	0.3517
average of P vs average of X	0.6680	0.1048	0.3525	0.1141	0.1724	0.3963	0.9510
average of P vs average of C	0.0014	0.0194	<.0001	<.0001	<.0001	<.0001	0.3390
average of L vs average of C	<.0001	0.0323	<.0001	<.0001	<.0001	<.0001	0.0840
average of L vs average of X	0.0006	0.0620	0.0484	0.0019	0.0114	0.1205	0.3227
average of C vs average of X	0.0027	0.0011	<.0001	<.0001	<.0001	<.0001	0.3668